WAVE INDUCED OSCILLATIONS IN HARBORS WITH CONNECTED BASINS

by

Jiin-Jen Lee and Fredric Raichlen

W. M. Keck Laboratory of Hydraulics and Water Resources
Division of Engineering and Applied Science
CALIFORNIA INSTITUTE OF TECHNOLOGY
Pasadena, California

Report No. KH-R-26

August 1971

WAVE INDUCED OSCILLATIONS IN HARBORS WITH CONNECTED BASINS

by

Jiin-Jen Lee
Research Fellow in Civil Engineering
(1969-1970)

and

Fredric Raichlen
Associate Professor of Civil Engineering

Supported by

U. S. Army Corps of Engineers
Contract No. DA-22-079-CIVENG-64-11

W. M. Keck Laboratory of Hydraulics and Water Resources
Division of Engineering and Applied Science
California Institute of Technology
Pasadena, California

Report No. KH-R-26

ABSTRACT

A linear, inviscid theory, termed the coupled basins theory, has been developed to analyze the response to periodic incident waves of an arbitrary shape harbor containing several interconnected basins. The region of consideration is divided into an open-sea region and several inner-basin regions (the number depending on the harbor geometry). The solution in each region is formulated as an integral equation in terms of the normal velocity at the entrance and/or at the common boundaries between regions. An approximate method is used to solve the integral equation by converting it to a matrix equation. The initially unknown boundary condition at the entrance is determined by matching the wave amplitudes and their normal derivatives at the harbor entrance and at all the common boundaries. The solution for the response and the amplitude distribution within the complete harbor can then be obtained.

It has been found that the coupled-basins theory gives results which agree well with experiments both for an irregular shape harbor as well as for a harbor composed of two connected circular basins. Various aspects of the response of harbors composed of several types of circular connected basins as well as circular harbors with rectangular entrance channels have been investigated. It is found that to a first approximation the response of a coupled harbor system can be constructed by superposing the response of the individual harbors.

Certain aspects of the effect of viscous dissipation on harbor resonance are discussed. Some attention is given to problems of scaling model results to the prototype harbor.

ACKNOWLEDGMENTS

The writers wish to express their appreciation to Professor Vito A. Vanoni for his continuing interest and many helpful suggestions throughout the course of the study.

The writers also would like to thank Mr. Elton F. Daly, supervisor of the shop and laboratory, for his contribution in the construction and maintenance of the experimental equipment. Appreciation is also due to Mr. Robert L. Greenway who assisted with the construction of the apparatus; Mr. Carl Green who prepared the drawings; and Mrs. Arvilla F. Krugh who typed the entire manuscript.

This research was supported by the U. S. Army Corps of Engineers under Contract DA-22-079-CIVENG-64-11. The experiments were conducted in the W. M. Keck Laboratory of Hydraulics and Water Resources at the California Institute of Technology.

TABLE OF CONTENTS

TABLE OF CONTENTS (Continued)

LIST OF FIGURES

LIST OF FIGURES (Continued)

LIST OF FIGURES (Continued)

CHAPTER 1

INTRODUCTION

Waves which propagate from the open-sea into bays and harbors usually experience changes in wave direction, shape, and amplitude due to the local bathymetry and horizonal geometry of the embayment. The harbor shape and the internal reflections associated with the harbor boundary can cause amplification or attenuation of the incident wave system. This phenomenon usually is referred to as harbor resonance, seiche, or harbor surging and can be the cause of significant damage to moored ships and adjacent structures especially if the resonant period of the ship-mooring system is close to that of a mode of oscillation of the harbor. In addition, the currents induced by these harbor oscillations can create navigational hazards near the entrance and within the harbor.

For an existing harbor that experiences operational problems due to the effect of resonant oscillations, corrective action must be taken to reduce or eliminate such oscillations. In the case of new construction an attempt should be made to use a harbor geometry that will be free from possible resonance effects for the local wave conditions. In either case an analytical method for predicting resonance and the associated wave amplitudes is quite useful for preliminary investigations as well as providing a guide for experimental studies if they are deemed necessary. The existing methods, to be discussed, are not advanced to the state where the resonance characteristics of a harbor can be determined

accurately analytically; however, as mentioned, these methods certainly can assist the engineer in early design stages, in assessing existing problems, or in conducting experiments in the laboratory.

1.1 PREVIOUS HARBOR RESONANCE STUDIES

Previous analytical and experimental studies of harbor resonance can be divided into two groups. The first deals with the problem of wave-induced oscillations in harbors of simple geometry such as circular, rectangular, or combinations of these simple shapes, e.g., McNown (1952), LeMehaute (1961), Miles and Munk (1961), Ippen and Goda (1963), Raichlen and Ippen (1965), Miles (1970), and Carrier, Shaw, and Miyata (1971). The second group of investigations is concerned primarily with harbors of complicated geometry, e.g., Knapp and Vanoni (1945), Wilson (1959, 1960), Wilson, Hendrickson and Kilmer (1965), Leendertse (1967), Hwang and Tuck (1970), Lee (1969), and Lee and Raichlen (1970). In this section the work of these investigators will be briefly discussed in the order just presented.

McNown (1952) investigated some of the response characteristics of a circular harbor of constant depth excited by wave incident upon a small entrance gap. In his analysis it was assumed that the crest of a standing wave (antinode) occurred at the entrance when the harbor was in resonance. A similar method was applied to rectangular harbors by Kravtchenko and McNown (1955). Thus, for resonant motions, this assumption led to a boundary condition identical to that for a completely closed basin. Therefore, the wave periods associated with resonant oscillations would be those which correspond to the eigenvalues for the

free oscillations of a completely closed circular (or rectangular) basin. Due to this assumption this method can determine only approximately the resonant periods of a harbor of simple planform.

Other theoretical work on rectangular harbors include Aptés (1957) study of a rectangular harbor with an entrance connected to a relatively long wave channel and the study by Biesel and LeMehaute (1955, 1956) and LeMehaute (1960, 1961) for rectangular harbors with various types of entrances. Apté obtained a theoretical solution for the amplitude distribution within the partially closed harbor by matching the entrance velocities between two domains: the harbor and the attendant wave channel. Although agreement between theory and experiments was good the analysis did not attack the problem of a harbor connected to the open-sea. LeMehaute's method was based on complex number calculus and was applied to a rectangular harbor connected to an infinitely long but relatively narrow channel. He superimposed various incident, reflected, and transmitted waves incorporating an empirical reflection coefficient and attenuation parameter to obtain a solution.

The problem of a rectangular harbor connected directly to the open-sea was first investigated by Miles and Munk (1961). They included the effect of the wave radiation from the harbor mouth to the open-sea thereby limiting the maximum wave amplitude within the harbor for the inviscid case to a finite value even at resonance. They also considered, in a general fashion, an arbitrary shape harbor and formulated the problem as an integral equation in terms of a Green's function; however, no attempt was made to solve the resulting expression for harbors of

complicated shape. In the case of a rectangular harbor, Miles and Munk applied this general formulation and found for periodic waves that narrowing the harbor entrance leads to an enhancement of harbor surging (oscillation) instead of a reduction. This phenomenon was termed the "harbor paradox". The increasing wave amplification at resonance as the entrance width decreased was also found by LeMehaute (1955) and Ippen and Goda (1963).

Ippen and Goda (1963) employed the Fourier transformation method to evaluate the waves radiated from the entrance of a rectangular harbor to the open-sea and the method of separation of variables for the region inside of the rectangular harbor. A solution for the response was obtained by matching average amplitudes from the two regions at the entrance. They found good agreement between experiments and the theory.

Ippen and Raichlen (1962) and Raichlen and Ippen (1965) have studied, both theoretically and experimentally, the wave-induced oscillations in a rectangular harbor connected to a larger highly reflective rectangular wave basin. They found that the response characteristics of the harbor were radically different from a similar prototype harbor connected to the open-sea. The response curve of the former was characterized by a large number of closely spaced resonant maxima where for the harbor connected to the open-sea only several distinct resonant modes of oscillation would be experienced for the same wave period range. It was pointed out that to reduce the coupling effect of the reflection of the wave energy which is radiated from the harbor entrance efficient wave absorbers were necessary

in the main wave basin. A subsequent study by Ippen, Raichlen, and Sullivan (1962) showed that the coupling effect is indeed significantly reduced by wave absorbers in the main wave basin.

Most recently, Miles (1970) re-examined the "harbor paradox" using electrical circuit analogy and used as examples a coupled rectangular and circular harbor connected to the open-sea. Carrier, Shaw and Miyata (1971) also theoretically studied resonant oscillations in harbors of special shapes (rectangular, circular, or circular sectors) connected to the open-sea through a rectangular entrance channel and found that for inviscid conditions the length of the entrance channel affects both the wave amplification at resonance within the harbor and the frequency bandwidth of the response near resonance.

Attempts to study the problem of wave induced oscillations in harbors of complicated geometry began with the two independent hydraulic model studies by Knapp and Vanoni (1945) and Wilson (for work in the period of 1942 to 1951, see Wilson (1959, 1960)). Knapp and Vanoni's study was in connection with harbor improvements at the Naval Operating Base, Terminal Island, California (the present East and West Basins of Long Beach Harbor). One purpose of the study was to choose the optimum mole alignment and in this connection the characteristic response of the basin was also determined. Wilson's work dealt with the problem of surging in Table Bay Harbor, Capetown, South Africa and the interaction of moored vessesl with wave-induced oscillations in the harbor. Through experimental studies certain proposed modifications were suggested for reducing the harbor surging.

Although hydraulic model studies usually can provide reliable information on harbor surging and the investigator can develop corrective procedures using the model, generally these models are expensive and require a considerable amount of time to operate intelligently. Therefore, many researchers have been searching for a method to theoretically determine the wave-induced oscillations in harbors of arbitrary shape. Such theoretical results at the very least provide a guide for initial calculations and for the experimental program if indeed a model study is deemed necessary.

Wilson, Hendrickson, and Kilmer (1965) and Leendertse (1967) have studied numerically the three-dimensional oscillations in bays or harbors of arbitrary shape and variable depth by using finite-difference techniques. Both methods require that the wave condition at the open boundary (or at the harbor entrance) be assumed or specified from field data. Recently two independent studies on wave oscillations in an arbitrary shape harbor with constant depth have been reported by Hwang and Tuck (1970) and Lee (1969, 1970) and also Lee and Raichlen (1970). Hwang and Tuck obtained their solution by superimposing the scattered wave pattern along the entire reflecting boundary (including the coastline) to the standing wave system; they have confirmed their analysis by comparing with the experimental results obtained by Ippen and Goda (1963) for a fully open rectangular harbor. In Lee (1969) the domain of interest was divided into two regions: a region which defines the limit of the harbor and the open-sea region. Solutions in each region were obtained in terms of the unknown boundary condition at the entrance with the

response determined by matching the solutions at the harbor entrance. This theoretical analysis has been confirmed experimentally applying the theory to two circular harbors, a rectangular harbor, and a constant depth model of the East and West Basins of the Long Beach Harbor.

1.2 DESCRIPTION OF PRESENT STUDY

The present study is an extension of the studies by Lee (1969) and Lee and Raichlen (1970). As just mentioned, in those studies, the entire domain was divided (at the harbor entrance) into two regions: (1) the harbor region which forms the interior limit of the harbor boundary and (2) the open-sea region. The solution in each region was formulated as an integral equation in terms of the unknown boundary condition at the harbor entrance. A method was used to solve for the integral equation by converting it to a matrix equation. In this method the harbor boundary was divided into a sufficiently large number of straightline segments, thus, continuous integration in the solution is replaced by discrete summation along the harbor boundary. The final solution was obtained by matching the solutions obtained from both regions at the harbor entrance. This method has been successfully applied to harbors of several geometrical shapes including a complicated harbor geometry. In principle, this method can be applied to a harbor of any arbitrary shape connected to the open-sea as long as the water depth in both regions can be assumed constant. However, in order to realize a prescribed accuracy for the numerical calculations, the ratio of the length of the straightline boundary segments to the wave length must be kept within certain limits. It was found that to insure good experi-

mental agreement this ratio should be less than one-tenth. This requirement implies that for a harbor with a very complicated shape or short waves the storage space of a digital computer must be quite large to handle the problem and the computation time on such a computer may be fairly long.

In order to improve this aspect of the analysis the present study was initiated. A method has been developed where the harbor region is divided into several subregions, and the same method as just described is used to form a solution in each region in terms of the unknown boundary condition at the common boundary which separates adjacent regions. In this way both the required computer storage and the computation time are reduced significantly. As an example, the size of the computer storage for the computer program presented by Lee (1969) for the Long Beach Harbor Model was 206,000 bytes on the IBM 360/75. (Each eight binary "bit" is referred to as a byte; four bytes form a word.) The execution time for one wave number ($k = 2.35\ ft^{-1}$) including the compilation of the main program was 28.9 sec. Excluding the time required for compiling the main program, the computation time was 24.0 sec. By applying the coupled-basins method to compute the response characteristics of the same Long Beach Harbor Model (with the interior harbor now divided into two regions: the East Basin and the West Basin) the computer storage on the same IBM 360/75 computer was reduced to 145,000 bytes while the execution time for the same wave number was now 23.4 sec (including the compilation of the main program). Subtracting the time for compilation of the program from this, the actual computation time was 13.0 sec. Thus, immediate advantages of the

present method are clearly seen and more complicated harbor geometries can be studied for a given computer size as well as investigating shorter waves than could be investigated with the method of Lee (1969).

The coupled-basins theory which was developed is presented in Chapter 2. The experimental results obtained for a model of the East and West Basins of Long Beach Harbor reported by Lee (1969) were used as initial confirmation of the present theory. In addition, experiments were conducted using an arrangement of two connected circular basins and a harbor which consists of a circular segment with a rectangular channel connecting it to the open-sea. In Chapter 4 theoretical results are compared to these experiments for the three cases.

The second objective of this investigation was to study in detail certain aspects of the response of coupled basins of simple geometry compared to the response of the individual basins alone. This aspect of harbor resonance is quite important considering that one method of expanding harbors is to add additional slips and side basins. Before construction takes place it is important that the effect of these basins on the main harbor be completely understood. Several different arrangements of circular-coupled basins and circular-rectangular-coupled basins have been investigated theoretically in this connection and the analytical results are presented in Sections 4.2 and 4.3. In addition to the response characteristics of such harbors, the amplitude distribution in a coupled-circular harbor is presented for a particular arrangement for several values of the wave number parameter ka (the product of the wave number k and the radius a). The effect of a rectangular entrance canal on the

response of a circular harbor is presented in Section 4.3.2. This aspect of the problem was not pursued in detail, but was investigated primarily to determine the effect on the response of one basin with a particular shape of one with a different shape; these results indicate a fruitful area of further study. In connection with this preliminary study of entrance channel effects, the effect of the side-channel resonators on the response of harbors with entrance channels was briefly investigated theoretically with results also presented in Section 4.3.2. A qualitative discussion of the effect of energy dissipation on the harbor response is presented in Section 4.4 with some attention given to the problem of scaling model results to the corresponding prototype.

CHAPTER 2

THEORETICAL ANALYSIS

The theoretical analysis for the wave induced oscillations in harbors which are composed of coupled basins with arbitrary shape and a constant depth is presented in this chapter. The complete harbor is divided into several regions, and the solution to the boundary value problem in each region is formulated as an integral equation. This integral equation is approximated by a matrix equation which can be solved using a high-speed digital computer. The final solution is obtained using matching conditions at the harbor entrance and the common boundaries between regions, i.e., equating, at the entrance as well as at the common boundaries, the wave amplitudes and their normal derivatives obtained from the solutions in each region.

2.1 DEVELOPMENT OF THE HELMHOLTZ EQUATION

Assuming an irrotational flow, a velocity potential, Φ, can be defined such that the fluid particle velocity can be expressed as $\vec{u} = \nabla\Phi$. Thus, from the continuity equation for an incompressible fluid, Laplace's equation is obtained:

$$\nabla \cdot \vec{u} = \nabla^2 \Phi = 0. \tag{1}$$

A solution of Φ is sought in the following form:

$$\Phi(x, y, z;t) = \frac{1}{-i\sigma} f(x, y)\, Z(z)\, e^{-i\sigma t}, \tag{2}$$

where σ is the angular frequency defined as $2\pi/T$ (T is the wave period),

$\lambda = \sqrt{-1}$, and f(x, y), termed the wave function, describes the variation of Φ in the x, y direction. (The coordinate system is defined in Fig. 1.) Substituting Eq. 2 into Eq. 1 one obtains:

$$\frac{1}{f}\left(\frac{\partial^2 f}{\partial x^2}+\frac{\partial^2 f}{\partial y^2}\right) = -\frac{1}{Z}\frac{\partial^2 Z}{\partial z^2} \ . \tag{3}$$

If Eq. 3 is equated to a constant, say $-k^2$, then the following equations are obtained:

$$\frac{d^2 Z}{dz^2} - k^2 Z = 0 \ , \tag{4}$$

$$\frac{\partial^2 f}{\partial x^2} + \frac{\partial^2 f}{\partial y^2} + k^2 f = 0 \ . \tag{5}$$

The boundary condition at the bottom and the linearized dynamic free surface condition are respectively:

$$\frac{\partial \Phi}{\partial z}(x, y, -h; t) = 0 \ , \tag{6.a}$$

$$\eta(x, y; t) = A_i f(x, y)\, e^{-\lambda\sigma t} = -\frac{1}{g}\left(\frac{\partial \Phi}{\partial t}\right)_{z=0} \ , \tag{6.b}$$

where the depth h is assumed constant, η is the displacement of water surface from the still water level, A_i is the amplitude at the crest of the incident wave, and g is the acceleration of gravity.

The function Z(z) which satisfies Eqs. 4 and 6 can be found as:

$$Z(z) = -\frac{A_i g \cosh k(h+z)}{\cosh kh} \ .$$

Thus, the velocity potential Φ becomes:

$$\Phi(x, y; t) = \frac{1}{\lambda\sigma}\,\frac{A_i g \cosh k(h+z)}{\cosh kh}\, f(x, y)\, e^{-\lambda\sigma t} \ . \tag{7}$$

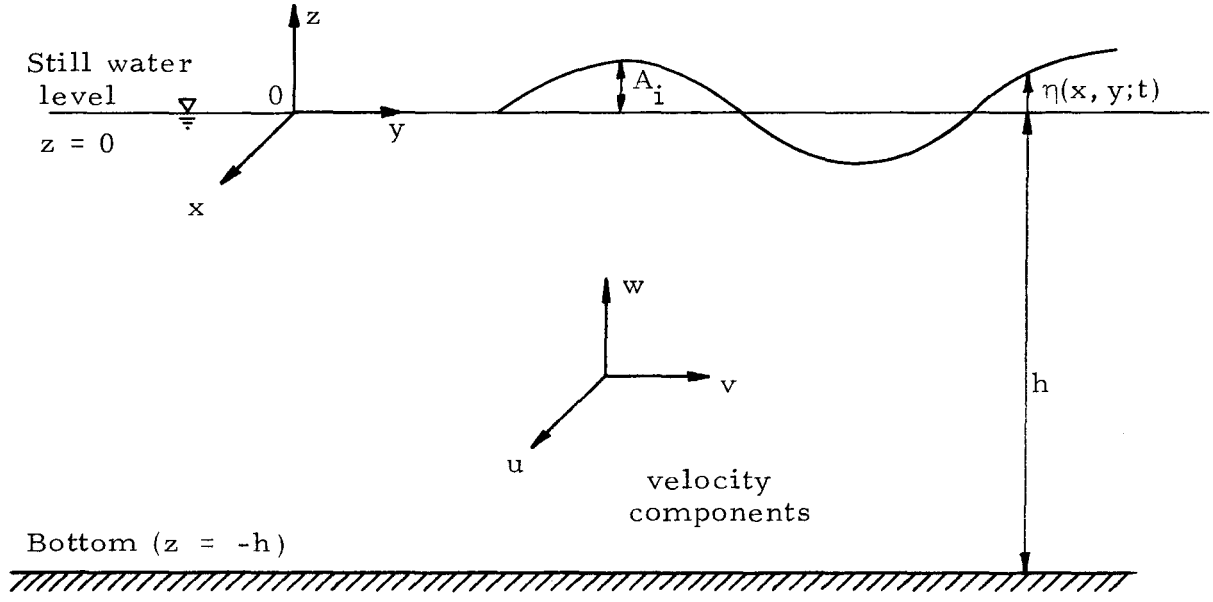

Fig. 1 Definition sketch of the coordinate system

Substituting Eqs. 6b and 7 into the linearized kinematic free surface condition, $\partial\eta/\partial t = (\partial\Phi/\partial z)_{z=0}$, the well known "dispersion relation" for water waves is obtained: $\sigma^2 = gk \tanh(kh)$; therefore, the arbitrary constant k used in Eqs. 4 and 5 is the wave number defined as $2\pi/L$ (L is the wave length).

To complete the expression for the velocity potential, the main problem which remains is to determine the wave function, f(x, y), which satisfies Eq. 5, known as the Helmholtz equation, and the boundary condition that there is no flow through solid boundaries (such as the coastline and the boundary of the harbor in this problem) and also the radiation condition which will be discussed later.

2.2 SOLUTION OF THE HELMHOLTZ EQUATION FOR COUPLED BASINS

The procedure for determining the wave function, f(x, y), and thus the response of the harbor to periodic incident waves can be outlined as follows:

(i) The domain of interest shown in Fig. 2 is divided into several regions: the infinite ocean region (Region I), and regions bounded by the limits of the harbor and various interior divisions (Region II-1, Region II-2, Region II-3).

(ii) The function f_1 in Region I is expressed in terms of the unknown value of the normal derivative $\partial f_1/\partial n$ at the harbor entrance. The function f_{21} in Region II-1 is expressed in terms of the unknown value of $\partial f_{21}/\partial n$ both at the harbor entrance and at the common boundaries between other basins in Region II, e.g., line $\overline{CD}$ and $\overline{EF}$ in Fig. 2. Similarly, the function f_{22} in Region II-2 (or the function f_{23} in Region II-3)

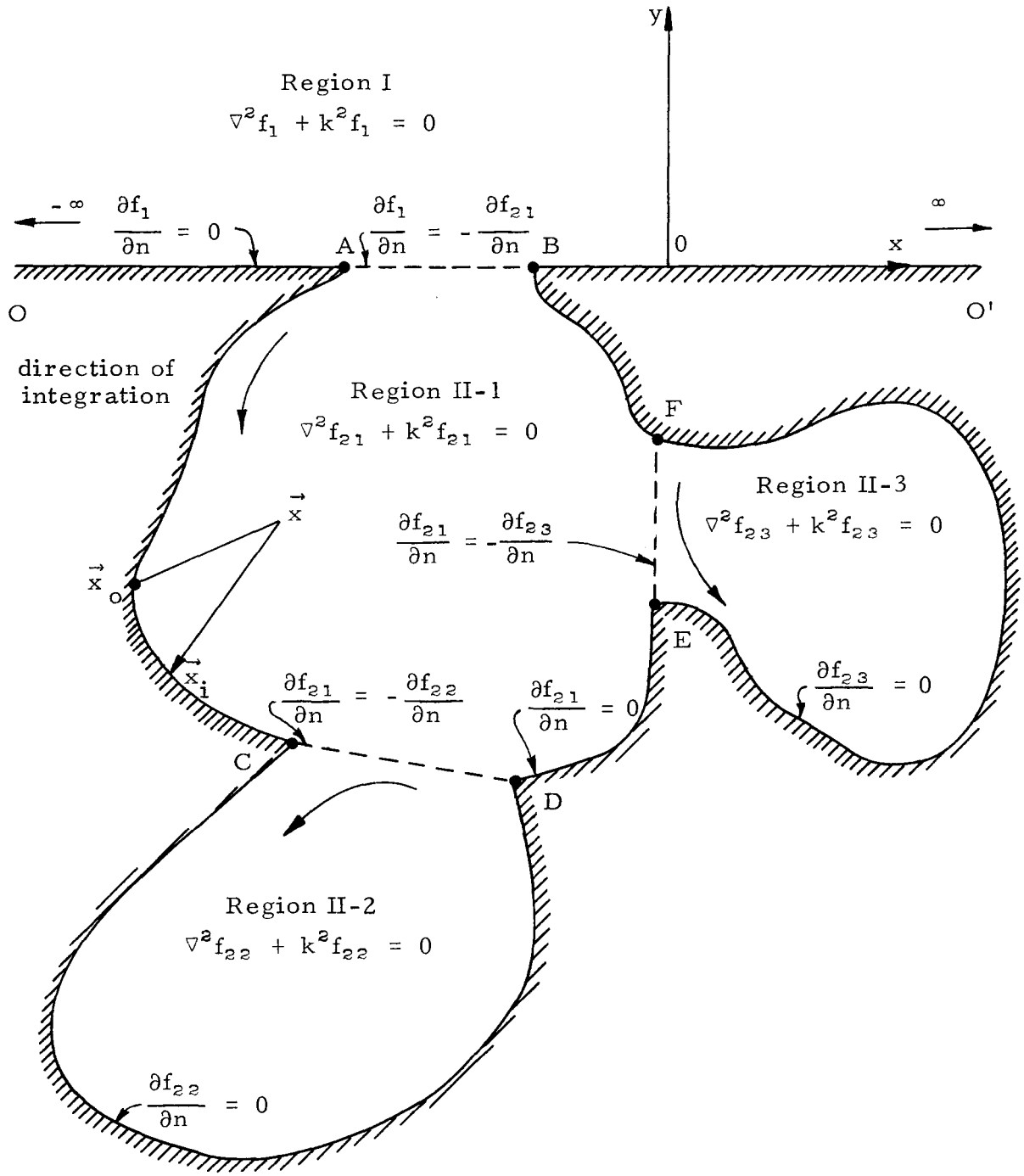

Fig. 2 A Definition Sketch of an Arbitrary Shape Harbor Containing Coupled-Basins

is determined in terms of the unknown value of $\partial f_{22}/\partial n$ (or $\partial f_{23}/\partial n$) at the common boundary between Regions II-1 and II-2 (or between Regions II-1 and II-3). It is noted that the functions of f_1, f_{21}, f_{22}, ... all must satisfy the Helmholtz equation, $\nabla^2 f + k^2 f = 0$, in the respective region.

(iii) At the boundaries between regions the wave functions and the normal derivatives are equated to solve ultimately for the value of the normal derivative at the harbor entrance, $\partial f_1/\partial n$. This is denoted as the "continuity" condition and can be formulated as:

$f_1 = f_{21}$, $\partial f_1/\partial n = -\partial f_{21}/\partial n$ at the entrance to the open-sea (boundary $\overline{AB}$ as shown in Fig. 2),

$f_{21} = f_{22}$, $\partial f_{21}/\partial n = -\partial f_{22}/\partial n$ at the imaginary boundary between Regions II-1 and II-2, (boundary $\overline{CD}$ as shown in Fig. 2),and

$f_{21} = f_{23}$, $\partial f_{21}/\partial n = -\partial f_{23}/\partial n$ at the imaginary boundary between Regions II-1 and II-3 (boundary $\overline{EF}$ as shown in Fig. 2).

This matching procedure is done simultaneously. The negative sign in the normal derivative appearing in the formulated matching conditions is the result of the adapted sign convention that the outward normal to the domain of interest is considered positive.

(iv) Once the normal derivative, $\partial f/\partial n$, at each common boundary is determined, the wave function f within each basin can be evaluated.

This method can be applied to an arbitrary number of coupled interior basins, although the example to be discussed (Fig. 2) only has three obvious interior regions.

2.2.1 The Function f_{21} in Region II-1

The function f_{21} at any position $\vec{x}$ inside Region II-1 can be expressed in terms of the values of f_{21} and $\partial f_{21}/\partial n$ at the boundary of the region by applying Weber's solution of the Helmholtz equation (see Baker and Copson (1950) or Lee (1969)):

$$f_{21}(\vec{x}) = -\frac{i}{4}\int_s \left[f_{21}(\vec{x}_o)\frac{\partial}{\partial n}(H_o^{(1)}(kr)) - H_o^{(1)}(kr)\frac{\partial}{\partial n}(f_{21}(\vec{x}_o)) \right] ds(\vec{x}_o) , \quad (8)$$

where $\vec{x}_o$ is the position vector of a point on the boundary, $H_o^{(1)}(kr)$ is the zero order Hankel function of the first kind, n is directed outward and normal to the boundary, and r is the distance $|\vec{x}-\vec{x}_o|$. The contour integration is to be performed along the boundary of the region moving in a counterclockwise direction.

Eq. 8 shows that the wave function $f_{21}(\vec{x}_o)$ must be known at all boundaries of Region II-1 before the function $f_{21}(\vec{x})$ at any interior point can be obtained. To obtain a solution, the wave function at the boundary, $f_{21}(\vec{x}_o)$, is expressed in terms of the normal derivative of the wave function at the boundaries between Region II-1 and Regions II-2 and II-3 and that at the harbor entrance. This is accomplished by modifying Eq. 8 by allowing the field point $\vec{x}$ to approach a boundary point $\vec{x}_i(x_i, y_i)$ from the interior of

the region (see Fig. 2). Thus, if the boundary is sectionally smooth, Eq. 8 becomes (see Lee, 1969 for this derivation):

$$f_{21}(\vec{x}_i) = -\frac{\lambda}{2}\int_S \left[f_{21}(\vec{x}_o)\frac{\partial}{\partial n}\left[H_o^{(1)}(kr)\right] - H_o^{(1)}(kr)\frac{\partial}{\partial n} f_{21}(\vec{x}_o)\right] ds(\vec{x}_o) , \qquad (9)$$

where $r = |\vec{x}_i - \vec{x}_o|$.

This integral equation (Eq. 9) cannot be solved analytically for an arbitrarily shaped boundary; however, an approximate method can be applied. Eq. 9 is expressed in discrete form by dividing the boundary of Region II-1 into a sufficiently large number of straight line segments (N_1):

$$f_{21}(\vec{x}_i) = -\frac{\lambda}{2}\sum_{\substack{j=1 \\ j\neq i}}^{N_1} \left[f_{21}(\vec{x}_j)\frac{\partial}{\partial n}H_o^{(1)}(kr_{ij}) - H_o^{(1)}(kr_{ij})\frac{\partial}{\partial n} f_{21}(\vec{x}_j)\right]\Delta s_j$$

$$- \frac{\lambda}{2} f_{21}(\vec{x}_i)\int_0^{\frac{1}{2}\Delta s_i} 2\left[-kH_1^{(1)}(kr)\frac{\partial r}{\partial n}\right]dr + \frac{\lambda}{2}\frac{\partial}{\partial n} f_{21}(\vec{x}_j)\int_0^{\frac{1}{2}\Delta s_i} 2H_o^{(1)}(kr)dr, \qquad (10)$$

where $r_{ij} = |\vec{x}_i - \vec{x}_j|$. The notation and the numbering system used for the straight-line segments are shown in Fig. 3. The segments are numbered starting at the right-hand-corner of the harbor entrance and then proceeding counterclockwise. (It should be noted that for the other two regions, Region II-2 and Region II-3, the numbering system starts at the right-hand-corner of the common boundary between regions and then also progresses counterclockwise.)

Eq. 10 can be expressed in matrix form as:

$$\underline{F_1} = -\frac{\lambda}{2}(G_n\underline{F_1} - G\underline{P_1}) , \qquad (11)$$

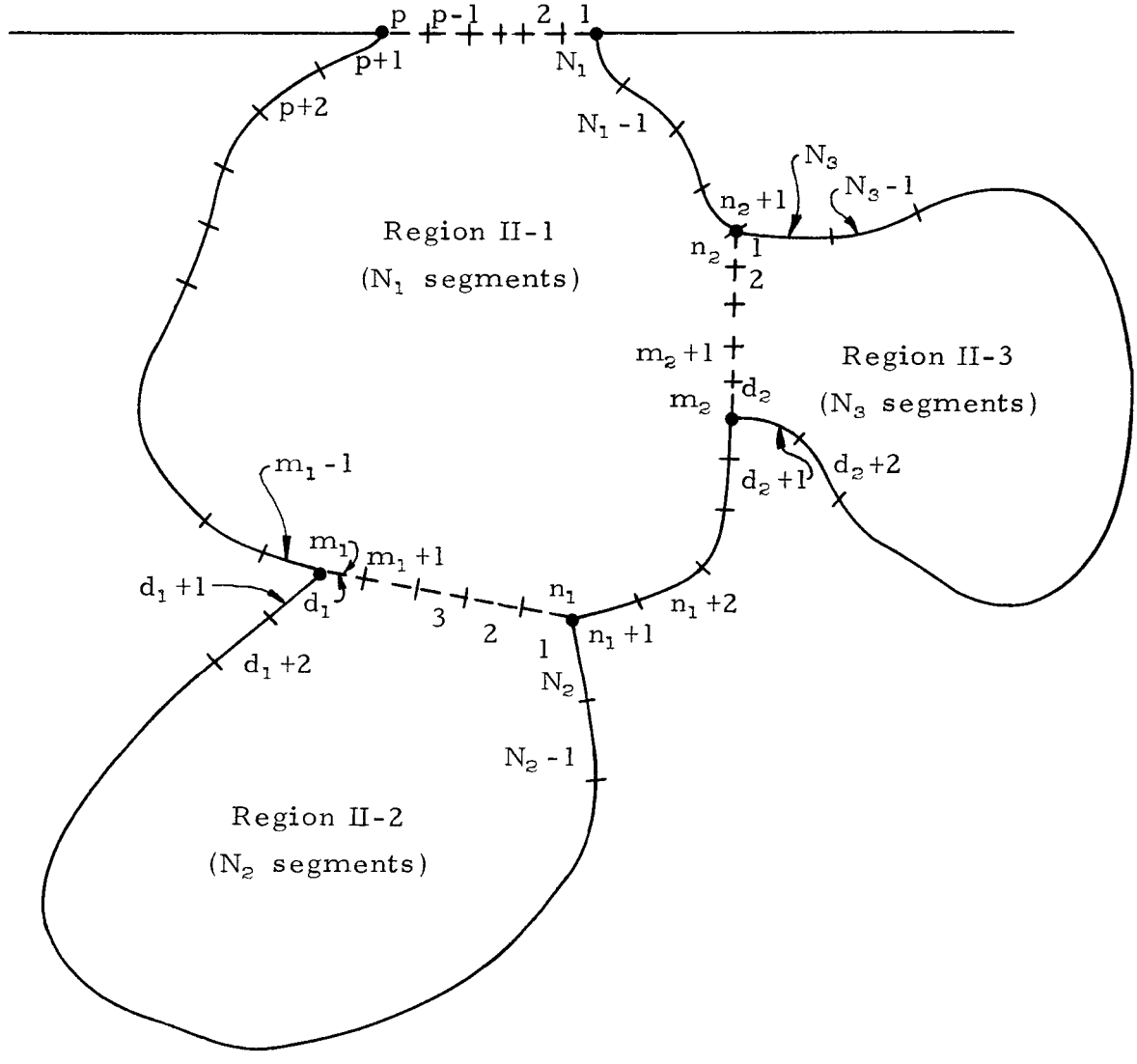

Note: Entrance to the open-sea: p segments

Common boundary between Regions II-1 and II-2: d_1 segments

Common boundary between Regions II-1 and II-3: d_2 segments

Fig. 3 A Definition Sketch of the Harbor Boundary Approximated by Straight-Line Segments

where:

$$\underline{F_1} = f_{21}(\vec{x}_i) \qquad (i = 1, 2, \ldots\ldots N_1), \qquad (12.a)$$

$$\underline{P_1} = \frac{\partial}{\partial n} f_{21}(\vec{x}_i) \qquad (i = 1, 2, \ldots\ldots N_1), \qquad (12.b)$$

$$(G_n)_{ij} = -kH_1^{(1)}(kr_{ij})\left[-\frac{x_i - x_j}{r_{ij}}\left(\frac{\partial y}{\partial s}\right)_j + \frac{y_i - y_j}{r_{ij}}\left(\frac{\partial x}{\partial s}\right)_j\right]\Delta s_j$$

$$(\text{for } i, j = 1, 2, \ldots\ldots N_1;\ i \neq j), \qquad (12.c)$$

$$(G_n)_{ii} = \frac{\lambda}{\pi}\left(\frac{\partial x}{\partial s}\frac{\partial^2 y}{\partial s^2} - \frac{\partial^2 x}{\partial s^2}\frac{\partial y}{\partial s}\right)_i \Delta s_i \quad (\text{for } i = 1, 2, \ldots\ldots N_1), \qquad (12.d)$$

$$(G)_{ij} = H_o^{(1)}(kr_{ij})\Delta s_j \qquad (\text{for } i, j = 1, 2, \ldots\ldots N_1;\ i \neq j), \qquad (12.e)$$

$$(G)_{ii} = \left\{1 + \lambda\frac{2}{\pi}\left[\log\left(\frac{k\Delta s_i}{4}\right) - 0.42278\right]\right\}\Delta s_i$$

$$(\text{for } i = 1, 2, \ldots\ldots N_1). \qquad (12.f)$$

For the derivation of the diagonal elements of the matrices G_n and G (Eqs. 12.d and 12.f), the asymptotic expressions for the Hankel functions are used, i.e., $H_1^{(1)}(kr) \sim -\lambda\frac{2}{\pi}\left(\frac{1}{kr}\right)$ and $H_o^{(1)}(kr) \sim 1 + \lambda\frac{2}{\pi}$ $(\log\frac{kr}{2} + \gamma)$ as $kr \to 0$ ($\gamma = 0.577216$, Euler's constant). Detailed derivations of Eqs. 12 are given by Lee (1969).

The vector $\underline{P_1}$ in Eq. 11 involves the unknown value of $\partial f_{21}/\partial n$ at the harbor entrance and at the common boundaries between Regions II-1 and II-2, and Regions II-1 and II-3. Since the value of $\partial f_{21}/\partial n$ at solid boundary is zero, the vector $\underline{P_1}$ can be expressed as follows:

$$
\underline{P_1} = \begin{pmatrix}
\frac{\partial}{\partial n} f_{21}(\vec{x}_1) \\
\frac{\partial}{\partial n} f_{21}(\vec{x}_2) \\
\vdots \\
\frac{\partial}{\partial n} f_{21}(\vec{x}_p) \\
\vdots \\
\frac{\partial}{\partial n} f_{21}(\vec{x}_{m_1}) \\
\vdots \\
\frac{\partial}{\partial n} f_{21}(\vec{x}_{n_1}) \\
\vdots \\
\frac{\partial}{\partial n} f_{21}(\vec{x}_{m_2}) \\
\vdots \\
\frac{\partial}{\partial n} f_{21}(\vec{x}_{n_2}) \\
\vdots \\
\frac{\partial}{\partial n} f_{21}(\vec{x}_{N_1})
\end{pmatrix} = \begin{pmatrix}
C_1 \\ C_2 \\ \vdots \\ C_p \\ 0 \\ \vdots \\ C_{m_1} \\ \vdots \\ C_{n_1} \\ 0 \\ \vdots \\ C_{m_2} \\ \vdots \\ C_{n_2} \\ 0 \\ \vdots \\ 0
\end{pmatrix} = \begin{pmatrix}
1 & 0 & \cdots & 0 & 0 & \cdots & 0 & 0 & \cdots & 0 \\
0 & 1 & 0 & \cdots & & & & & & \\
0 & 0 & & & & & & & & \\
\vdots & & & & & & & & & \\
 & & & & 1 & & & & & \\
0 & 0 & \cdots & 0 & 0 & & & & & \\
0 & 0 & \cdots & 0 & 0 & & & & & \\
 & & & & & 1 & 0 & 0 & & \\
 & & & & & 0 & & & & \\
 & & & & & & & & & \\
 & & & & & 0 & & 1 & & \\
 & & & & & 0 & 0 & 0 & 0 & \\
 & & & & & & & & 0 & \cdots & 0 \\
 & & & & & & & & 1 & 0 & 0 \\
 & & & & & & & & 0 & & \\
 & & & & & & & & & & \\
 & & & & & & & & 0 & & 1 \\
 & & & & & & & & & & 0 \\
 & & & & & & & & & & \\
 & & & & & & & & & & \\
 & & & & & & & & & & \\
 & & & & & & & & & & \\
0 & \cdots & 0 & 0 & \cdots & 0 & 0 & \cdots & 0 & & 0
\end{pmatrix} \begin{pmatrix}
C_1 \\ C_2 \\ \vdots \\ C_p \\ C_{m_1} \\ \vdots \\ C_{n_1} \\ C_{m_2} \\ \vdots \\ C_{n_2}
\end{pmatrix} \tag{13}
$$

Eq. 13 can be written in a simpler fashion as:

$$\underline{P}_1 = U_1 \cdot \underline{C} \quad , \tag{14}$$

where U_1 is a N_1 x D matrix as defined in Eq. 13, (in which $D = p + d_1 + d_2$ and p is the total number of segments at the entrance to the open-sea, d_1 is the total number of segments at the common boundary between Regions II-1 and II-2, and d_2 is the total number of segments at the common boundary between Regions II-1 and II-3). The vector $\underline{C}$ in Eq. 14 consists of the unknown values of $\partial f_{21}/\partial n$ at the harbor entrance, and at the common boundaries between Regions II-1 and II-2 as well as between Regions II-1 and II-3.

Substituting Eq. 14 into Eq. 11 and rearranging, one obtains:

$$\underline{F}_1 = \left(\frac{i}{2}G_n + I\right)^{-1}\left(\frac{i}{2}GU_1\right)\underline{C}$$

$$= M_1 \underline{C} \quad , \tag{15}$$

where $M_1 = \left(\frac{i}{2}G_n + I\right)^{-1}\left(\frac{i}{2}GU_1\right)$ is a N_1 x D matrix and can be computed directly, since the matrices G_n, G, U_1 are known matrices at this stage of the development (I is an identity matrix).

Eq. 15 shows that the value of $f_{21}(\vec{x}_1)$ on the boundary of Region II-1 can be expressed as a function of the values of $\partial f_{21}/\partial n$ at the harbor entrance and those at the common boundaries. The vector $\underline{C}$, i.e., the normal derivatives, will be determined through a matching procedure which will be described in Subsection 2.2.5.

2.2.2 The Function f_{22} in Region II-2

Following a procedure which is similar to that used in Subsection 2.2.1, the function $f_{22}(\vec{x})$ at any position $\vec{x}$ inside Region II-2 can be expressed in terms of the values of f_{22} and $\partial f_{22}/\partial n$ on the boundary as:

$$f_{22}(\vec{x}) = -\frac{\lambda}{4}\int_S \left[f_{22}(\vec{x}_o)\frac{\partial}{\partial n} H_o^{(1)}(kr) - H_o^{(1)}(kr)\frac{\partial}{\partial n} f_{22}(\vec{x}_o) \right] ds(\vec{x}_o) , \quad (16)$$

where $r = |\vec{x} - \vec{x}_o|$.

By allowing the interior point $\vec{x}$ to approach a boundary point $\vec{x}_i$ the following integral equation (analogous to Eq. 9) is obtained:

$$f_{22}(\vec{x}_i) = -\frac{\lambda}{2}\int_S \left[f_{22}(\vec{x}_o)\frac{\partial}{\partial n} H_o^{(1)}(kr) - H_o^{(1)}(kr)\frac{\partial}{\partial n} f_{22}(\vec{x}_o) \right] ds(\vec{x}_o) , \quad (17)$$

where $r = |\vec{x}_i - \vec{x}_o|$.

The approximate method used in Region II-1 is applied; thus Eq. 17 can be written as a matrix equation:

$$\underline{F}_2 = -\frac{\lambda}{2}\left(G_n \underline{F}_2 - G\underline{P}_2 \right) , \quad (18)$$

where: $\underline{F}_2 = f_{22}(\vec{x}_i)$ $\qquad i = 1, 2, \ldots\ldots, N_2$

and: $\underline{P}_2 = \frac{\partial}{\partial n} f_{22}(\vec{x}_i)$ $\qquad i = 1, 2, \ldots\ldots, N_2$;

the matrices G_n and G are each an $N_2 \times N_2$ matrix. The elements of the matrices G_n and G can be calculated from the same expressions given in Eqs. 12c, 12d, 12e, 12f. Of course, it is realized that the index i or j referred to in these equations represents the boundary points of the Region II-2.

The vector $\underline{P}_2$ involves the unknown values of $\partial f_{22}/\partial n$ at the common boundary between Region II-1 and Region II-2. Thus, using the conditions described at the beginning of Section 2.2 (see iii) the vector $\underline{P}_2$ can be related to the value of $\partial f_{21}/\partial n$ at the common boundary.

The vector $\underline{P}_2$ can thus be written as follows:

$$\underline{P}_2 = \begin{pmatrix} \frac{\partial}{\partial n} f_{22}(\vec{x}_1) \\ \frac{\partial}{\partial n} f_{22}(\vec{x}_2) \\ \vdots \\ \frac{\partial}{\partial n} f_{22}(\vec{x}_{d_1}) \\ \vdots \\ \frac{\partial}{\partial n} f_{22}(\vec{x}_{N_2}) \end{pmatrix} = \begin{pmatrix} -C_{n_1} \\ -C_{n_1-1} \\ \vdots \\ -C_{m_1} \\ 0 \\ 0 \\ \vdots \\ 0 \end{pmatrix} = \begin{pmatrix} 0 & \cdots & 0 & -1 \\ 0 & \cdots & -1 & 0 \\ \vdots & \iddots & & \vdots \\ -1 & \cdots & 0 & 0 \\ 0 & 0 & \cdots & \vdots \\ \vdots & & & \vdots \\ 0 & \cdots & 0 & 0 \end{pmatrix} \begin{pmatrix} C_{m_1} \\ \vdots \\ C_{n_1-1} \\ C_{n_1} \end{pmatrix} = U_2 \cdot \underline{C}_2, \quad (19)$$

where the matrix U_2 is a N_2 x d_1 matrix with the antidiagonal elements of the first d_1 rows and d_1 columns equal to -1 and with the other

elements equal to zero. The vector $\underline{C}_2$ is a d_1 dimensional vector with its elements equal to the $(p+1)^{th}$ element to $(p+d_1)^{th}$ element of the vector $\underline{C}$ defined in Eq. 13.

Substituting Eq. 19 into Eq. 18 and solving for the vector $\underline{F}_2$, the following matrix equation is obtained:

$$\underline{F}_2 = \left(\frac{\lambda}{2} G_n + I\right)^{-1} \left(\frac{\lambda}{2} G U_2\right) \underline{C}_2 = M_2 \underline{C}_2 \tag{20}$$

where M_2 is a $N_2 \times d_1$ matrix which can be calculated directly. It should be stressed that the matrices G_n, G in Eq. 20 are different from the matrices G_n, G in Eq. 15 although the formulas for calculating them are the same. This is because they are based on the boundary points of two different regions. From Eq. 20, the value of f_{22} at the boundary of Region II-2 can be expressed in terms of the unknown value of $\partial f_{21}/\partial n$ at the common boundary between Regions II-1 and II-2.

2.2.3 The Function f_{23} in Region II-3

The value of $f_{23}(\vec{x}_i)$ on the boundary of Region II-3 can be formulated exactly the same way as was done in Eq. 17:

$$f_{23}(\vec{x}_i) = -\frac{\lambda}{2} \int_s \left[f_{23}(\vec{x}_o) \frac{\partial}{\partial n} H_o^{(1)}(kr) - H_o^{(1)}(kr) \frac{\partial}{\partial n} f_{23}(\vec{x}_o) \right] ds(\vec{x}_o), \tag{21}$$

where $r = \left| \vec{x}_i - \vec{x}_o \right|$.

Eq. 21 can then be approximated by the following matrix equation:

$$\underline{F}_3 = -\frac{\lambda}{2} \left(G_n \underline{F}_3 - G \underline{P}_3 \right), \tag{22}$$

where $\underline{F}_3 = f_{23}(\vec{x}_i)$, $i = 1, 2, \ldots N_3$

$\underline{P}_3 = \frac{\partial}{\partial n} f_{23}(\vec{x}_i)$, $i = 1, 2, \ldots N_3$, and

the matrices G_n and G are both $N_3 \times N_3$ matrices, their elements can be calculated by applying the formulas which are given in Eq. 12c, 12d, 12e, and 12f to the boundary points of Regions II-3.

Similar to Eq. 19, the vector $\underline{P}_3$ can be expressed as follows:

$$\underline{P}_3 = \begin{pmatrix} \frac{\partial}{\partial n} f_{23}(\vec{x}_1) \\ \frac{\partial}{\partial n} f_{23}(\vec{x}_2) \\ \vdots \\ \frac{\partial}{\partial n} f_{23}(\vec{x}_{d_2}) \\ \vdots \\ \frac{\partial}{\partial n} f_{23}(\vec{x}_{N_3}) \end{pmatrix} = \begin{pmatrix} -C_{n_2} \\ -C_{n_2-1} \\ \vdots \\ -C_{m_2} \\ 0 \\ \vdots \\ 0 \end{pmatrix} = \begin{pmatrix} 0 & \cdots & -1 \\ \cdots & & 0 \\ \cdots & & \cdots \\ \cdots & & \cdots \\ \cdots & & \cdots \\ -1 & 0 \cdots & 0 \\ 0 & 0 \cdots & 0 \\ \cdots & & \cdots \\ \cdots & & \cdots \\ \cdots & & \cdots \\ 0 & \cdots & 0 \end{pmatrix} \begin{pmatrix} C_{m_2} \\ \vdots \\ C_{n_2} \end{pmatrix} = U_3 \underline{C}_3 , \quad (23$$

where the matrix U_3 is a $N_3 \times d_2$ matrix with the antidiagonal elements of the first d_2 rows and d_2 columns equal to -1 and the remaining elements equal to zero. The vector $\underline{C}_3$ is a d_2 dimensional vector with its elements equal to the last d_2 elements of the vector $\underline{C}$ defined in Eq. 13.

Substituting Eq. 23 into Eq. 22 and solving for the vector $\underline{F}_3$, one obtains:

$$\underline{F}_3 = \left(\frac{i}{2}G_n + I\right)^{-1}\left(\frac{i}{2}GU_3\right)\underline{C}_3 = M_3\underline{C}_3 \quad , \tag{24}$$

where M_3 is a $N_3 \times d_2$ matrix which can be calculated directly.

If the region forming the boundary of the harbor is divided into more than three regions, i.e., more than Region II-1 and II-2, and II-3, an approach similar to that used in Subsections 2.2.2 and 2.2.3 can be used to formulate the solutions for additional regions.

In order to solve for the unknown vector $\underline{C}$ defined in Eq. 13, the solution in Region I (the open-sea region) must first be obtained. This is presented in the following subsection.

2.2.4 The Function f_1 in Region I (Open-Sea)

The solution f_1 of the Helmholtz equation in Region I can be considered as composed of three separate parts: a function f_i representing an incident wave, a function f_r representing a reflected wave considered to occur as if the harbor entrance were closed, and a function f_3 (termed the radiated wave function) representing a correction to f_r due to the presence of the harbor.

Thus the wave amplitude, $\eta_1(x, y;t)$ in Region I can be expressed as:

$$\eta_1(x, y;t) = A_i f_1 e^{-i\sigma t}$$

$$= A_i(f_i + f_r + f_3) e^{-i\sigma t} \quad . \tag{25}$$

The incident wave function, f_i, can be specified in an arbitrary fashion; for example, a periodic incident wave with the wave ray at an angle α to the coastline (x-axis as shown in Fig. 2) can be represented as $f_i(x, y) = \exp[ik(x \cos \alpha + y \sin \alpha)]$. The reflected wave function f_r can be obtained from: $f_r(x, y) = f_i(x\ ,\ -y)$. For the case of a periodic incident wave with wave ray perpendicular to the coastline ($\alpha = 90^o$), the function $f_i(x, y)$ can be represented by $\frac{1}{2}e^{iky}$ (the factor $\frac{1}{2}$ is chosen for convenience). In the following discussion, the incident waves will be considered as normally incident to the coast line; this condition also was treated experimentally in this study.

The major problem in defining the open-sea wave system, i.e., the function f_1, is to evaluate the radiated wave function f_3 which must also satisfy the Helmholtz equation:

$$\frac{\partial^2 f_3}{\partial x^2} + \frac{\partial^2 f_3}{\partial y^2} + k^2 f_3 = 0 \quad , \tag{26}$$

and the following boundary conditions:

(i) $\frac{\partial f_3}{\partial n} = 0$ at the coastline (boundary $\overline{AO}$ and $\overline{BO'}$ of Fig. 2)

(ii) $\frac{\partial f_3}{\partial n} = -\frac{\partial f_{21}}{\partial n}$ at the harbor entrance (boundary $\overline{AB}$ of Fig. 2), and

(iii) $\lim_{r\to\infty} f_3 = 0$, this is called the radiation condition

(where $r = \sqrt{x_2 + y_2}$) .

The function f_3 which satisfies Eq. 26 and the boundary condition is obtained using Weber's solution of the Helmholtz equation:

$$f_3(\vec{x}) = -\frac{i}{4}\int_S [f_3(\vec{x}_o)\frac{\partial}{\partial n} H_o^{(1)}(kr) - H_o^{(1)}(kr)\frac{\partial}{\partial n} f_3(\vec{x}_o)]\, ds(\vec{x}_o) \quad , \tag{27}$$

where $\vec{x}_o$ is the source point $(x_o, 0)$ along the x-axis, $\vec{x}$ is the field point (x, y) in the open-sea region, $r = \sqrt{(x - x_o)^2 + y^2}$, and the integration is to be performed along the x-axis. It should be noted that the fundamental solution $H_o^{(1)}(kr)$ is necessary to satisfy boundary condition (iii) above, i.e., the radiation condition, (see Lee, 1969 for a detailed discussion).

In order to solve for the value of f_3 at the harbor entrance in terms of the value of $\partial f_3/\partial n$ at the entrance, the field point $\vec{x}$ is allowed to approach the x-axis at the point $(x_i, 0)$, thus, from Eq. 27 one obtains the following integral equation (similar to Eq. 9):

$$f_3(x_i, 0) = -\frac{\lambda}{2}\int_S \left[f_3(x_o, 0)\frac{\partial}{\partial n} H_o^{(1)}(kr) - H_o^{(1)}(kr)\frac{\partial}{\partial n} f_3(x_o, 0)\right] ds(x_o, 0) \quad , \quad (28)$$

where $r = |x_i - x_o|$.

Substituting the boundary conditions associated with Eq. 26 into Eq. 28, and expanding the terms inside the integral, the following simplified equation results:

$$f_3(x_i, 0) = -\frac{\lambda}{2}\int_{\overline{AB}} H_o^{(1)}(k|x_i - x_o|)\frac{\partial}{\partial n}\left[f_{21}(x_o, 0)\right]dx_o$$

$$\approx -\frac{\lambda}{2}\sum_{\substack{j=1 \\ j\neq i}}^{p} H_o^{(1)}(k|x_i - x_j|)\, C_j \Delta s_j - \frac{\lambda}{2} C_i \int_o^{\frac{1}{2}\Delta s_i} 2\left[1 + \lambda\frac{2}{\pi}\left(\log\left(\frac{kr}{2}\right) + \gamma\right)\right]dr \quad , \quad (29)$$

where x_i and x_j are the mid-points of the i^{th} and j^{th} segments of the harbor entrance respectively, Δs_j is the length of the j^{th} segment, the term C_j in Eq. 29 is the value of $\partial f_{21}/\partial n$ at the mid-point of the j^{th} entrance segment,

and p is, as mentioned before, the total number of segments into which the entrance is divided. (The symbol γ in Eq. 29 is referred to as Euler's constant which is equal to 0.577216.)

Once the value of $f_3(x_i, 0)$ at the entrance is determined from Eq. 29, the value of $f_1(x_i, 0)$ at the harbor entrance can be obtained by adding the contribution of f_i and f_r to f_3; thus:

$$f_1(\vec{x}_i) = 1 + \sum_{j=1}^{p} H_{ij} C_j \tag{30}$$

for $i = 1, 2, \ldots p$. The first term on the right-hand side of Eq. 30 represents the incident plus reflected wave if the entrance is closed. This amplitude is unity since for convenience the amplitude of the incident wave was chosen as one-half. The matrix H_{ij} in Eq. 30 represents the contribution of the function f_3 and it is rewritten in matrix form from Eq. 29, where $H_{ij} = -\frac{\lambda}{2} H_o^{(1)}(kr_{ij})\Delta s_j$ for $i, j = 1, 2, \ldots p$; $i \neq j$, and $H_{ii} = -\frac{\lambda}{2}\left[1 + \lambda\frac{2}{\pi}\left(\log\left(\frac{k\Delta s}{4}\right) - 0.42278\right)\right]\Delta s_i$, for $i = 1, 2, \ldots p$.

At this stage of the development the solution of the Helmholtz equation: $\nabla^2 f + k^2 f = 0$, for each region has been formulated in terms of the value of the unknown derivative $\partial f/\partial n$ at each common boundary between interior regions and at the harbor entrance. In the next subsection, a matching procedure is discussed which results in a solution for the harbor response for the individual basins from these solutions.

2.2.5 Matching Solutions at the Harbor Entrance and the Common Boundaries Between Regions

The solutions for the wave function, f, for the various regions are summarized as follows:

(a) At the harbor entrance between Region I and Region II-1:

$$f_1(\vec{x}_i) = 1 + \sum_{j=1}^{p} H_{ij} C_j \qquad \begin{matrix} i = 1,2, \ldots p \\ j = 1,2, \ldots p \end{matrix} \tag{31a}$$

$$f_{21}(\vec{x}_i) = \sum_{j=1}^{D} (M_1)_{ij} C_j \qquad \begin{matrix} i = 1,2, \ldots p \\ j = 1,2, \ldots p, p+1, \ldots D \end{matrix} \tag{31b}$$

(where $D = p + d_1 + d_2$)

(b) At the common boundary between Regions II-1 and II-2:

$$f_{21}(\vec{x}_i) = \sum_{j=1}^{D} (M_1)_{ij} C_j \qquad \begin{matrix} i = m_1, m_1+1, \ldots n_1 \\ j = 1,2, \ldots D \end{matrix} \tag{31c}$$

$$f_{22}(\vec{x}_i) = \sum_{j=1}^{d_1} (M_2)_{ij} (C_2)_j , \qquad \begin{matrix} i = d_1, d_1-1, d_1-2, \ldots 2, 1 \\ j = 1,2, \ldots d_1 \end{matrix} \tag{31d}$$

(c) At the common boundary between Regions II-1 and II-3:

$$f_{21}(\vec{x}_i) = \sum_{j=1}^{D} (M_1)_{ij} C_j , \qquad \begin{matrix} i = m_2, m_2+1, \ldots n_2 \\ j = 1,2, \ldots D \end{matrix} \tag{31e}$$

$$f_{23}(\vec{x}_i) = \sum_{j=1}^{d_2} (M_3)_{ij} (C_3)_j \qquad \begin{matrix} i = d_2, d_2-1, d_2-2, \ldots 2, 1 \\ j = 1,2, \ldots d_2 \end{matrix} \tag{31f}$$

Because of the sign convention used in the contour integration (the counterclockwise direction is positive in each region) the rows of the matrix M_2 in Eq. 31d are interchanged so that the equation for every segment will correspond to that of Eq. 31c. Similarly, the rows of the matrix M_3 in

in Eq. 31f are interchanged so that they will correspond to those of Eq. 31e.

The matching procedure consists of equating Eq. 31a to Eq. 31b, Eq. 31c to Eq. 31d, and Eq. 31e to Eq. 31f simultaneously. Thus, one obtains the following matrix equation:

$$M_A \underline{C} = \underline{S} + H_A \underline{C} \tag{32}$$

where:

1) M_A is a D x D matrix consisting the first p rows, the $m_1{}^{th}$ row to $n_1{}^{th}$ row, and the $m_2{}^{th}$ row to $n_2{}^{th}$ row of the matrix M_1 whose elements are defined in Eqs. 12, 14, and 15:

$$M_A = \begin{pmatrix} (M_1)_{11} & (M_1)_{12} & \cdots & (M_1)_{1D} \\ \vdots & \vdots & \cdots & \vdots \\ \vdots & \vdots & \cdots & \vdots \\ (M_1)_{p1} & (M_1)_{p2} & \cdots & (M_1)_{pD} \\ (M_1)_{m_1 1} & (M_1)_{m_1 2} & \cdots & (M_1)_{m_1 D} \\ \vdots & \vdots & \cdots & \vdots \\ (M_1)_{n_1 1} & (M_1)_{n_1 2} & \cdots & (M_1)_{n_1 D} \\ (M_1)_{m_2 1} & (M_1)_{m_2 2} & \cdots & (M_1)_{m_2 D} \\ \vdots & \vdots & \cdots & \\ (M_1)_{n_2 1} & (M_1)_{n_2 2} & \cdots & (M_1)_{n_2 D} \end{pmatrix}$$

2) $\underline{C}$ is a D x 1 column vector consisting of the values of $\partial f_{21}/\partial n$ at every segment representing the harbor entrance and the common boundaries between regions and is defined as:

$$\left[C_1 \; C_2 \; . \; . \; C_p \; C_{m_1} \; . \; C_{n_1} \; C_{m_2} \; . \; C_{n_2} \right]$$

3) $\underline{S}$ is a D x 1 column vector with its first p elements representing the value of the incident wave plus the reflected wave at the harbor entrance, these are equal to unity, and with the other elements equal to zero. Thus, it is defined as: [1 1 . . 1 0 . . . 0]

4) H_A is a D x D matrix defined as:

$$H_A = \begin{pmatrix}
H_{11} & H_{12} & . & H_{1p} & 0 & . & 0 & 0 & . & 0 \\
H_{21} & H_{22} & . & H_{2p} & . & . & . & . & . & . \\
. & . & . & . & . & . & . & . & . & . \\
H_{p1} & H_{p2} & . & H_{pp} & 0 & . & 0 & 0 & . & 0 \\
0 & . & . & 0 & (M_2)_{d_1 1} & . & (M_2)_{d_1 d_1} & 0 & . & 0 \\
. & . & . & . & . & . & . & . & . & . \\
0 & . & . & 0 & (M_2)_{11} & . & (M_2)_{1 d_1} & 0 & . & 0 \\
0 & . & . & 0 & 0 & . & 0 & (M_3)_{d_2 1} & . & (M_3)_{d_2 d_2} \\
. & . & . & . & . & . & . & . & . & . \\
0 & . & . & 0 & 0 & . & 0 & (M_3)_{11} & . & (M_3)_{1 d_2}
\end{pmatrix}$$

Thus, Eq. 32 can be solved for the unknown vector $\underline{C}$ as follows:

$$\underline{C} = \left(M_A - H_A \right)^{-1} \cdot \underline{S} \tag{33}$$

The unknown value of $\partial f_{21} / \partial n$ at the harbor entrance is equal to the first p elements of the vector $\underline{C}$, the value of $\partial f_{21} / \partial n$ at the common boundary between Regions II-1 and II-2 is equal to the next d_1 elements of the vector $\underline{C}$, and the value of $\partial f_{21} / \partial n$ at the common boundary between Regions II-1 and II-3 is equal to the last d_2 elements of the vector $\underline{C}$.

Once the vector $\underline{C}$ is obtained from Eq. 33, the value of the wave function at the boundary of each region can be determined. The wave function f_{21} at the boundary of Region II-1 can be obtained from Eq. 15, while the value of f_{22} at the boundary of Region II-2 can be obtained from Eq. 20 and f_{23} at the boundary of Region II-3 can be obtained from Eq. 24.

The value of wave function f at any position within each region can be determined after the vector $\underline{C}$ and the wave function f at the boundary of each region are evaluated. For example, for an arbitrarily chosen point $\vec{x}$ in Region II-1 the value of $f_{21}(\vec{x})$ can be calculated by the following discrete form of Eq. 8:

$$f_{21}(\vec{x}) = -\frac{\lambda}{4}\left\{\sum_{j=1}^{N_1} f_{21}(\vec{x}_j)\left[-kH_1^{(1)}(kr)\frac{\partial r}{\partial n}\right]\Delta s_j - \sum_{j=1}^{D} H_o^{(1)}(kr)C_j\Delta s_j\right\} \tag{34}$$

where $\vec{x}_j$ is the mid-point of the j^{th} boundary segment in Region II-1, and $r = |\vec{x} - \vec{x}_j|$. In an analogous manner, similar expressions can be used to determine the wave functions in Regions II-2 and II-3.

The response of a harbor to incident waves is described by a parameter called the "amplification factor". This is the ratio of the wave amplitude $\eta_{2i}(x, y)$ at any position (x, y) inside the harbor (i = 1 refers to Region II-1, i = 2 refers to Region II-2, and i = 3 refers to Region II-3), to the sum of the incident plus the reflected wave amplitude at the coastline with the harbor entrance closed:

$$R = \frac{|\eta_{2i}(x, y;t)|}{|A_i(f_i + f_r)e^{-\lambda\sigma t}|} = \frac{|A_i f_{2i}(x, y)e^{-\lambda\sigma t}|}{|A_i \cdot 1 \cdot e^{-\lambda\sigma t}|} = |f_{2i}(x, y)| \tag{35}$$

The value of f_{21}, f_{22}, or f_{23} is a complex number; therefore, in computing the amplification factor, R, the absolute value must be taken.

CHAPTER 3

EXPERIMENTAL APPARATUS & PROCEDURES

In general the experimental equipment used for this study is described by Lee (1969) and only will be summarized here. An overall view of the experimental equipment is shown in Fig. 4.

The wave basin used is 1 ft 9 in. deep, 15 ft 5 in. wide, and 31 ft 5 in. long with vertical walls of 3/4 in. marine plywood and a floor constructed of 1 in. marine plywood. The bottom of the wave basin is horizontal to within at least ±0.02 in. and has been treated with a layer of polyester resin approximately 1/8 in. thick to provide a water-tight seal.

The wave generator is of the pendulum type 11 ft 8 in. long and 2 ft high located at one end of the basin, and is designed to operate either as a paddle- or piston-type wave generator; for a detailed description, the interested reader is referred to Raichlen (1965). The wave generator is driven by two arms connected to independent cranks which in turn are connected through a pulley system to a 1-1/2 hp variable speed motor. The cranks allow for a maximum stroke of ±6 in. and they can be adjusted to within 0.001 in. of each other. Wave periods ranging from 0.34 sec to 3.8 sec can be obtained with this system.

The wave period is determined by measuring the rotational speed of one crank of the wave generator. This is accomplished by attaching a disc with 360 evenly spaced holes arranged at its outer edge to the

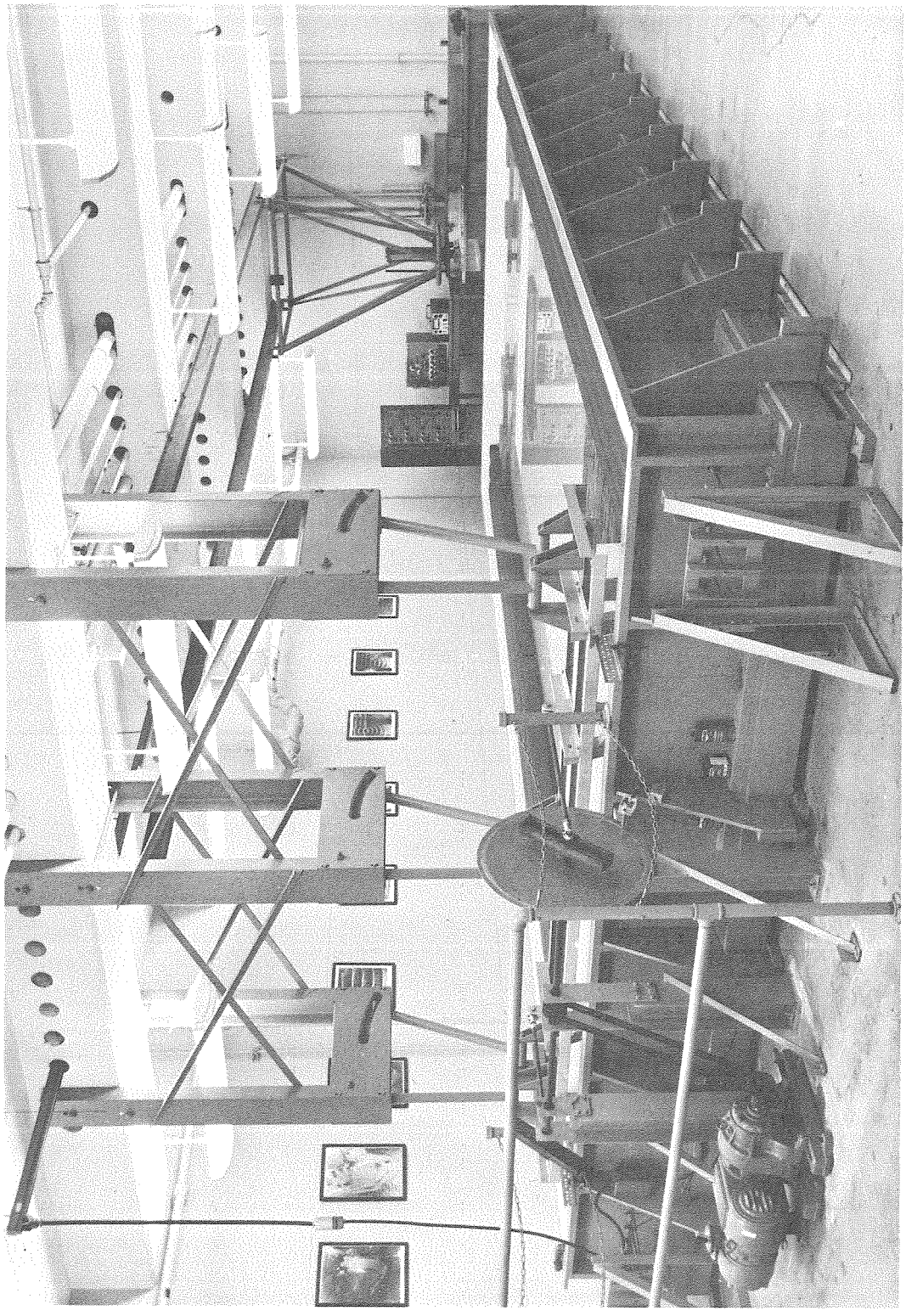

Fig. 4 An Over-All View of the Experimental Equipment

crank and then counting the number of holes passing a light-photocell arrangement in a fixed period of time with an electronic counter. Wave amplitudes are measured electronically using resistance wave gages and an oscillograph recorder with the gages calibrated before and after an experiment (a duration of approximately one hour). A calibration curve representing an average over the duration of an experiment is used in reducing the experimental data; generally these curves are linear over the range of wave heights used and show very little change during an experiment (see Lee (1969)).

In order to simulate the open-sea in the laboratory two wave energy dissipators are used around the boundaries of the basin: a wave filter placed in front of the wave generator, and wave absorbers located along the side-walls of the wave basin. The wave filter is 11 ft 9 in. long, 1 ft 4 in. high and 5 ft thick in the direction of wave propagation. It is constructed of 70 layers of galvanized iron wire screen with each screen spaced 0.8 in. apart. The wire diameter of the screens is 0.011 in. with 18 wires per inch in one direction and 14 wires per inch in the other. The wave absorbers, placed along the side-walls of the basin are each 1 ft 6 in. high, 1 ft 10 in. thick, and 30 ft long and consist of 50 layers of the same galvanized iron screen as used in the wave filter with a 3/8 in. space between screens. These wave absorbers are supported by structural frames outside the wave basin; one of these structural frames can be seen in Fig. 4. Sodium dichromate ($Na_2 Cr_2 O_7$) was added to the water in the basin to control corrosion of the galvanized wire screens. This additive was used in a concentration of 500 ppm (by weight) with the pH of the

water maintained between 6.2 to 6.5 to insure its proper functioning as a corrosion inhibitor.

The wave filter and wave absorbers used have reflection coefficients which are less than 20% for the experimental range of depths, wave heights, and wave periods. This means that the amplitude of a wave which passes through the absorber (or filter) and reflects from the wall (or wave machine) and then passes back through the absorber (or filter) to the main wave basin is reduced by more than 80%. A more detailed discussion of the characteristics of the dissipation system is given by Lee (1969).

Experiments were conducted in a well defined coupled harbor to test the theory which is described in Chapter 2. The harbor consisted of two circular basins with the same diameter connected together on the axis which is perpendicular to the "coastline". The first basin of the harbor had a 60° opening which communicated directly with the "open-sea" and a 10° opening diametrically opposite connected to the 10° opening of the second basin of the harbor. Each harbor was 1 ft 6 in. in diameter and 1 ft 3 in. high. The model used is shown in the photograph presented in Fig. 5. It is seen in Fig. 5 that the two cylinders which make up the harbor are connected top and bottom to lucite reinforcing plates which were used to keep the basins circular. The edges of the entrance between the two basins and at the "open-sea" do not have a zero thickness as assumed in the theory, but due to construction limitations this thickness was approximately 1/2 in. for the former and 1/4 in. for the latter. The two vertical lucite plates to either side of the main harbor entrance shown in Fig. 5 fitted into the existing end wall of the basin to form a perfectly

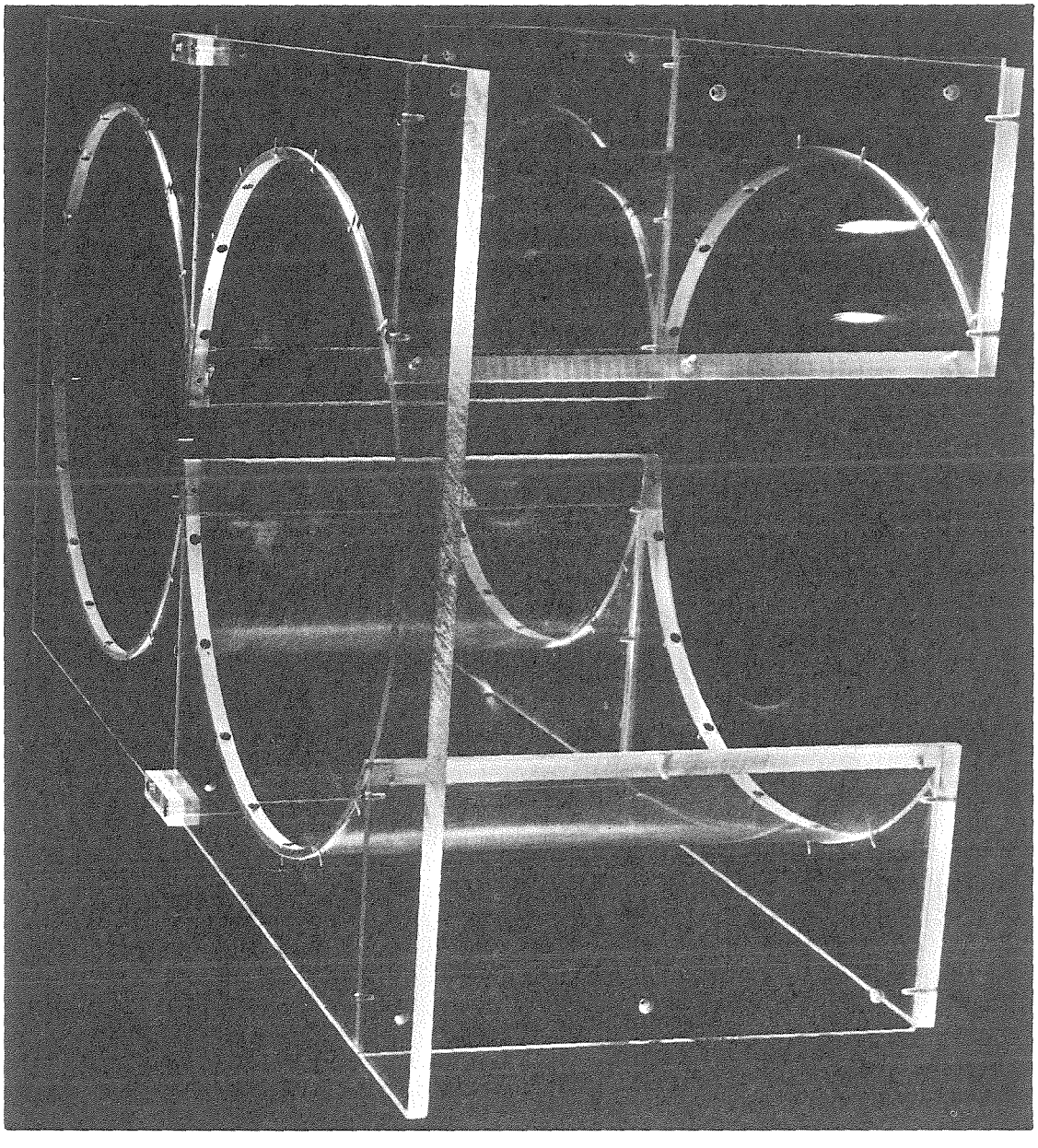

Fig. 5 Photograph of the Model of the Coupled Circular Basins

reflecting "coastline"; the "coastline" is located 27 ft 6 in. from and parallel to the wave paddle. The water depth in the basin for all experiments was 1.0 ft.

CHAPTER 4

PRESENTATION AND DISCUSSION OF RESULTS

Theoretical results obtained using the method developed in Chapter 2 are presented here along with some limited experimental results. The effect of interconnected basins in a harbor on the overall harbor response is discussed relative to the response of the individual basins.

4.1 A MODEL OF THE EAST AND WEST BASINS OF LONG BEACH HARBOR

A model of the East and West Basins of Long Beach Harbor was studied previously, both theoretically and experimentally, by Lee (1969). The theoretical results of that study were obtained by dividing the domain of interest into two regions: the open-sea region (Region I) and the harbor domain (Region II). The boundary of Region II was divided into 75 segments (with two segments for the harbor entrance) to obtain a numerical solution; this subdivision is shown in Fig. 6. (The theory presented in Lee (1969) was referred to therein as the "arbitrary-shape harbor theory"; herein it will be referred to as the "single-basin theory".)

The validity and accuracy of the coupled-basins theory, presented in Chapter 2, was tested initially using the model of Long Beach Harbor which, as can be seen in Fig. 6, is essentially composed of two basins (the East and the West Basins). For the analytical model the harbor was

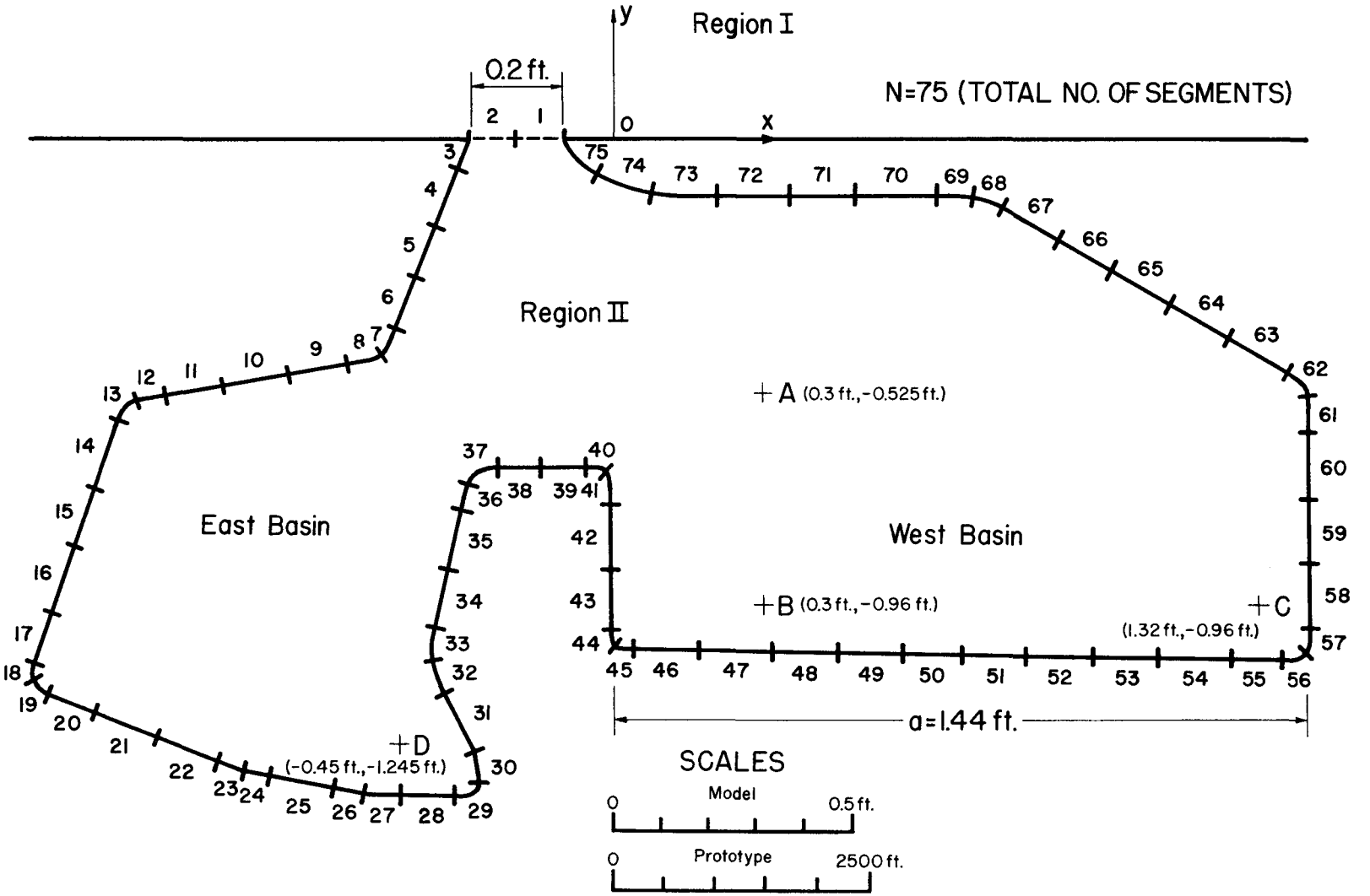

Fig. 6 Configuration Used in Single Basin Theory for Analytical Model of East and West Basins of Long Beach Harbor California

divided at the junction of the East and West Basins; this division is shown in Fig. 7. The boundary of Region II-1 (the West Basin) is divided into 50 segments with two segments for the entrance to the open-sea, and four segments for the common boundary between the East and West Basins. The boundary of Region II-2 (the East Basin), shown in Fig. 7, is divided into 34 segments including four segments for the common boundary between Regions II-1 and II-2.

Response curves have been obtained using the coupled-basins theory and are presented in Figs. 8 through 11 for four different locations in Long Beach Harbor. The ordinate is the ratio of the wave amplitude at the particular location to the open-sea standing wave amplitude (Eq. 35) and the abscissa is the product of the wave number and a characteristic harbor length, a, (in the model a = 1.44 ft, in the prototype a = 6768 ft). In these figures, both the experimental results and the theoretical results for the harbor treated as one basin are presented for comparison (see Lee (1969)). Figs. 8 through 11 show that the present results agree well with the previous single-basin theory throughout the full range of ka which was investigated. Only small differences between the theories can be seen in the response at resonance which is the region where both theories are somewhat unreliable because both theories neglect viscous and non-linear effects. Actually the maximum difference between the two theoretical results is less than 3%. Since both theoretical curves agree well with each other and with the experimental results at all four locations, it can be concluded that the wave amplitude distribution within the harbor is also predicted correctly by the coupled-basins theory.

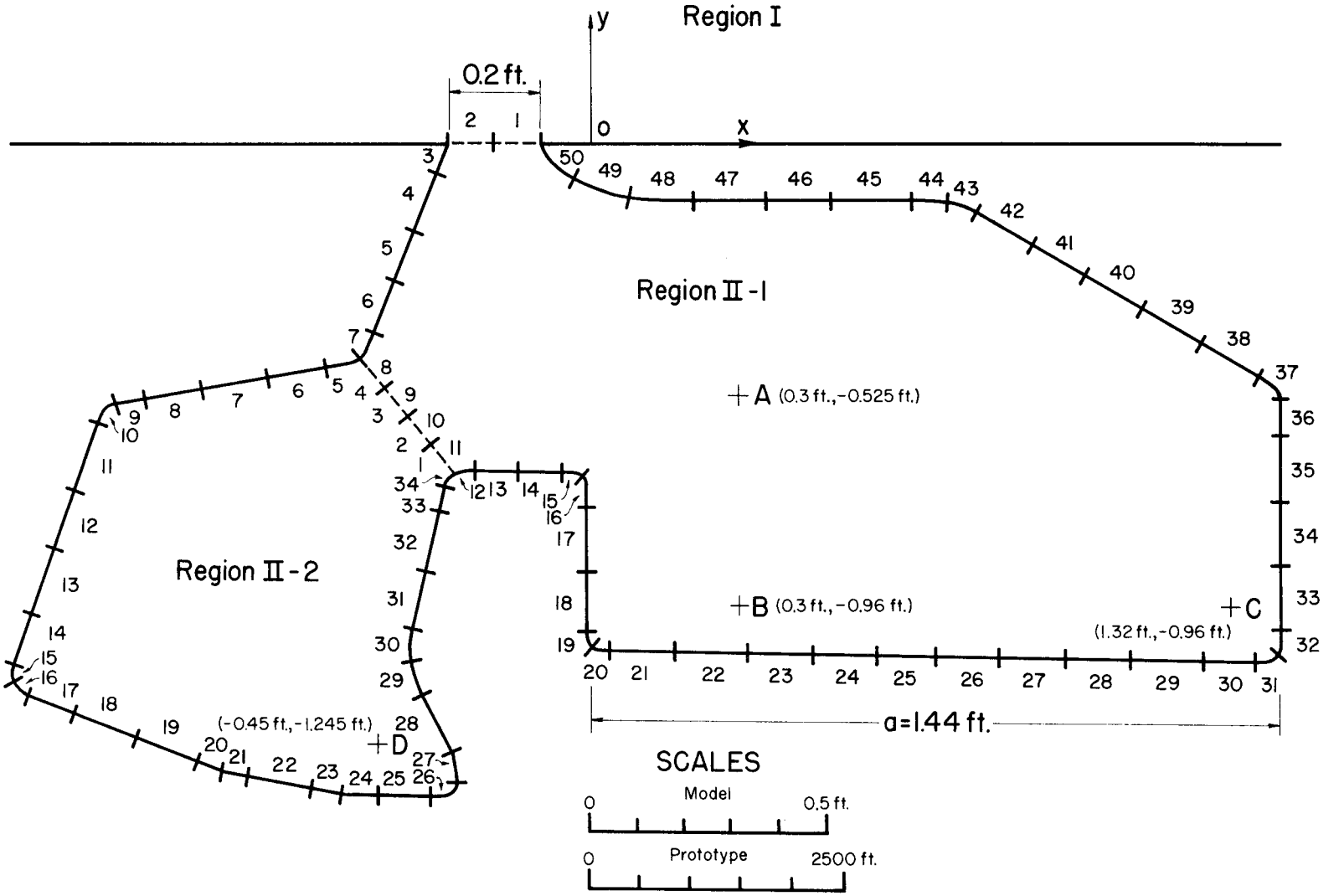

Fig. 7 Configuration Used in Coupled-Basins Theory for Analytical Model of East and West Basins of Long Beach Harbor, California

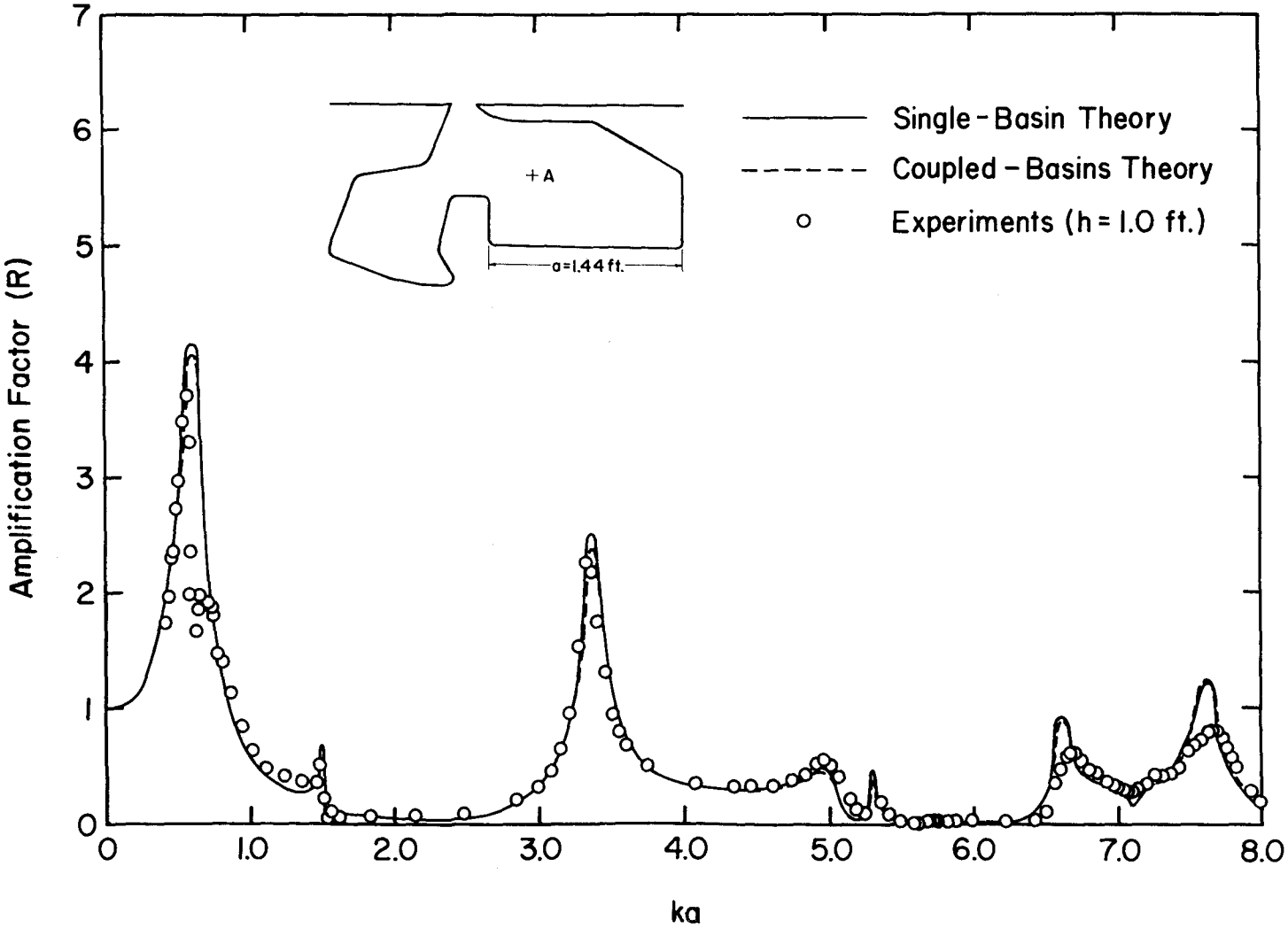

Fig. 8 Response Curve at Position A of the Long Beach Harbor Model

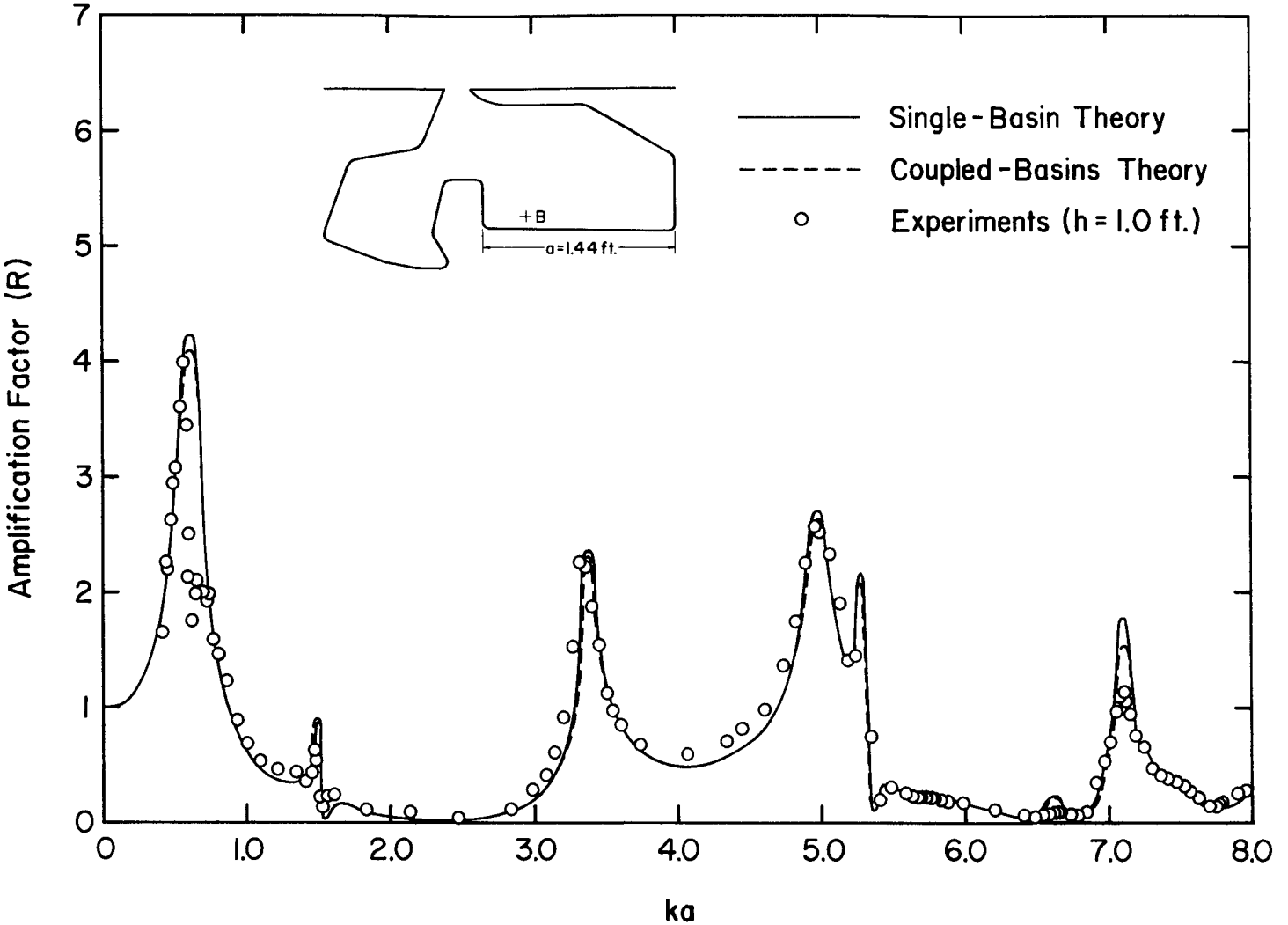

Fig. 9 Response Curve at Position B of the Long Beach Harbor Model

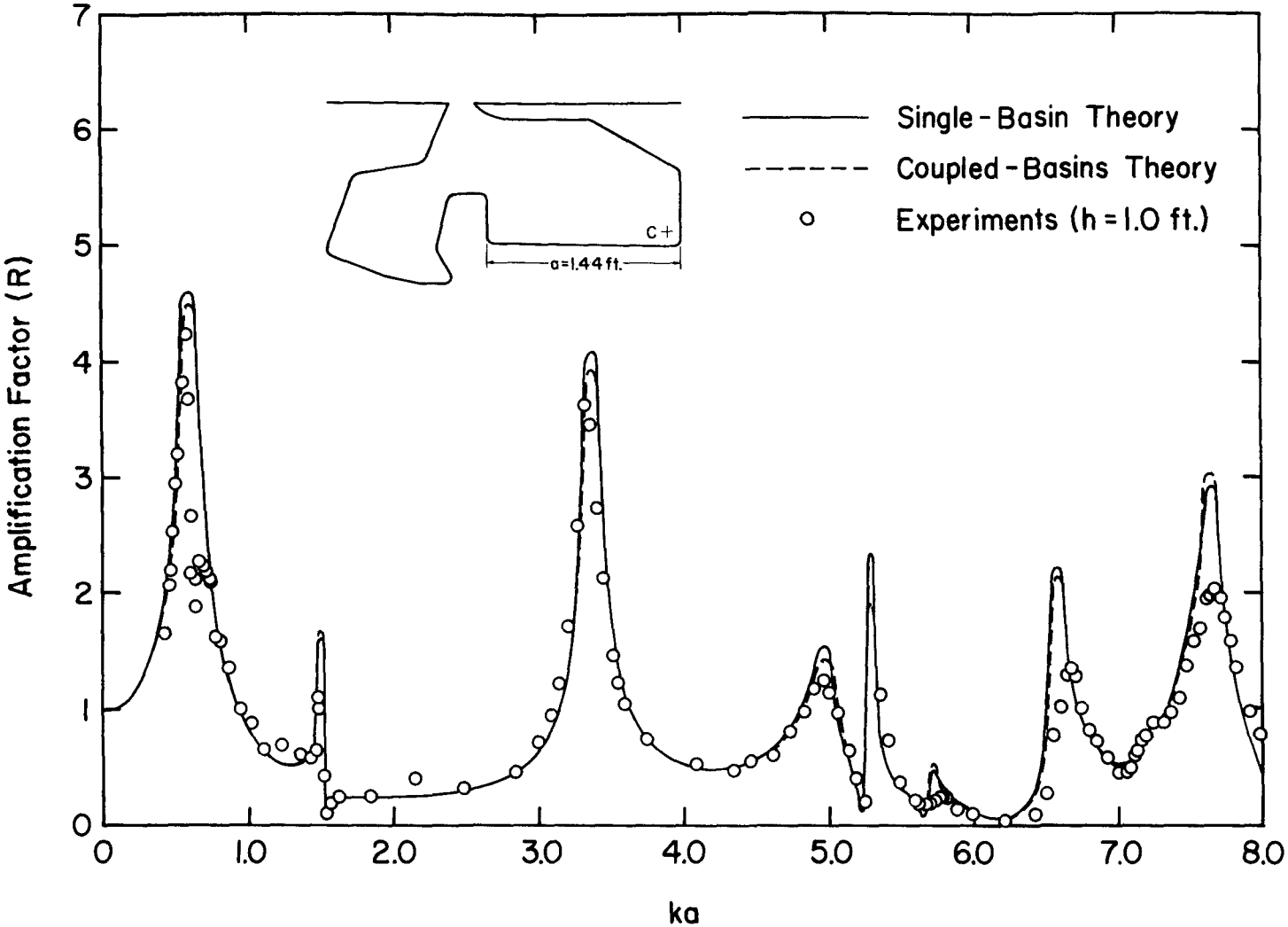

Fig. 10 Response Curve at Position C of the Long Beach Harbor Model

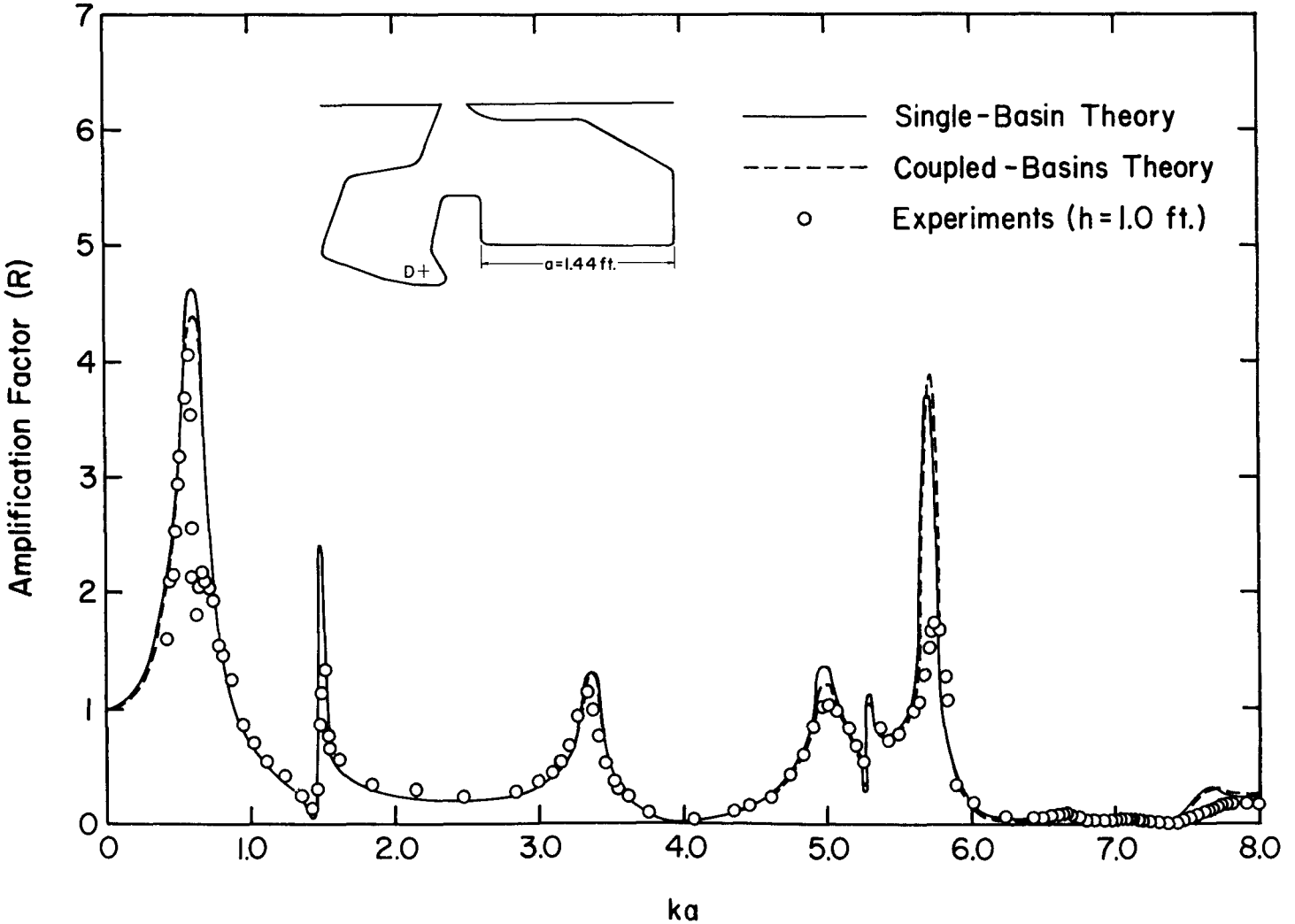

Fig. 11 Response Curve at Position D of the Long Beach Harbor Model

4.2 THE RESPONSE OF A CIRCULAR BASIN WITH A 10^{o} OPENING CONNECTED TO A CIRCULAR HARBOR WITH A 60^{o} OPENING

Theoretical and experimental results have been obtained for a coupled-harbor consisting of two circular basins: the first with a 10^{o} opening connected to a second basin which has a 60^{o} entrance which opens directly on the open-sea (see Fig. 5). The response curves for two positions in each of the basins are presented in Figs. 12 through 15 where the ordinate is the amplification factor and the abscissa is the wave number parameter ka (the product of the wave number and the harbor radius). In the experiments the radius of each circular basin is 0.75 ft and the depth of the water in both the harbor and the "open-sea" was 1.0 ft.

The boundary of Basin A was subdivided, in applying the coupled-basins theory, into 38 segments with six of these at the harbor entrance and two at the common boundary between Basins A and B. Basin B was divided into 37 segments including two segments at the boundary between Basins A and B.

Figs. 12 through 15 show that the theoretical results agree reasonably well with the experiments except near resonance for the range of ka covered. Near the various resonant modes of oscillation the amplification predicted by theory is greater than that measured experimentally; however, the resonant frequencies are accurately predicted by the theory. The differences in amplification mentioned are probably due to viscous dissipation which affects the experiments but does not enter the inviscid

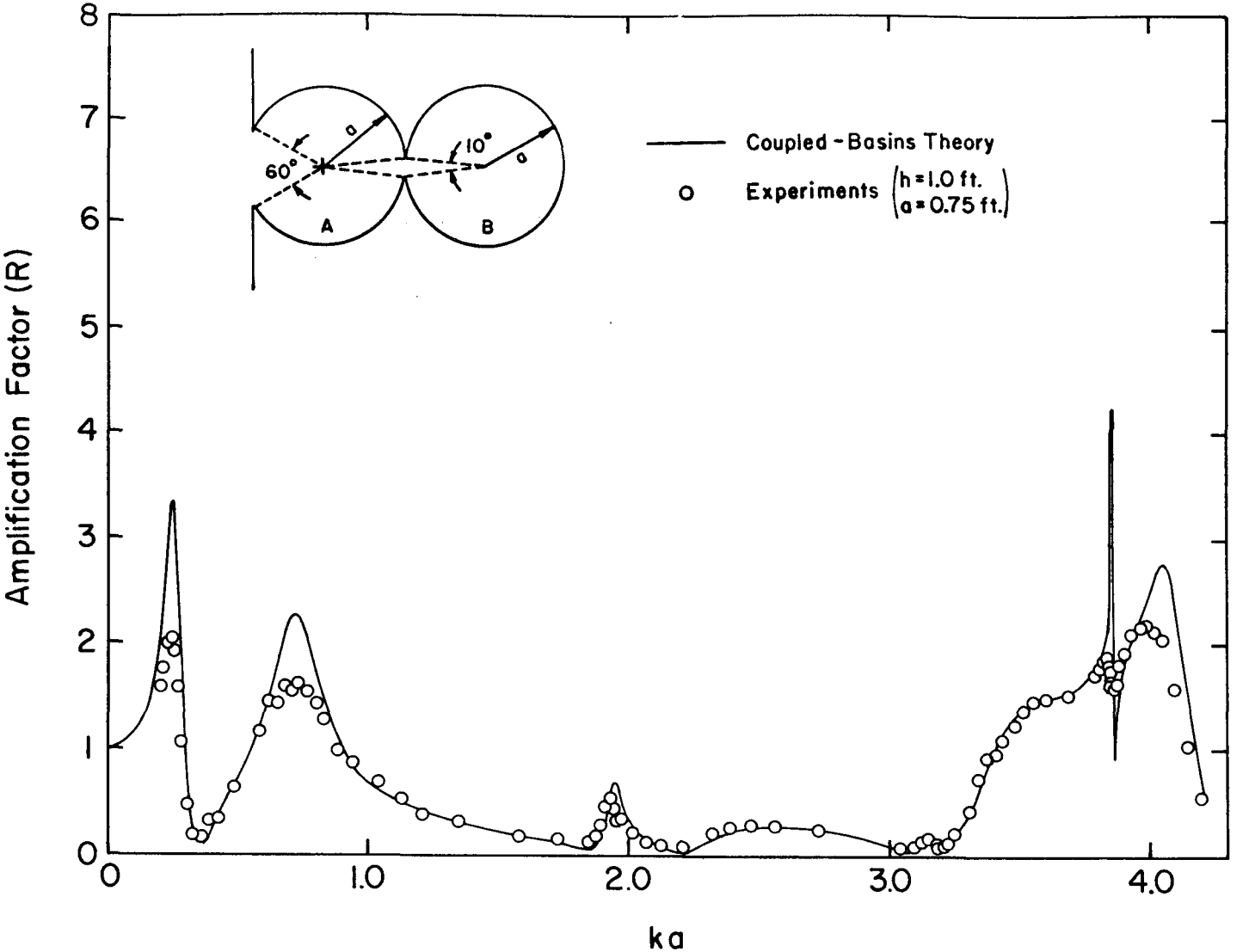

Fig. 12 Response Curve at Center of Basin A for Two Coupled-Circular Harbors ($\theta_A = 60^o$, $\theta_B = 10^o$, $a_A = a_B$)

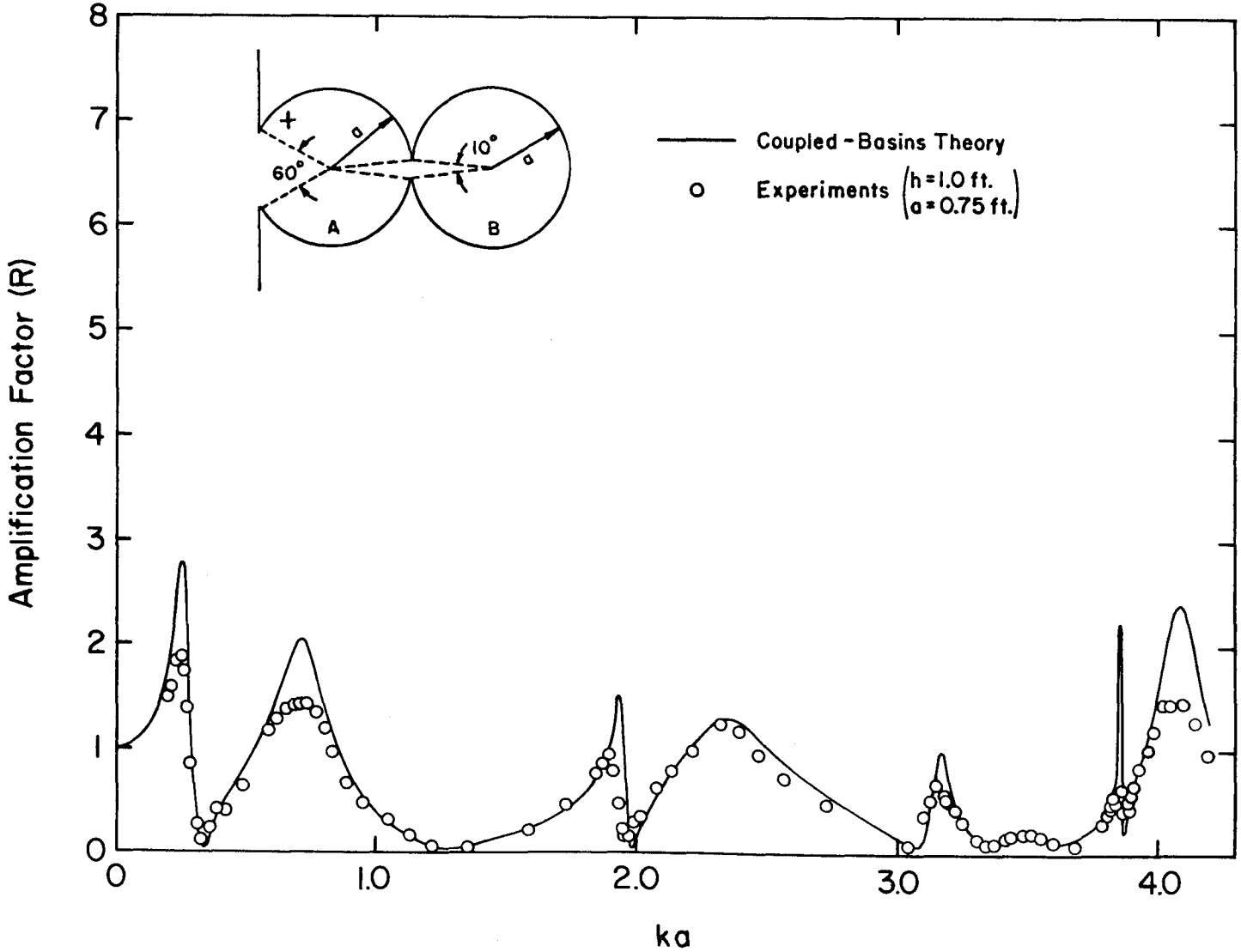

Fig. 13 Response Curve at r/a = 0.934, $\theta = 45^{\circ}$ in Basin A for Two Coupled Circular Harbors ($\theta_A = 60^{\circ}$, $\theta_B = 10^{\circ}$, $a_A = a_B$)

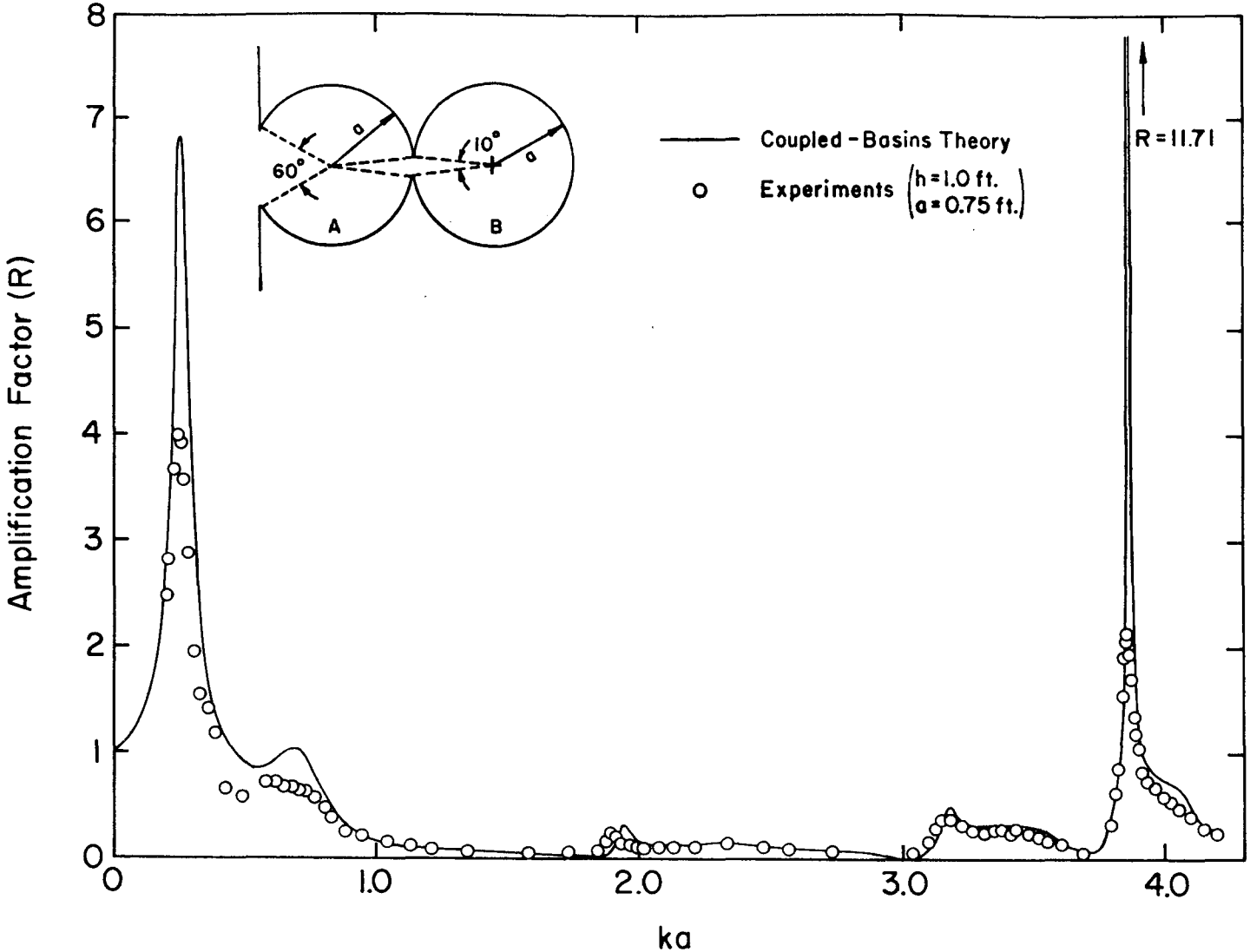

Fig. 14 Response Curve at Center of Basin B for Two Coupled-Circular Harbors ($\theta_A = 60^o$, $\theta_B = 10^o$, $a_A = a_B$)

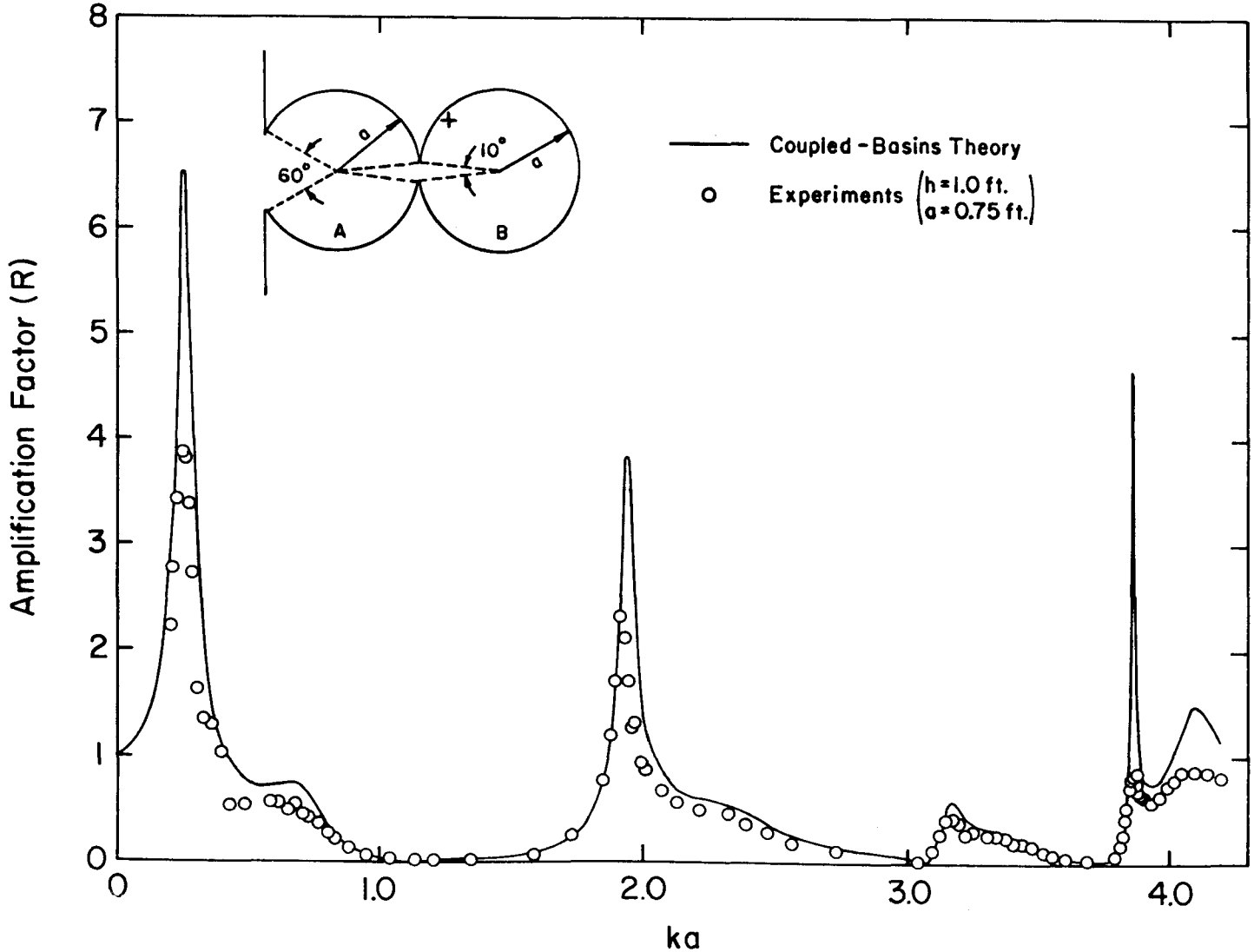

Fig. 15 Response Curve at r/a = 0.934, $\theta = 45^{\circ}$ in Basin B for Two Coupled Circular Harbors ($\theta_A = 60^{\circ}$, $\theta_B = 10^{\circ}$, $a_A = a_B$)

coupled-basins theory. Similar differences were reported by Lee (1969) in connection with the application of the single-basin theory. It is interesting to note that some of the largest responses are associated with peaks with very narrow bandwidths, and in the experiments these responses are significantly attenuated. In fact, in some cases these maxima have almost disappeared in the experiments due to viscous effects. Thus, viscosity can play an important role in minimizing resonance effects. Some comments on the effect of viscous dissipation on harbor response will be presented in Section 4.4.

In each of these response curves eight maxima appear; however, some of these resonant conditions are not immediately apparent from the figures. The reason for this is that Figs. 12 through 15 refer to the response at a particular location in one harbor as a function of the wave number parameter ka. Hence the effect of resonance for a particular wave number at one position in one basin may be important, but at another location no effect may be seen. Consider Fig. 13 for the range of ka between 1.8 and 3.0. There are two well-defined resonant maxima shown in that range for a positon $r/a = 0.934$, $\theta = 45^{o}$ in the first basin (A) whereas for the center of the second basin (B) (Fig. 14) only one, rather poorly defined maximum, is apparent for the same wave number range.

The effect of location can be eliminated when investigating resonance by plotting the maximum amplification, regardless of location, as a function of ka. The theoretical response curve defined in that way is presented in Fig. 16 for these two coupled circular basins. The eight resonant modes are immediately obvious. To see where these modes of oscillation

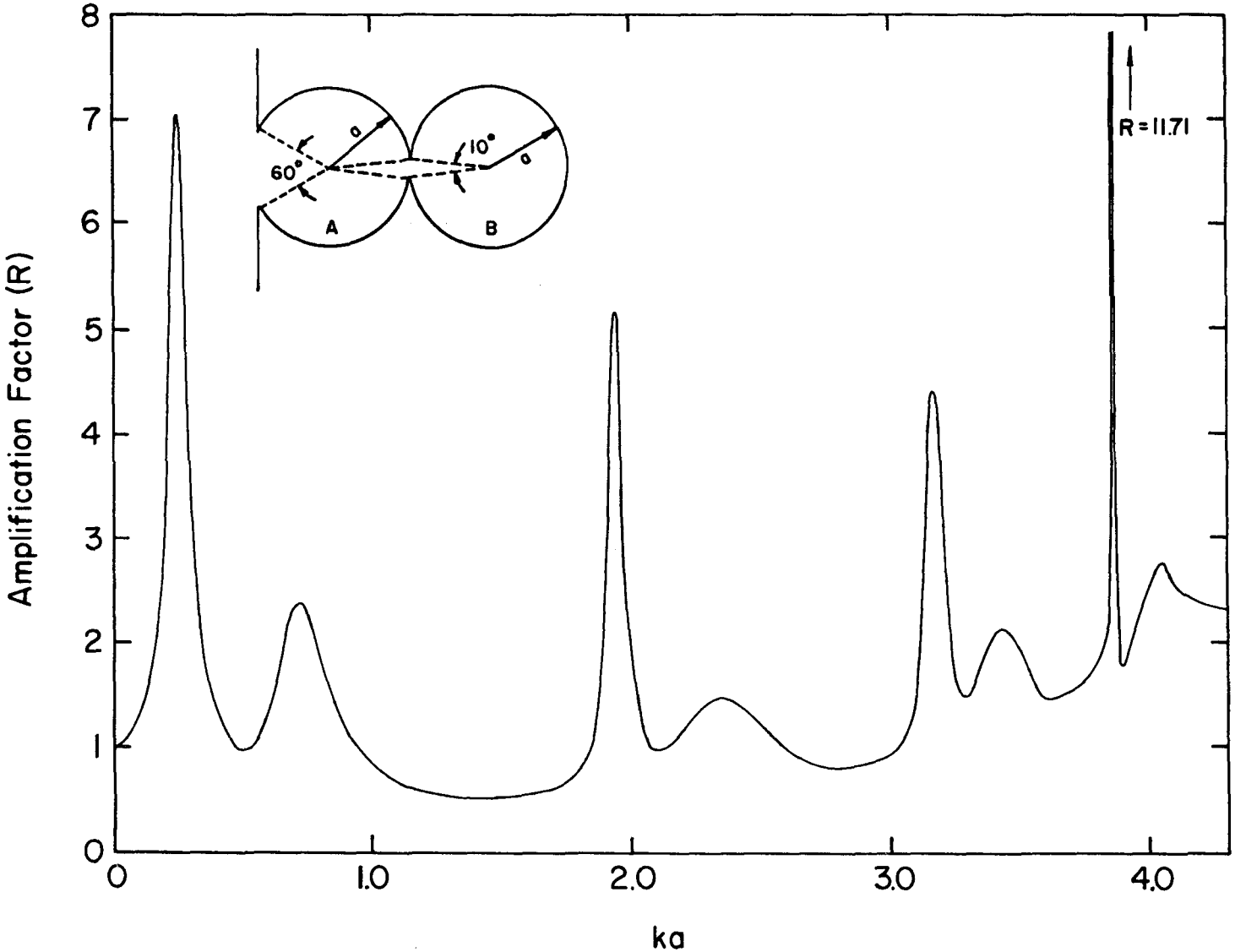

Fig. 16 Maximum Response Curve for Two Coupled Circular Harbors ($\theta_A = 60^o$, $\theta_B = 10^o$, $a_A = a_B$)

come from, the maximum response for a circular harbor with a 10^{o} entrance gap directly connected to the open-sea and a circular harbor with a 60^{o} opening directly connected to the open-sea has been determined using the "arbitrary harbor theory" presented by Lee (1969). These theoretical results are presented in Fig. 17 and show an increase in the amplification at resonance as the harbor entrance width decreases along with a corresponding shift of the maxima to smaller wave numbers. The former is referred to as the "harbor paradox" by Munk & Miles (1961). The latter effect is the shift of resonance toward closed basin resonance as the entrance width decreases.

One effect of coupling can be seen clearly by comparing Fig. 16 and Fig. 17. At first glance, Fig. 16 appears to be simply a combination of the two response curves presented in Fig. 17, i.e., the first, third, fifth, and seventh modes in Fig. 16 correspond to the four modes shown by solid lines in Fig. 17 and the second, fourth, sixth, and eighth modes of Fig. 16 agree qualitatively with the four modes by dashed lines in Fig. 17. Thus, it appears that the maximum response of this coupled-basin system is a combination of the response of the individual basins when each is connected directly to the open-sea. This suggests one problem which can arise in an actual harbor when it is enlarged by changing its configuration from a single basin to a system of interconnected slips. The original response of the harbor may be changed to a more complicated one with additional maxima for the same range of wave period. (However it is possible that this effect may not be too

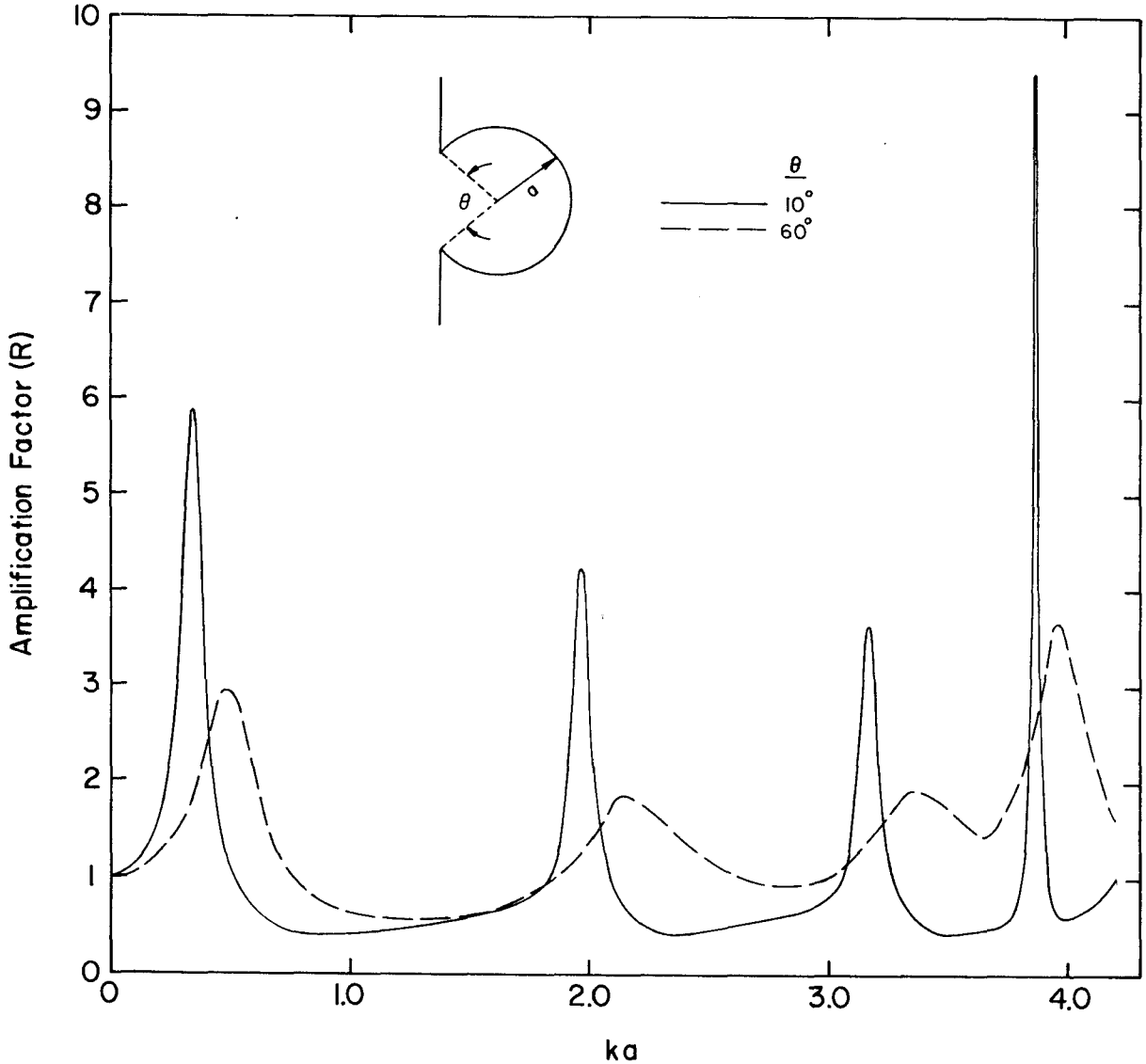

Fig. 17 Maximum Response Curves for Two Circular Harbors $\theta = 60^{\circ}$ and $\theta = 10^{\circ}$

serious due to the influence of viscous dissipation which tends to reduce the maximum amplification for modes of oscillation whose peaks have small wave number bandwidths.)

The shape of the water surface for the eight resonant modes of oscillation shown in Fig. 16 are presented in Figs. 18 through 25. These may be compared to similar distributions for the individual basins (10^{o} and 60^{o} openings) which have been presented previously by Lee (1969).

Fig. 18 shows the wave amplitude distribution inside the harbor for the first resonant mode of the coupled-basins system (ka = 0.26). The wave amplitude has been normalized with respect to that at location P (in the inner basin) which is a position at which the amplitude is very close to a maximum (the maximum is at the back-wall on the diameter of symmetry). The wave amplitude shown in Fig. 18 is relatively uniform within each basin; however, the average wave amplitude in the inner basin is about twice that in the outer basin. In addition, either positive or negative water surface displacements occur simultaneously in both the inner and outer basins. Therefore, this mode is usually referred to as the "pumping mode".

The wave amplitude distribution inside the harbor for the second mode of oscillation (ka = 0.72) is presented in Fig. 19. The maximum wave amplitude is located in the outer basin; the wave amplitude shown has been normalized with respect to that at location P (which is very close to the position of the maximum wave amplitude). Fig. 19 shows that positive water surface displacements exist in the outer basin while

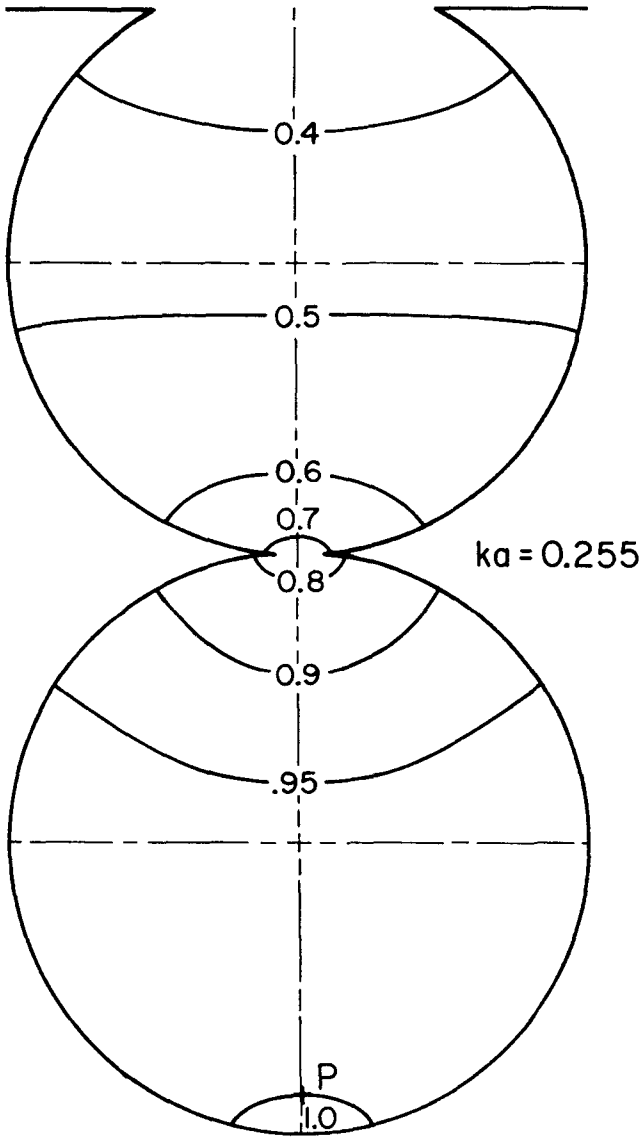

Fig. 18 Shape of Mode 1 (ka = 0.255); Two Coupled Circular Harbors

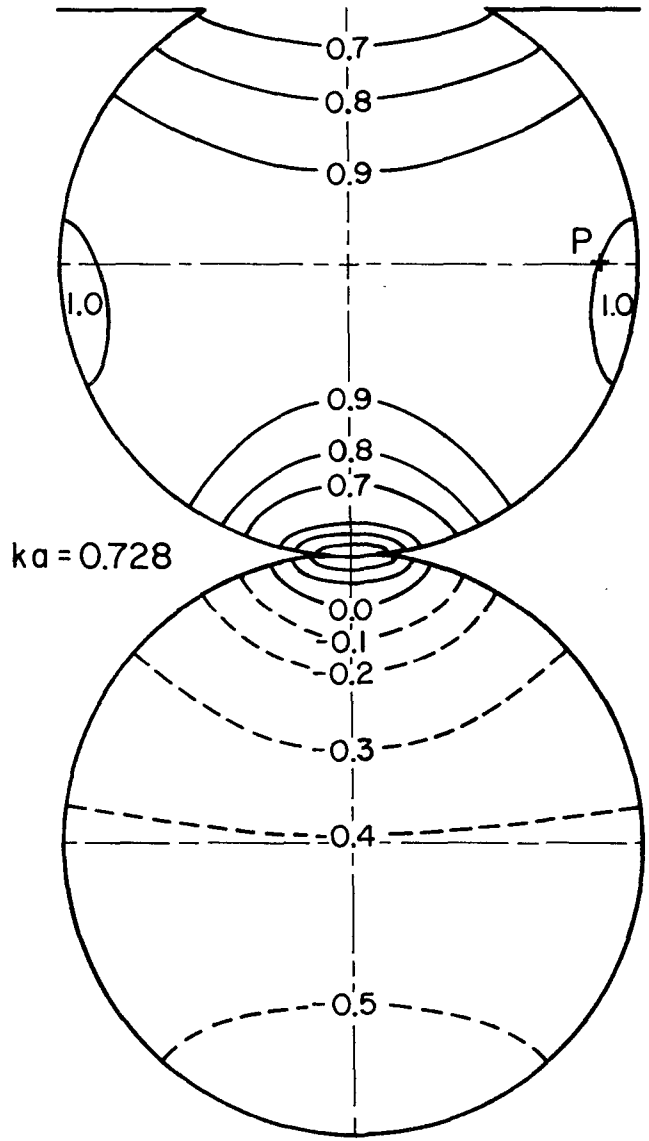

Fig. 19 Shape of Mode 2 (ka = 0.728); Two Coupled Circular Harbors

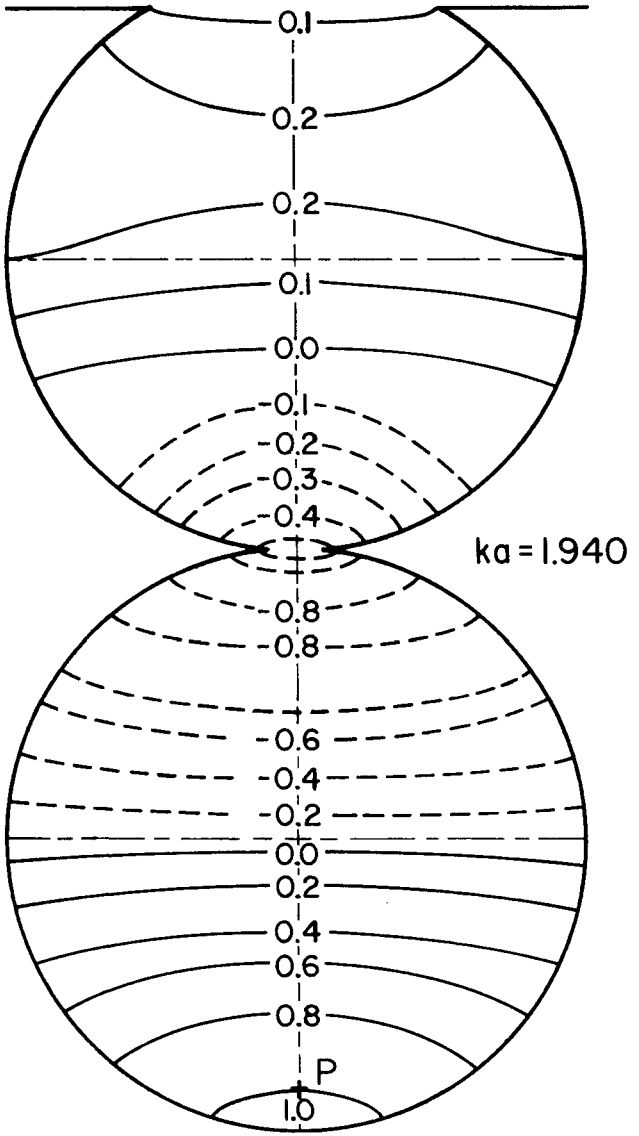

Fig. 20 Shape of Mode 3 (ka = 1.940); Two Coupled Circular Harbors

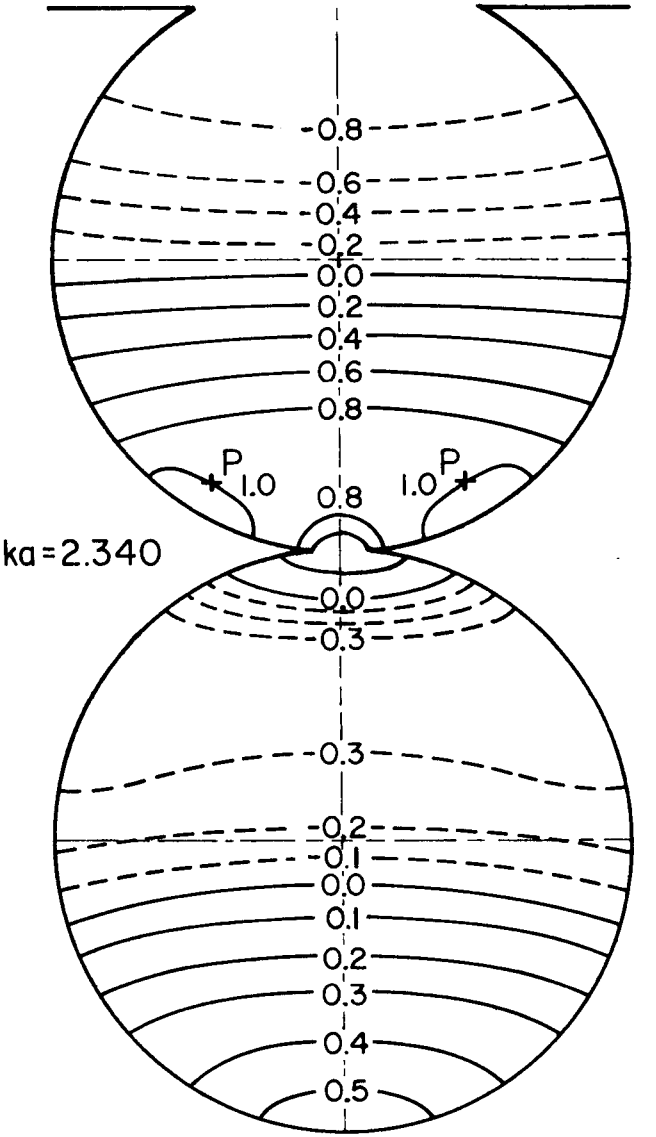

Fig. 21 Shape of Mode 4 (ka = 2.340); Two Coupled Circular Harbors

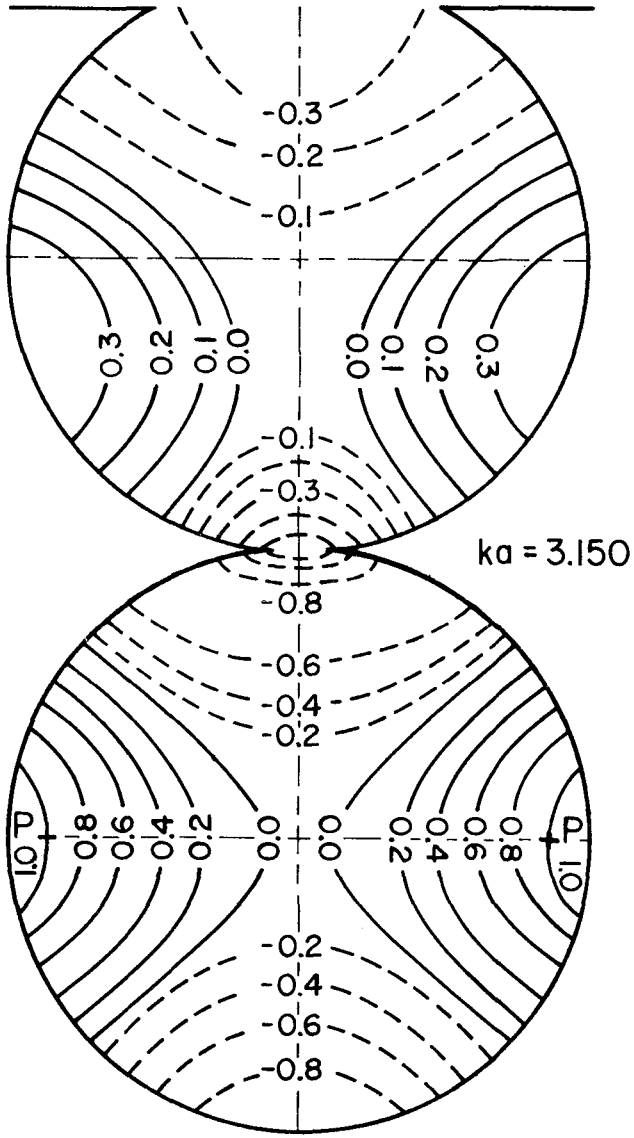

Fig. 22 Shape of Mode 5 (ka = 3.150); Two Coupled Circular Harbors

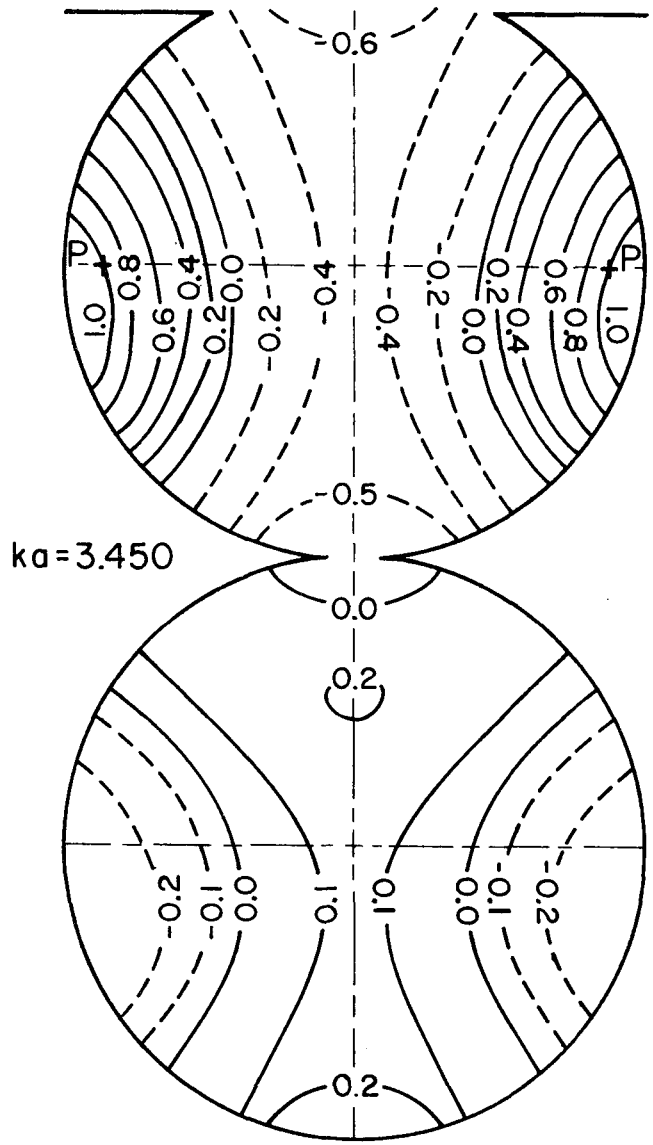

Fig. 23 Shape of Mode 6 (ka = 3.450); Two Coupled Circular Harbors

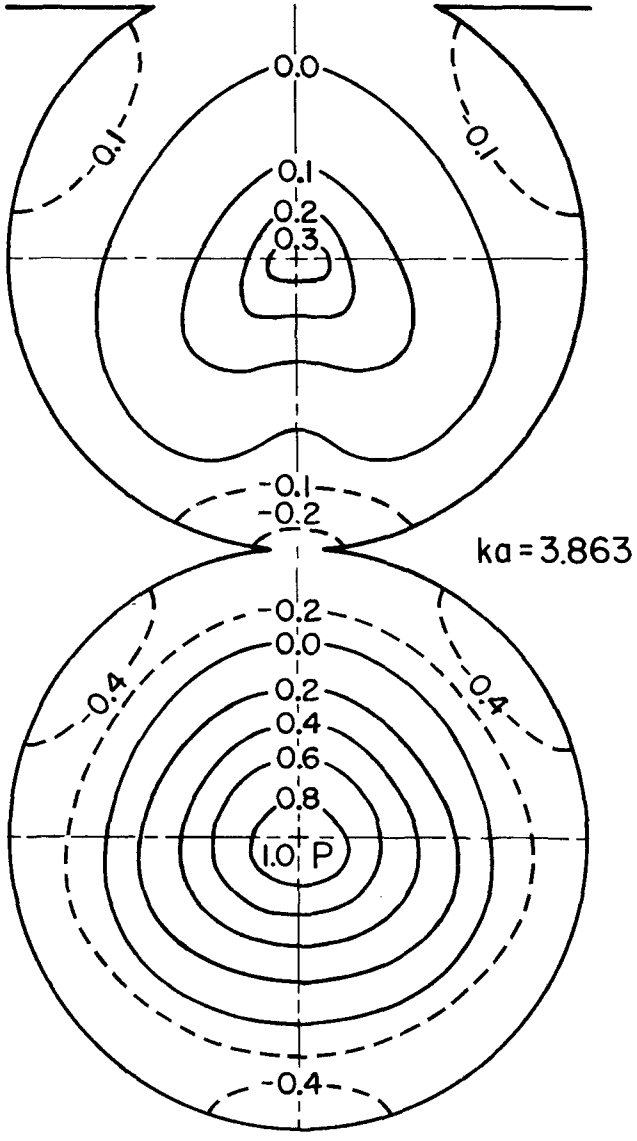

Fig. 24 Shape of Mode 7 (ka = 3.863); Two Coupled Circular Harbors

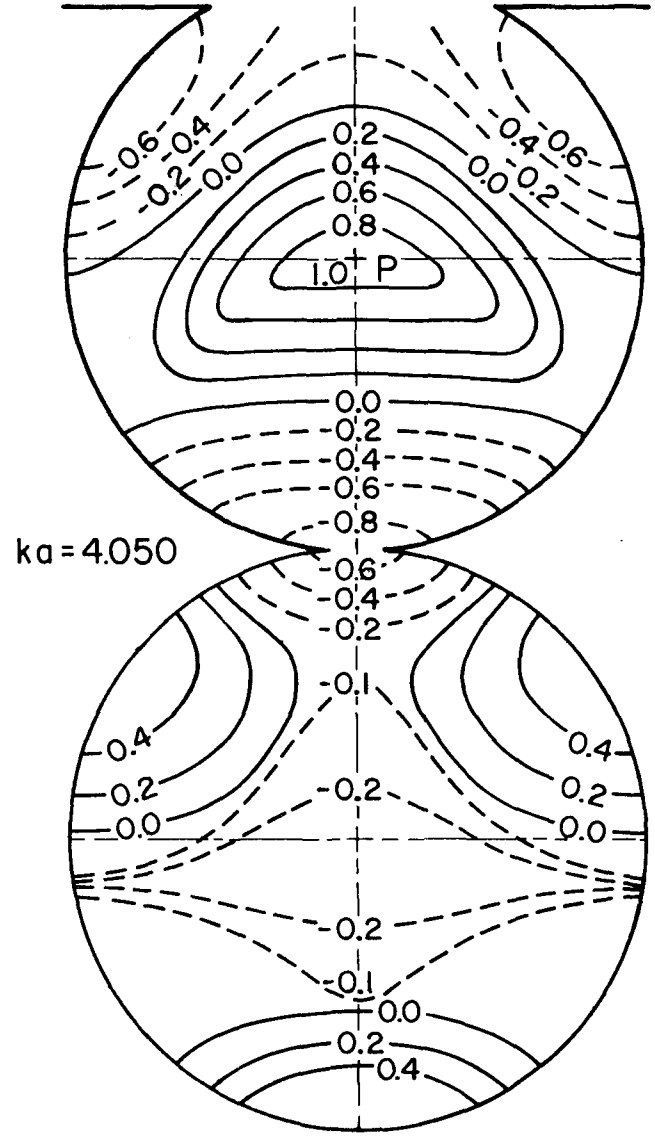

Fig. 25 Shape of Mode 8 (ka = 4.050); Two Coupled Circular Harbors

negative water surface displacements exist in the inner basin with a nodal line (line of zero wave amplitude) located near the common boundary between the outer and inner basins. Considering the out-of-phase motion in the two basins, this mode of oscillation may be called the "sloshing mode", i. e., sloshing between basins. The increased complexity of water surface oscillations with increasing wave number is seen by comparing Figs. 18 and 19.

Fig. 20 shows the wave amplitude distribution inside the harbor for value of ka = 1.94 which corresponds to the third resonant mode of oscillation. The normalized surface amplitude exhibits two nodal lines: one in the outer basin and one in the inner basin. Thus, for this value of ka a sloshing mode exists in each basin with the water surface at the inner part of the outer basin and the outer part of the inner basin moving in phase. In addition, for this mode the water surface displacement in the inner basin is at least twice the wave amplitudes in the outer basin.

The wave amplitude distribution inside the harbor for the fourth resonant mode (ka = 2.34) is presented in Fig. 21. The position of the maximum wave amplitude for this mode is in the outer basin near the entrance to the inner basin. There are three nodal lines in the harbor: one in the outer basin, one near the common boundary between the two basins (the entrance to the inner basin), and another near the center of the inner basin. Even though the water surface displacements in the inner basin are relatively small compared with those in the outer basin, the water surface shape for this value of ka is still approximately that

of a sloshing mode within each basin. However, this mode of oscillation is more complicated than the one shown in Fig. 20 in the sense that an additional nodal line exists near the common boundary between the two basins.

A wave amplitude distribution for the next resonant mode of oscillation (ka = 3.15) is presented in Fig. 22. For this mode the maximum wave amplitude occurs in the inner basin at the position $r = a$, $\theta = 90^{o}$ (and its symmetric counterpart at $\theta = 270^{o}$). There are two nodal lines in each basin with the nodal lines somewhat similar to the crossed nodal lines of the corresponding mode of oscillation for a closed circular basin. The mode shape for the inner basin is similar to the one shown in Fig. 6.23 of Lee (1969), while the mode shape for the outer basin is similar to that presented in Fig. 6.24 of Lee (1969) except near the entrance to the inner basin. As can be seen from Fig. 22 water surface displacements in the inner basin are significantly larger than those of the outer basin.

The mode shape for ka = 3.45 is presented in Fig. 23. This value of ka corresponds to the sixth resonant mode of oscillation shown in Fig. 16. For this mode, the maximum wave amplitude occurs in the outer basin at the position: $r = a$, $\theta = 100^{0}$ (and its symmetric counterpart $\theta = 260^{o}$). There are two nodal lines in the outer basin, another one near the entrance to the inner basin, and two nodal lines in the inner basin. Comparing Figs. 22 and 23 it is seen that the water surface shapes appear similar; however, corresponding regions in the basins are in phase in Fig. 22 (ka = 3.15) while they are out of phase in Fig. 23 (ka = 3.45).

The wave amplitude distribution inside the harbor for the seventh resonant mode of oscillations (ka = 3.86) is presented in Fig. 24. For this value of ka, the maximum wave amplitude occurs at the center of the inner basin, and the water surface displacements in the inner basin are much larger than those in the outer basin. The contour lines of constant amplitude near the center of the inner basin (including the nodal line) are nearly circular. It is also seen from Fig. 24 that water surface motions in the regions near the center of both the inner and outer basins are in phase.

Fig. 25 shows the wave amplitude distribution inside the harbor for ka = 4.05 (the eighth resonant mode of oscillation). The position of maximum wave amplitude is at the center of the outer harbor, and the shape of the water surface in the outer basin is similar to that shown in Fig. 6.26 of Lee (1969) for a circular harbor with a 60° opening coupled directly to the open-sea. For this wave number water surface displacements in the inner basin are small compared with those of the outer basin and in contrast to the distribution shown in Fig. 24 the water surface oscillations near the center of the two basins are out-of-phase.

Thus, although it is seen that the response of coupled basins and the amplitude distributions within a harbor can become quite complicated as individual basins are connected, it may be possible to investigate these facets of the problem by viewing the basins as separate units. For example, in the case of the coupled-circular harbor just discussed some aspects of the response and the water-surface displacements could be constructed from a knowledge of the response of the individual basins.

4.3 THE RESPONSE OF VARIOUS COUPLED-BASINS SYSTEMS

In Section 4.1, it has been shown that the response of the Long Beach Harbor Model obtained using the coupled-basins theory agrees well with the theoretical results (single-basin theory) and experimental data obtained by Lee (1969). This agreement demonstrates how well the present method can be applied to basins of arbitrary shape coupled together and excited by waves from the open-sea. In Section 4.2, experimental data for coupled-circular basins have also provided further evidence in support of the theoretical approach, although in the hydraulic model the effect of viscous dissipation does significantly reduce the amplification factor at resonance, especially for peaks where the wave number bandwidth is small.

In this section, the effect on the overall harbor response of coupling basins together will be explored analytically for various basin arrangements. For simplicity rectangular basins and circular basins of different radii and/or different openings are used. The purpose of this portion of the investigation was twofold: to show the applicability of the method developed, and to study the effect of coupling on harbor response. For this reason only the maximum response curve for each case will be presented and discussed.

4.3.1 Two Coupled Circular Harbors

In Fig. 26, the maximum response curve is presented for a circular harbor with a 10^{o} opening connected along its diameter of symmetry to another circular harbor of the same size also with a 10^{o}

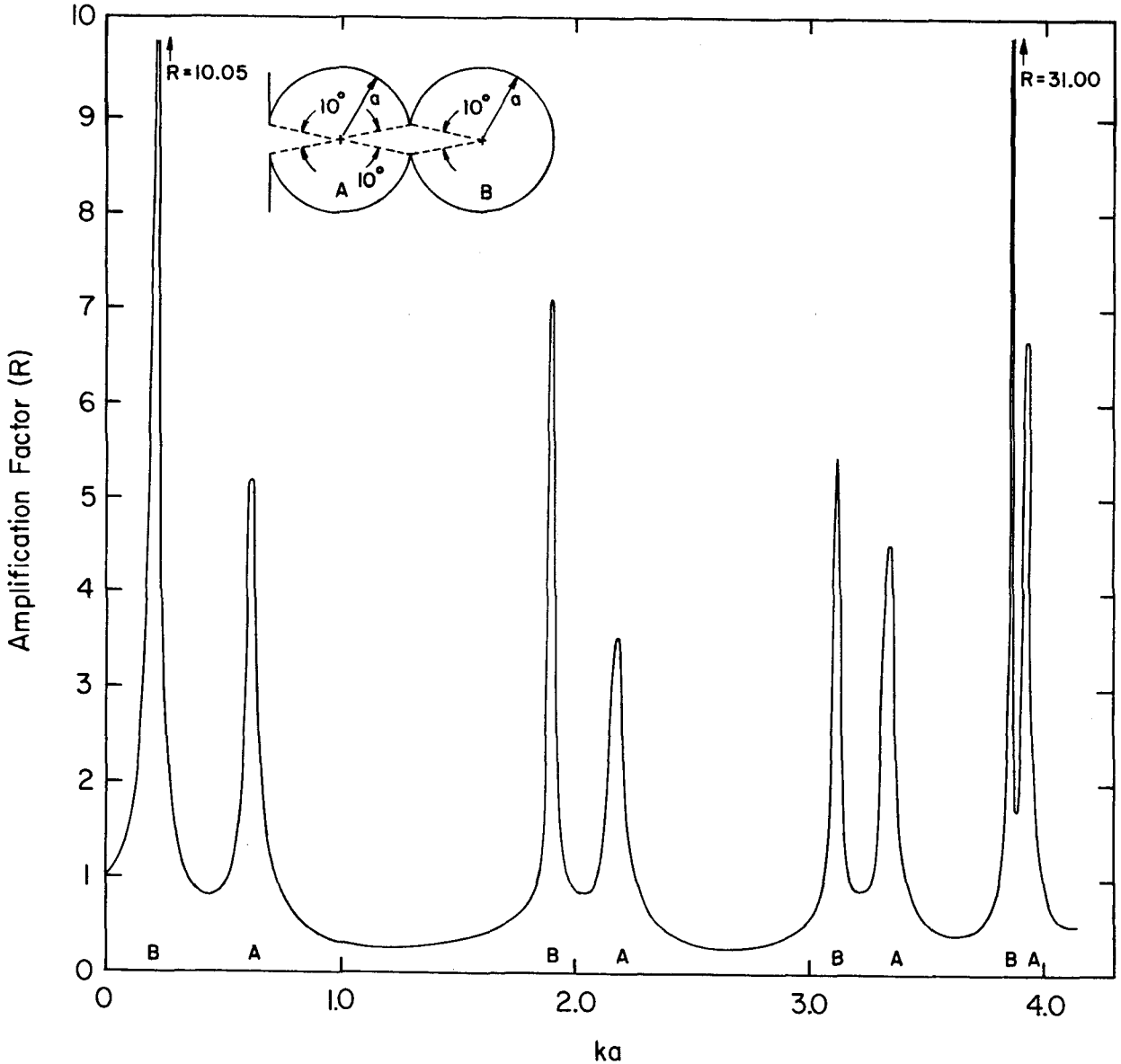

Fig. 26 Maximum Response Curve for Two Coupled Circular Harbors ($\theta_A = \theta_B = 10^o$, $a_A = a_B$)

opening. As before, the ordinate represents the maximum amplification factor defined as the maximum wave amplitude inside the harbor (regardless of the location) divided by the standing wave amplitude at the harbor entrance when the entrance is closed. The abscissa is the wave number parameter, ka, where a is the radius of the outer harbor (the same as the inner harbor for this case). From Fig. 26 it is seen that there are eight maxima in the range of ka presented corresponding to eight resonant modes of oscillation. The values of ka for these resonant modes are 0.210, 0.62, 1.90, 2.18, 3.11, 3.34, 3.85 and 3.93. The position at which the wave amplitude reaches the maximum is located in Basin B (inner basin) for the 1st, 3rd, 5th and 7th resonant modes of oscillation, and for the 2nd, 4th, and 6th and 8th resonant modes the maximum is in Basin A (outer basin). The location of each maximum as being in either Basin A or B is indicated in the figure along the abscissa. The effect of coupling on the harbor response can be inferred by comparing Fig. 26 with the response curve for a single circular harbor of 10^{o} opening connected to the open-sea, presented in Fig. 17. The response of these coupled basins appears to be composed of the resonant modes of the individual circular harbors with some differences in both the resonant wave number and the maximum amplification. Thus, Fig. 26 again demonstrates that the number of resonant modes of oscillation for a coupled basin is larger than the number of resonant modes for either basin alone, and for two identical basins connected the number of modes is increased by about a factor of two for a given wave number range.

The effect of the width of the harbor entrance on the response of the harbor is demonstrated from a comparison of Fig. 26 and Fig. 16; in the latter the outer harbor has a 60° opening. It is seen that the maximum amplification factor for most resonant modes for the example shown in Fig. 16 is less than that for the corresponding modes shown in Fig. 26; however, in contrast the wave-number-bandwidth for the resonant modes in Fig. 16 is generally greater than those of Fig. 26. These results again show that as the entrance width decreases the maximum wave amplification within the harbor increases while the wave number bandwidth near resonance decreases. However, the reader is reminded that for the prototype, viscous effects, which are not considered in the present theory, may be very important in limiting the maximum amplification at resonance especially for resonant peaks with narrow bandwidths. (This has been demonstrated by the experimental results presented in Figs. 12 through 15, and as mentioned will be discussed in Section 4.4.)

The response of two circular harbors with the entrances oriented at 90° to one another was investigated. The basins have the same diameter and each entrance has an included angle of 10°. The maximum response curve for this harbor system is presented in Fig. 27 where the ordinate and abscissa are defined earlier. There are eight maxima (four in each basin) in the response curve for the range of ka presented corresponding to eight resonant modes of oscillation. The values of ka for these resonant modes are: ka = 0.21, 0.62, 1.98, 2.10, 3.12, 3.35, 3.85, and 3.90. It is noted that the number of

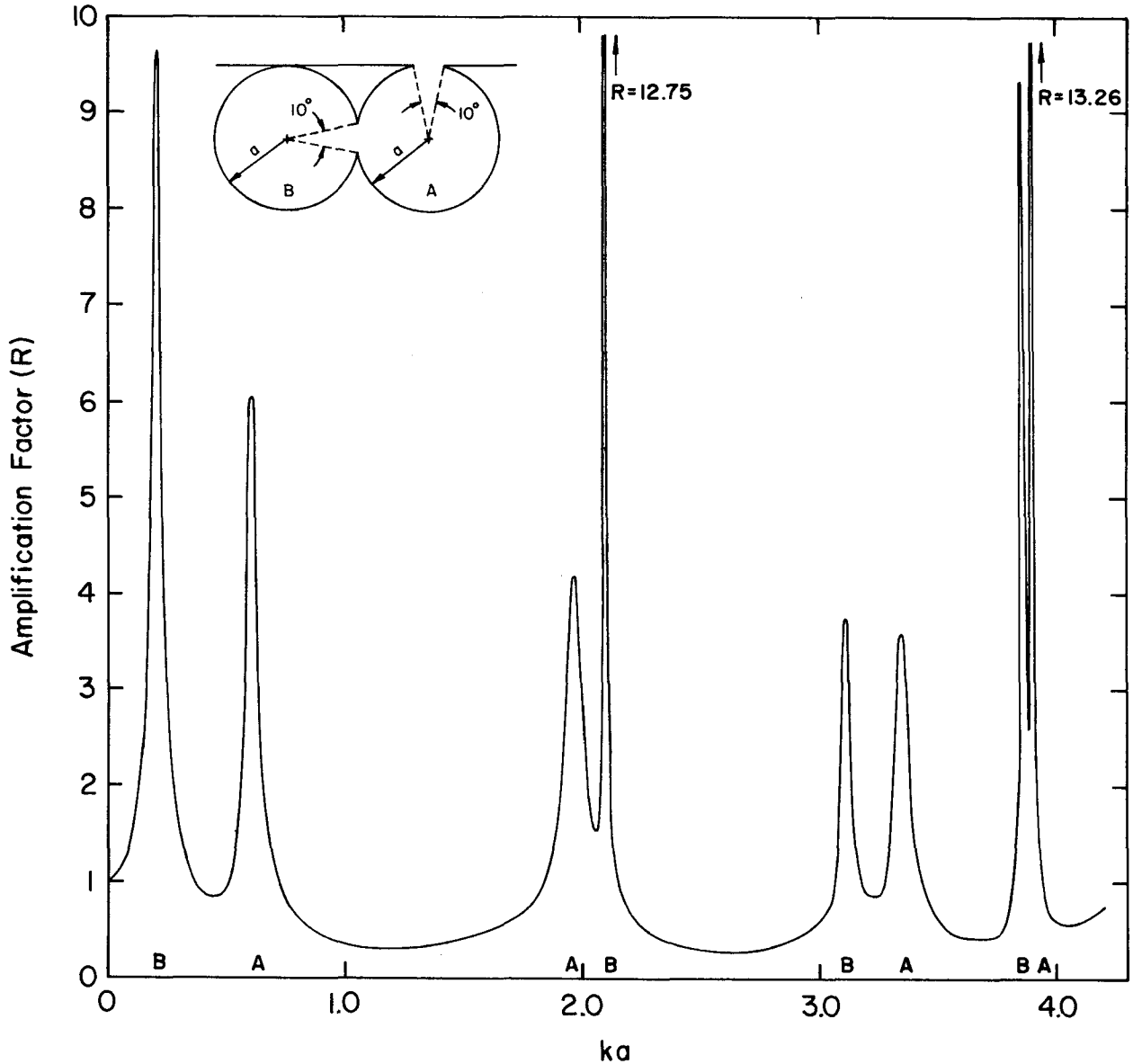

Fig. 27 Maximum Response Curve for Two Coupled Circular Harbors Connected at Right Angles ($\theta_A = \theta_B = 10^o$, $a_A = a_B$)

resonant modes of oscillation and the associated wave numbers for the arrangement shown in Fig. 27 are similar to the response curve presented in Fig. 26 suggesting that for these two harbors the coupling pattern does not alter the harbor response significantly. This is reasonable since this constant-depth circular harbor system has the same entrance width and only one characteristic dimension (the diameter of the harbor). Thus, the position of the boundary opening probably will not affect the response of the harbor very much for this range of wave lengths.

From Fig. 27 it is seen that the first two modes of oscillation are almost identical to the first two resonant modes shown in Fig. 26. This is reasonable since the basin dimensions are the same for the two cases but only the arrangement is different. For a small ratio of radius to wave length the effect on the harbor response of the arrangement should not be too important. The wave amplitude inside Basin B for the first mode (the pumping mode) is about twice the wave amplitude in Basin A, similar to the case shown in Fig. 26. The theoretical amplification at resonance for the other modes present in this wave number range does vary somewhat with basin arrangement but not significantly.

The maximum response curve for a circular harbor with a 10° opening coupled to another circular harbor with one-half the diameter is presented in Fig. 28. The larger harbor, which is connected to the open-sea, has a main entrance of 10° and a 10° opening in the backwall,

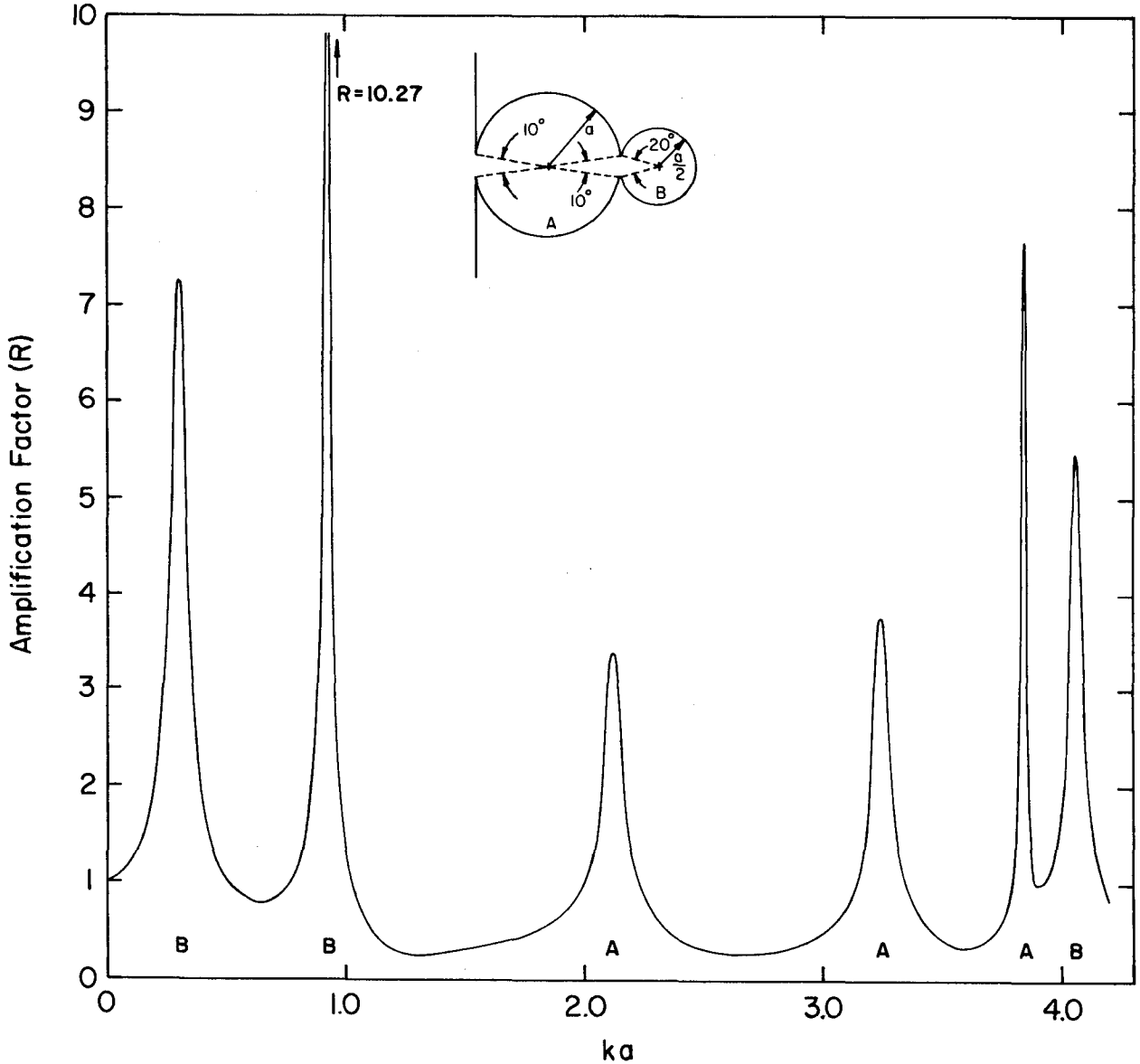

Fig. 28 Maximum Response Curve for Two Coupled Circular Harbors ($\theta_A = 10^o$, $\theta_B = 20^o$, $a_A = 2a_B$)

thus, the smaller basin has a 20^{o} opening. In the abscissa of Fig. 28 the characteristic dimension "a" is the radius of the larger basin (Basin A).

Fig. 28 shows six maxima corresponding to the six resonant modes of oscillation for the range of ka presented; the values of ka for these are: ka = 0.30, 0.92, 2.12, 3.24, 3.84 and 4.06. The position of the maximum amplitude for the first mode (the pumping mode) is at the center of the backwall of Basin B as it was with the other cases presented in the previous sub-sections. It is interesting to note that the position at which the maximum amplification is reached is in Basin A (the larger basin) for the third, fourth, and fifth resonant modes, and for the first, second, and sixth resonant modes the maximum amplification is in Basin B. The wave numbers of the modes at ka = 0.30, 2.12, 3.24, and 3.84 are similar to those of the four modes presented in Fig. 17 for a circular harbor with a 10^{o} opening. If the radius of the smaller basin (Basin B) is used as the normalizing dimension the wave number parameters for the two modes at ka = 0.92 and 4.06 become ka = 0.46 and 2.03 which are slightly greater than the values for the "pumping" and "sloshing" modes respectively for the single 10^{o} harbor. This is in the right direction since the inner harbor has a 20^{o} opening. Thus the results presented in Fig. 28 further demonstrate the fact that, for these shapes, the resonant modes of oscillation of coupled-basins are combinations of the resonant modes of the individual basins for the range of ka considered. Therefore, connecting one harbor to another does not necessarily improve the amplification characteristics of the

harbor system; however, it is possible that the wave amplitude amplification for some particular modes may be reduced if the proper geometry is found and if viscous effects are considered.

The maximum response curve for a circular harbor with a 60^{o} opening coupled to a circular harbor of one-half that size with a 20^{o} opening is presented in Fig. 29. Similar to the previous example, the characteristic dimension "a" which is used is the radius of the larger basin (Basin A). From Fig. 29 it is seen that there are five resonant modes of oscillation for the range of ka considered; the values of ka for these modes are: ka = 0.41, 0.97, 2.32, 3.39 and 3.88. For the first, second, and fifth modes (ka = 0.41, 0.97, and 3.88) the maximum wave amplitude occurs in the smaller basin (Basin B) while for the modes at ka = 2.32, 3.39 (third and fourth) the maximum response is in the larger basin (Basin A). By comparing Fig. 29 to Fig. 28 it is seen that except for the mode at ka = 3.88 the maximum amplification factor at resonance is smaller and the response near resonance has a larger wave number bandwidth for the example where the outer harbor has a 60^{o} opening than for the one with a 10^{o} opening. Thus, the effect of entrance width on the response of harbors to incident waves is further demonstrated.

The results presented in this section have demonstrated that the modes of oscillation which exist in coupled-circular-basins are closely related to the modes of the individual basins, and that resonance in one basin will affect the oscillations in the other. Moreover, for a particular range of ka, the modes of oscillation in coupled-basins appear to be a

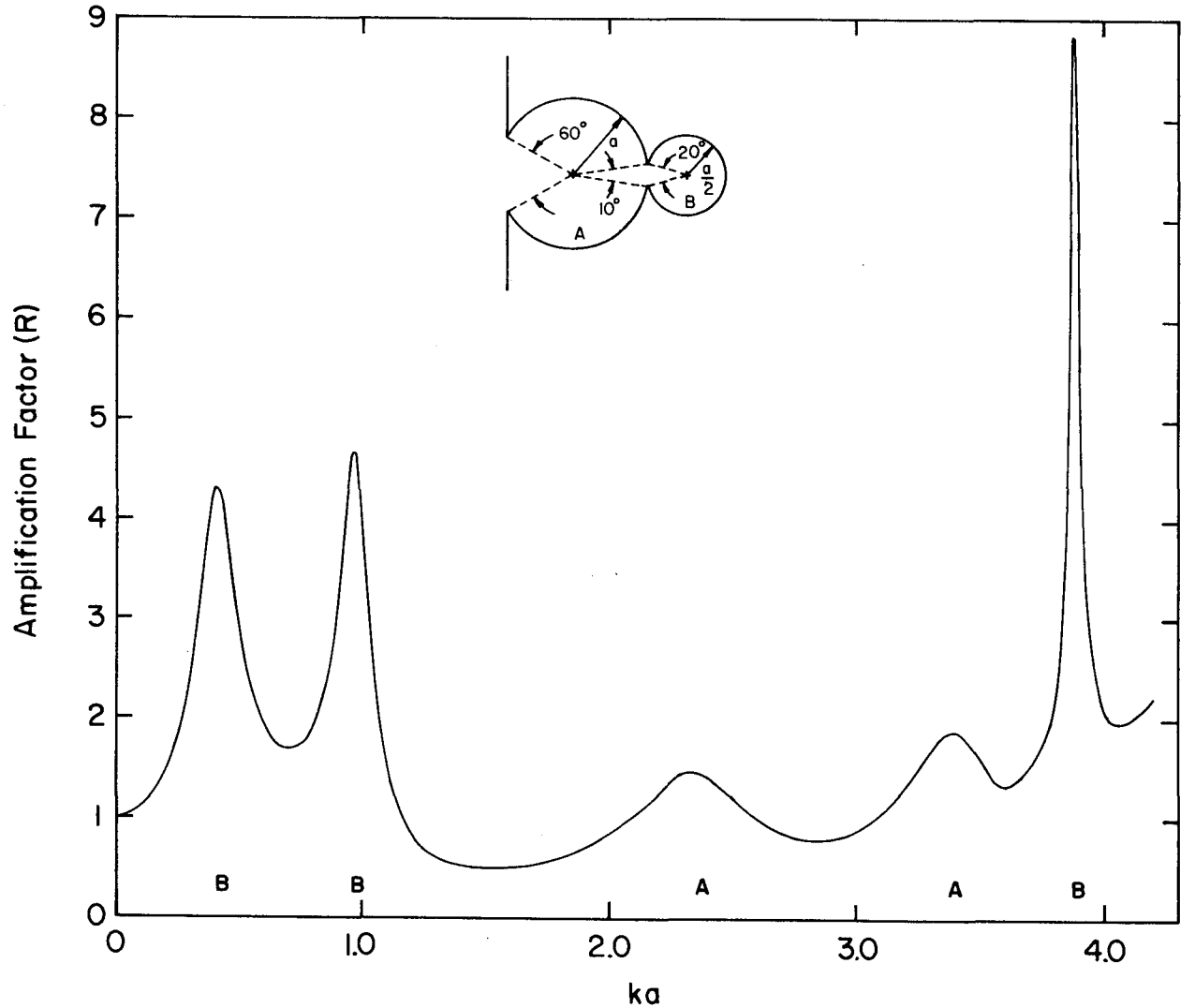

Fig. 29 Maximum Response Curve for Two Coupled Circular Harbors ($\theta_A = 60^o$, $\theta_B = 20^o$, $a_A = 2a_B$)

combination of the possible modes of oscillation of the individual basins. This is in agreement with the earlier work of Raichlen and Ippen (1965) in which it was found that a rectangular harbor connected to a highly reflective and larger rectangular wave basin had many more modes of oscillation compared to the response of the same harbor connected directly to the open-sea.

4.3.2 Rectangular and Circular Coupled Harbors

In the previous subsection examples of coupled circular harbors have been considered; in this subsection the response of circular harbors connected to rectangular entrance channels will be discussed. The entrance channel is a common feature of prototype harbors and the influence of the channel on the harbor response is therefore an important feature in the design of harbors.

The harbor model which was chosen for the theoretical investigation consists of a circular basin of constant depth with a radius of 0.75 ft and an entrance gap of 10^{o} included angle (an entrance width of 0.131 ft). Connected to this entrance is a channel 0.198 ft wide with a variable length. The other end of the channel is fully open and communicates directly with the open-sea. There is a difference in the width of the channel compared to the entrance width; the channel width was chosen to be the same as the rectangular channel investigated previously and reported by Lee (1969) and the dimension of the circular harbor were the same as that discussed previously herein.

The response curves for the maximum response anywhere in the harbor are presented in Figs. 30 through 33 for four different lengths of the entrance channel. These response curves were obtained by using the theory presented in Chapter 2 by dividing the entire domain into 3 regions: the open-sea region, the entrance channel region (Basin A), and the circular harbor region (Basin B). In all of these figures the ordinate is the maximum amplification factor in the harbor regardless of location and the abscissa is the product of the wave number and the radius of the circular basin. Indicated near the abscissa in these figures is the particular basin where the maximum occurs, e. g., "A" indicates the maximum occurs in the entrance channel and "B" denotes a maximum in the circular harbor. Considering the shortest entrance channel to be of unit length, the other three lengths studied were two, three, and four times that length.

The response with the shortest entrance channel, a length approximately one-third the diameter, is presented in Fig. 30. Five resonant modes of oscillation are evident for the range of ka investigated: three occur in the circular basin, one in the entrance channel, and one mode has maximum amplitudes in both basins. Referring to Fig. 17, it is noted that a circular harbor with a 10^{o} opening has four modes of oscillation over a range of ka up to about 4. 0. The values of the wave number parameter for the first, second, fourth and fifth modes of Fig. 30 are about the same as those for the four modes of oscillation of the 10^{o}-opening-harbor shown in Fig. 17. The amplification at resonance is different, in fact the amplification for the pumping mode is increased by nearly 45% by adding this fairly short channel.

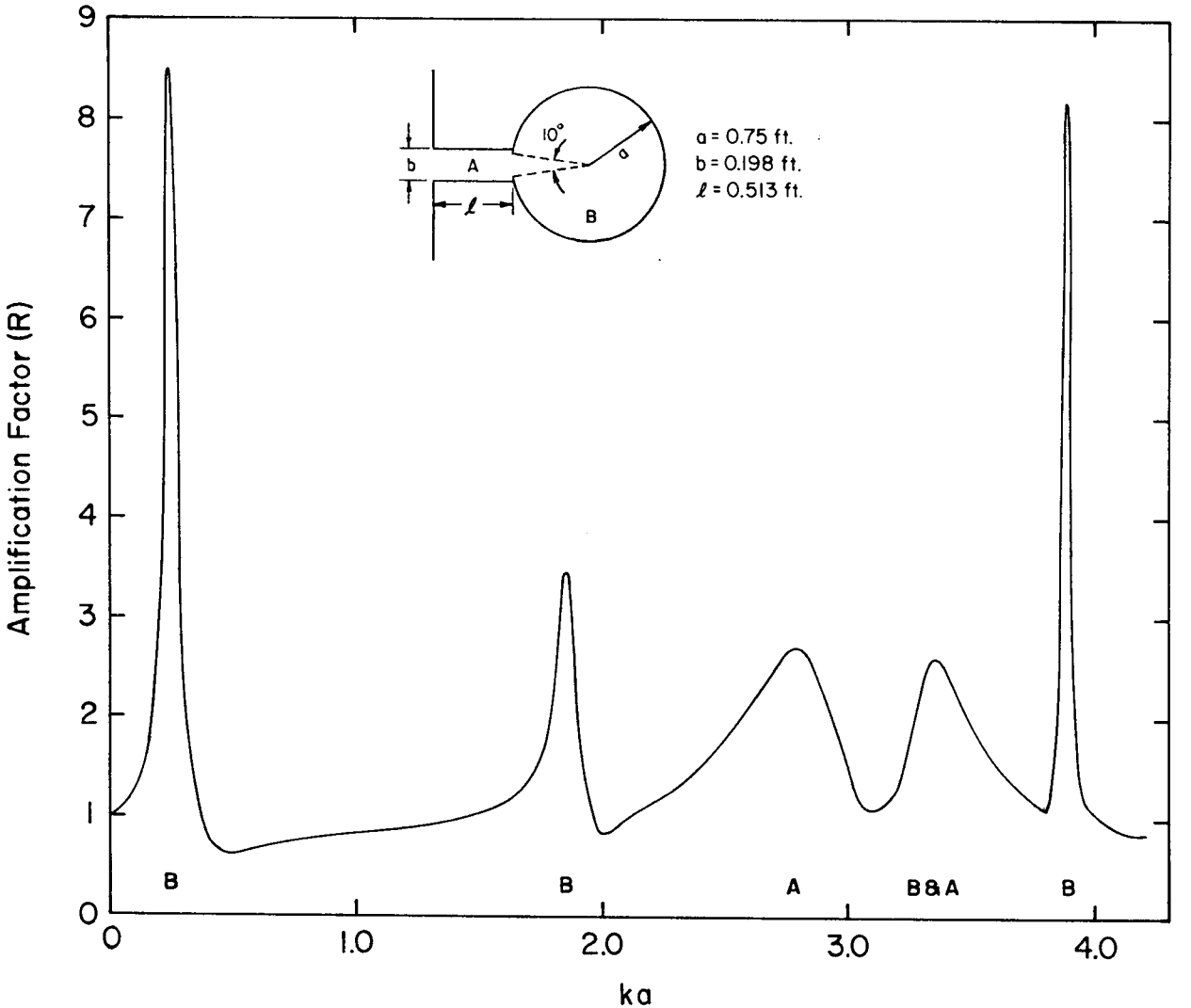

Fig. 30 Maximum Response Curve for Circular Harbor Coupled to Rectangular Entrance Channel ($\ell/a = 0.685$)

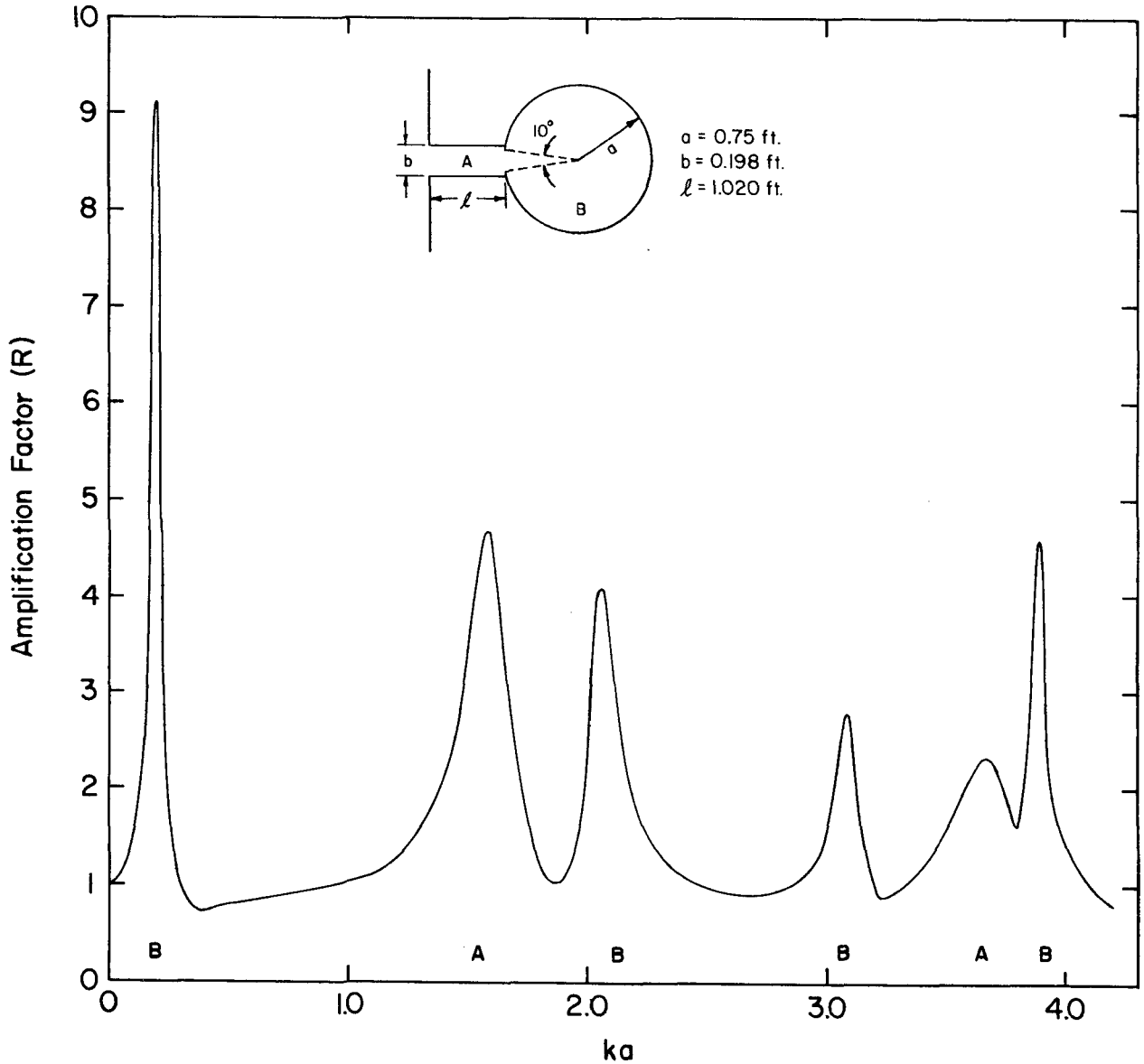

Fig. 31 Maximum Response Curve for Circular Harbor Coupled to Rectangular Entrance Channel ($\ell/a = 1.36$)

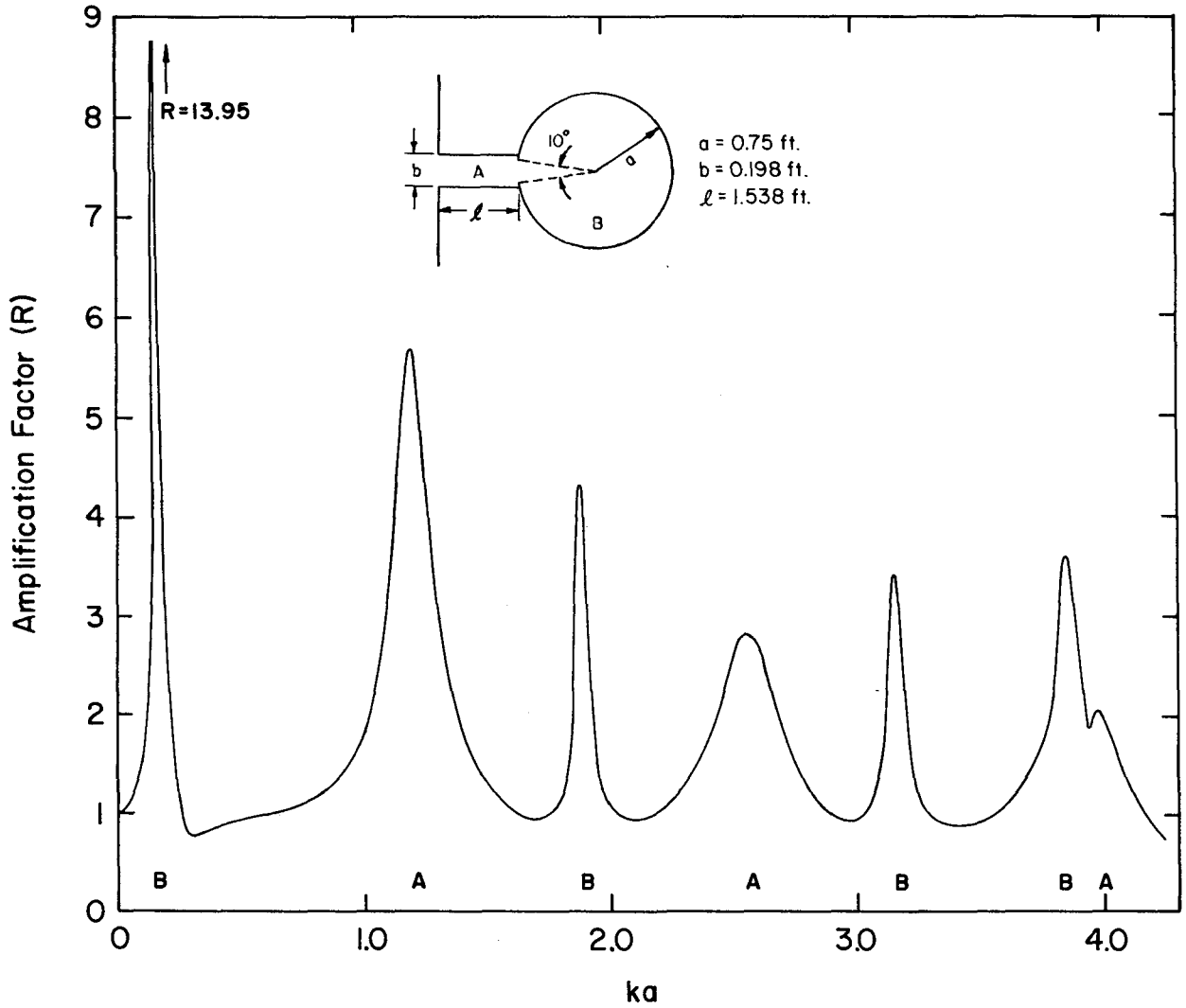

Fig. 32 Maximum Response Curve for Circular Harbor Coupled to Rectangular Entrance Channel ($\ell/a = 2.05$)

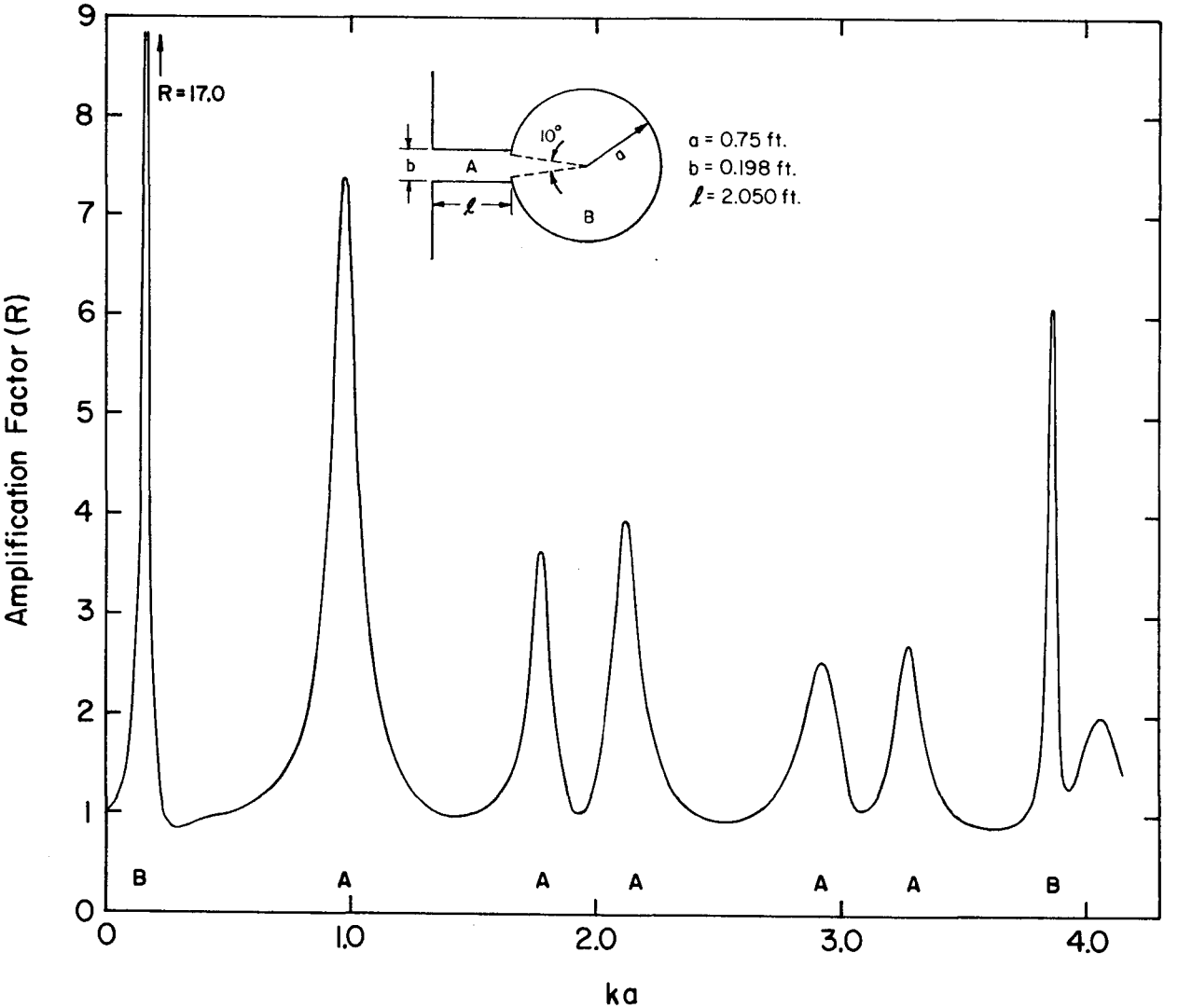

Fig. 33 Maximum Response Curve for Circular Harbor Coupled to Rectangular Entrance Channel ($\ell/a = 2.73$)

When the length of the entrance channel is doubled, as is shown in Fig. 31, an additional maximum is introduced in the response compared to Fig. 30 for the same wave number range. The four modes of the circular harbor become quite distinct and comparable in wave number to those shown in Fig. 17 for the same circular harbor connected directly to the open-sea. The two maxima shown in Fig. 31 at ka = 1.58 and 3.67 correspond to maximum amplitudes in the entrance channel. By multiplying these values by the ratio of the channel length to the harbor radius, ℓ/a, the wave number parameter may be expressed in terms of the channel length as: $k\ell$ = 2.14 and 4.83. The value of this parameter for the first two modes of a rectangular harbor (with the same aspect ratio) connected directly to the open-sea is: $k\ell$ = 1.32 and 4.2. Therefore, when the rectangular channel is connected between the open-sea and the circular basin the tendency is for the mode of oscillation to shift toward the closed rectangular basin mode ($k\ell = \pi$ and 2π). Nevertheless, these are identifiable as modes of resonance for the entrance channel.

Fig. 32 shows the maximum response curve when the length of the entrance channel is increased by 50% compared to the case shown in Fig. 31. For this configuration the four modes of the circular basin can still be recognized and are located at approximately the same values of ka as before, but the wave numbers for the modes of oscillation in the entrance channel have changed and the number of modes in the channel have now increased to three. Thus, there are now seven modes of oscillation for the range of the wave numbers shown, i.e., $0 < ka < 4.0$.

For the modes corresponding to channel resonance the values of the wave number parameter are: ka = 1.22, 2.56, and 3.97. When expressed in terms of the channel length these values become: $k\ell$ = 2.5, 5.25, and 8.23. Thus, for the increase in length, the parameter $k\ell$ approaches π, 2π, and 3π, the values for the first three modes of a narrow closed rectangular basin. In addition the amplification associated with these modes has increased. For the pumping mode the amplification has increased by 60% compared to the case with the entrance channel one-third this length.

When the length of the entrance channel is increased again by one-third (or four times that shown in Fig. 30) additional modes become evident as shown in Fig. 33. The pumping mode and the fourth mode of the circular harbor (ka = 3.85) are still evident, but other modes of the circular harbor have been masked by those of the rectangular entrance channel. These now appear at values of ka = 0.98, 1.78, 2.12, 2.92, 3.27, and 4.05 or in terms of the channel length at $k\ell$ = 2.67, 4.87, 5.78, 7.97, 8.93, and 11.08. The other modes that are introduced here ($k\ell$ = 4.87, 7.97, and 11.08) appear to be more comparable to the second, third, and fourth mode of a narrow rectangular harbor connected to the open-sea ($k\ell = \frac{3}{2}\pi$, $\frac{5}{2}\pi$, and $\frac{7}{2}\pi$). Again, for this case, the amplification of the pumping mode and other modes have increased with increasing entrance channel length.

In summary, with the addition of a rectangular entrance channel to the circular harbor, the modes of oscillation of the circular harbor are generally retained and additional modes due to the entrance channel are introduced. These latter modes may mask resonance in the circular

basin; however, the ratios of channel length to wave lengths for resonance are comparable to the closed basin and open harbor resonant modes one would expect for the rectangular basin alone. Another trend which is evident is that, for the four cases chosen, the amplification at resonance for the pumping mode increases with increasing channel length; for ratios of channel length to harbor radius of 0.68, 1.35, 2.05, and 2.74 the corresponding values of the amplification of the pumping mode are 8.5, 9.1, 13.95, and 17.0. This is compared to a value for the circular harbor alone of 5.9. Thus, again the response of a more complicated harbor appears qualitatively to be a combination of the response of the individual basins with certain effects relating to the influence of one basin type on the other.

Various investigators have proposed the use of side channel resonators to eliminate or at least reduce the effect of resonance on harbors (see Valembois (1953), James (1968)). These resonators are rectangular channels of various lengths which are connected perpendicular to the main entrance channel. Since the effect of the length of an entrance channel on the response of a circular harbor had been investigated, it was considered logical to extend this to a minimal investigation of the effect of resonators of two different lengths on the response of the harbor shown in Fig. 33. The channels were located approximately one-third of the length of the entrance channel from the open-sea with a width equal to the width of the entrance channel. The cases chosen were for lengths of the resonators equal to one-half and one-quarter of the length of the main channel. The maximum response curves for these two harbor systems are presented in Figs. 34 and 35.

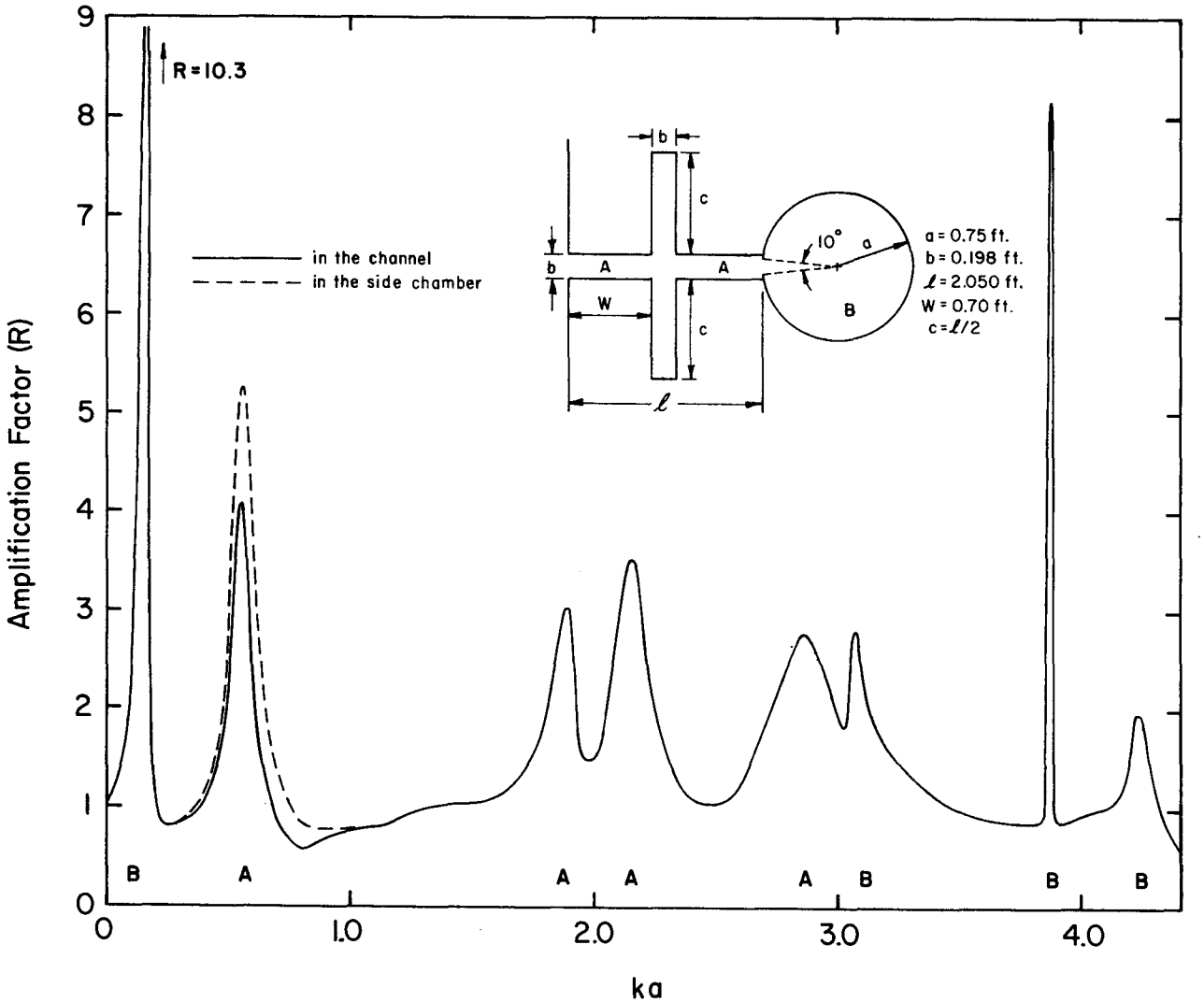

Fig. 34 Maximum Response Curve for Circular Harbor Coupled to Rectangular Entrance Channel with Side Chambers ($c/\ell = \frac{1}{2}$)

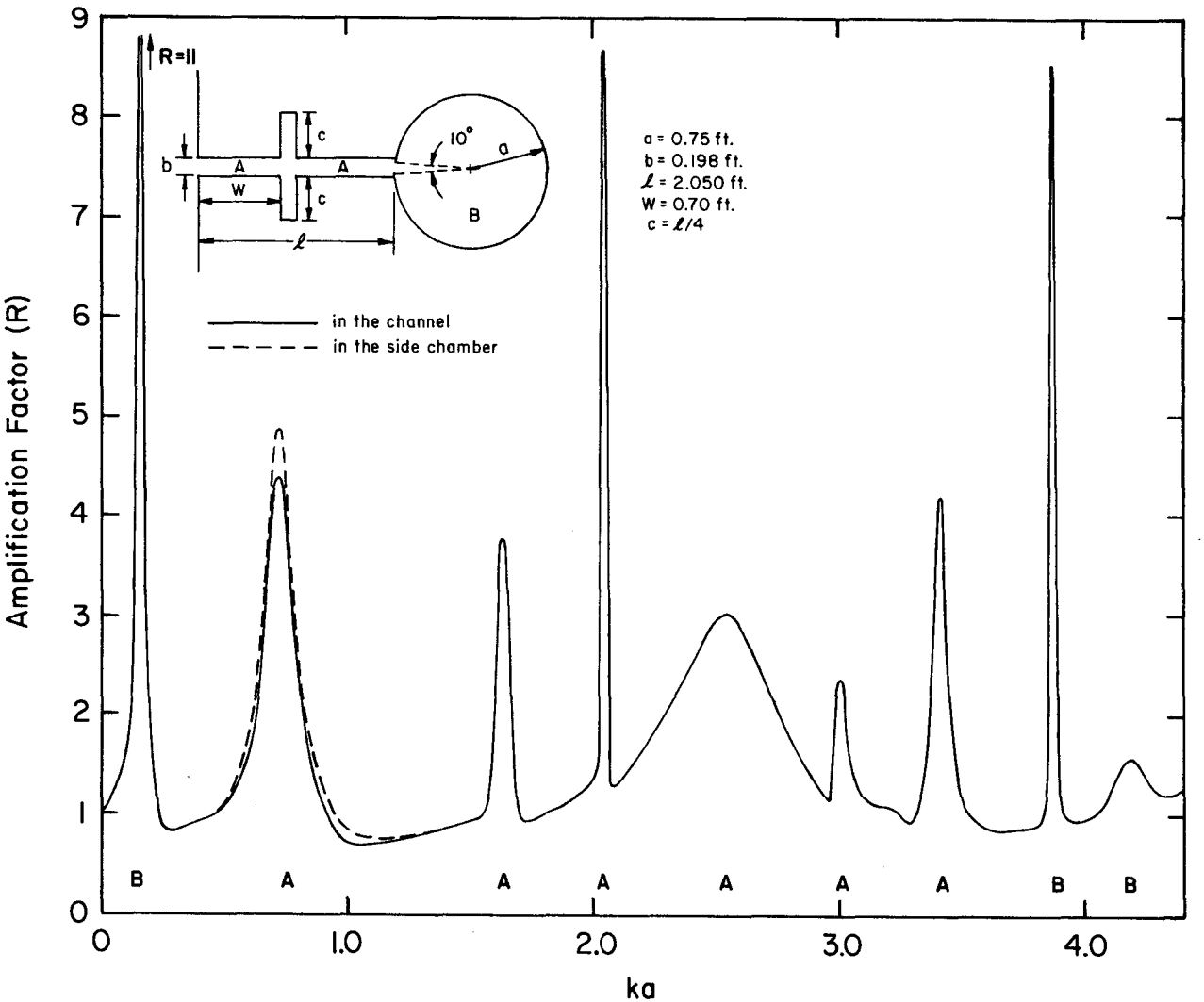

Fig. 35 Maximum Response Curve for Circular Harbor Coupled to Rectangular Entrance Channel with Side Chambers ($c/\ell = \frac{1}{4}$)

Fig. 34 shows the response curve presented with the ordinate and abscissa as previously defined for the case with the resonators one-half the length of the main entrance channel; the arrangement is shown in the inset in this figure. For this harbor system the wave number of the pumping mode has changed only slightly while its maximum response has been reduced from about seventeen to ten by the addition of the resonator. The next mode has been shifted to a smaller wave number and attenuated by a factor of nearly two by the resonator. It is noted that two curves are shown for this peak: one where resonance is in the entrance channel (the solid curve) and a curve for which resonance is in the side channel or resonator (the curve composed of long dashes). For this case, resonance in the side-channel dominates; however, with respect to the overall response of the harbor this is not considered important. The next four modes are not modified appreciably except for some shift in the resonant wave numbers. The seventh mode which is associated with resonance in the circular harbor is affected by the side channel resonators by both an increase in amplification compared to the case shown in Fig. 33 and by a decrease in the bandwidth of the peak. Although theoretically this appears to result in a more responsive harbor, the reduction in the bandwidth of the mode makes it more susceptible to viscous effects and hence the actual response may be less than for the corresponding mode shown in Fig. 33 (see Section 4. 4).

The response curve which is obtained when the length of the side channel resonator is halved is presented in Fig. 35. The peaks which are labeled as B (occurring in the circular basin) are similar in all three cases (Figs. 33, 34, and 35). There is a slight change in the maximum

amplification of the pumping and the second mode, but essentially the appearance is similar. However, the modes which correspond to resonance in the entrance channel are quite different with respect to wave number as well as amplification. Again viscous effects would probably modify these peaks significantly.

The objective of this phase of the investigation was only to demonstrate the applicability of the coupled basin theory to the evaluation of resonance in a complicated basin system and it certainly does not represent a comprehensive study of coupled basin systems, entrance channel effects, or the effect of side-channel resonation. The detailed study of the effect of location and dimensions of entrance channel and side-channel resonators would be an interesting extension to the present study.

4.3.3 Rectangular and Circular-Segment Coupled Harbor

The response of another example of coupled basins to periodic incident waves was considered. The harbor consisted of a rectangular entrance channel (connected to the open-sea with a fully open entrance) coupled to a circular sector of 140^{o} central angle. In Fig. 36, the response curve at the center of the backwall is presented; the harbor and the nomenclature used are shown in the inset in this figure. The ordinate is the amplification factor R, as previously defined, and the abscissa is the wave number parameter ka where a is the radius of the circular sector. This harbor has been studied previously by Carrier, Shaw, and Miyata (1971) employing a different method of analysis. The theoretical curve shown in Fig. 36 is obtained by using the coupled-basins theory presented in Chapter 2 with the harbor divided

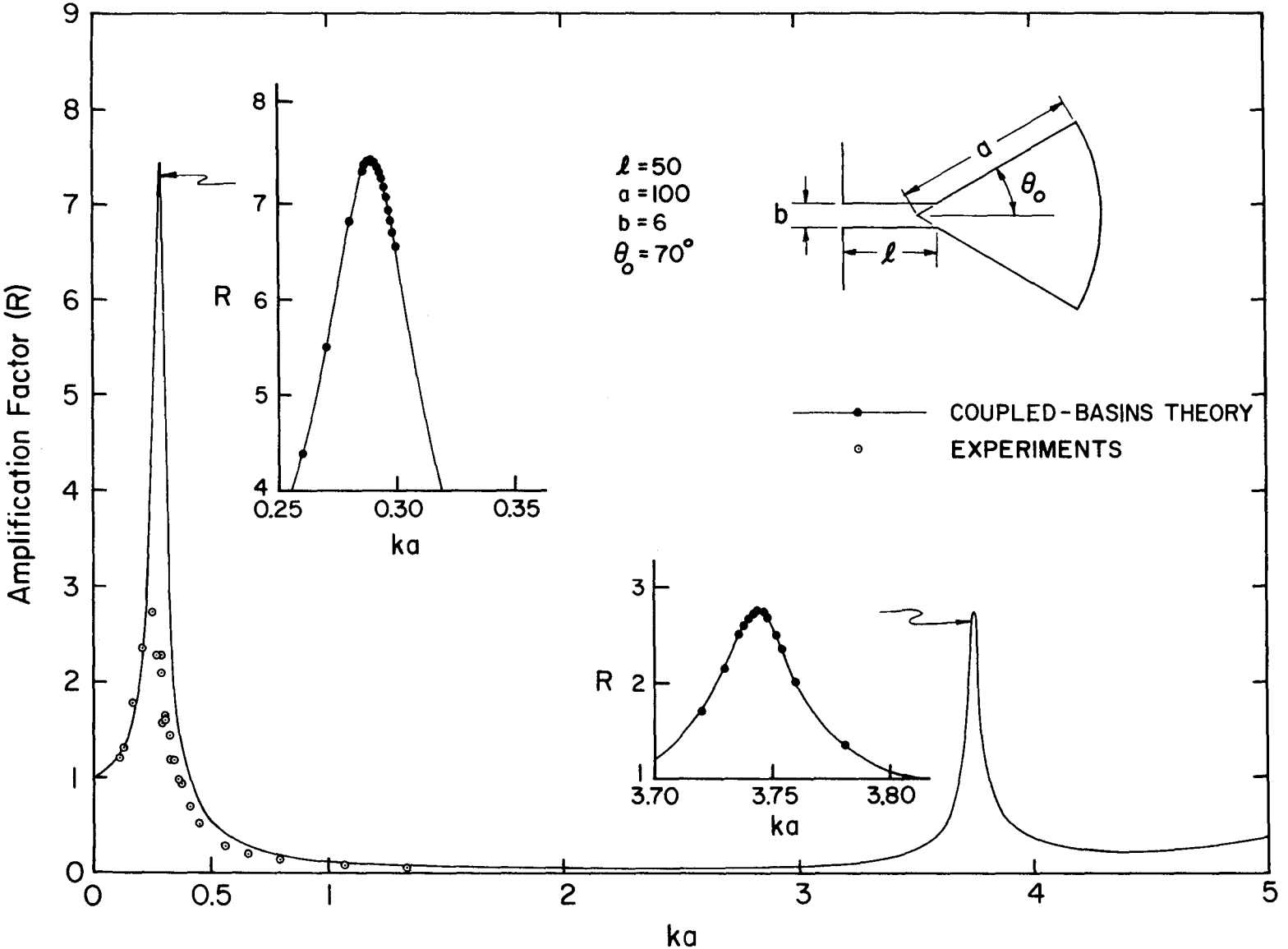

Fig. 36 Response Curve for a Circular-Segment Harbor with Entrance Channel; at Center of Backwall ($r = a$, $\theta = 0^{o}$)

into two regions: the rectangular entrance channel and the circular sector. The value of ka for the first two modes of oscillation are: ka = 0.289 and ka = 3.744. The first resonant mode of oscillation is a pumping mode where the maximum amplification (an amplification factor of 7.48) occurs at the center of the backwall. This value of amplification factor is very much smaller than the value reported by Carrier, Shaw, and Miyata (1971) in which they have reported an amplification factor of about 22. For the second resonant mode the amplification factor computed using the present theory is 2.75 which is close to the value of about 2.9 reported by Carrier, Shaw, and Miyata (1971).

Shown as insets in Fig. 36 are the computational details of the response near resonance for the two modes; the data from the coupled-basins theory are indicated by solid circles. It is seen that the maximum amplification was effectively determined for each mode of oscillation. Thus, it appears that the difference in the amplification factor for the pumping mode between the present theory and the theory of Carrier, Shaw, and Miyata can be attributed to differences between the methods rather than incomplete computations near resonance.

In addition to the theoretical results, some experiments were conducted in the laboratory for comparison. Due to certain experimental limitations and to cover the range of ka for the first mode of oscillation it was necessary to use a small harbor model. Referring to the sketch shown in Fig. 36, the dimensions of the harbor model used for the experiment were: $\theta_o = 70^o$, a = 3 in., ℓ = 1.5 in., b = 0.18 in. Experimental data are shown as open circles in Fig. 36. It is seen

that away from resonance the theory agrees reasonably well with the experiments. However, at resonance the maximum amplification measured was approximately 40% of the maximum predicted by the linear inviscid theory; this reduction was due undoubtedly to viscous effects which were quite important in these experiments because of the small width to depth ratio of the entrance channel.

The amplitude distributions determined theoretically for the first two mode of oscillation are presented in Figs. 37 and 38. Fig. 37 shows the water surface elevation for the pumping mode (ka = 0.289) increasing radially with distance from the entrance with the wave amplitudes inside the circular-sector region nearly uniform in the θ-direction at a given radius. The variation of the water surface elevation inside the harbor for the second mode of oscillation (ka = 3.744) is shown in Fig. 38. For this mode of oscillation the maximum wave amplitude occurs within the entrance channel relatively near the entrance to the circular segment region with a nodal line present inside the circular sector basin. Thus, negative water surface displacements are produced in the region near the backwall.

The results presented in this chapter have shown the applicability of the present theory in analyzing the coupled basins problem. For a complicated harbor geometry it may not be possible or economical to analyze the response using the method developed by Lee (1969); however, problems of computer storage size and economy of computation may be overcome using the present theory where the harbor region is divided into several basins. The boundary segment size in each basin must

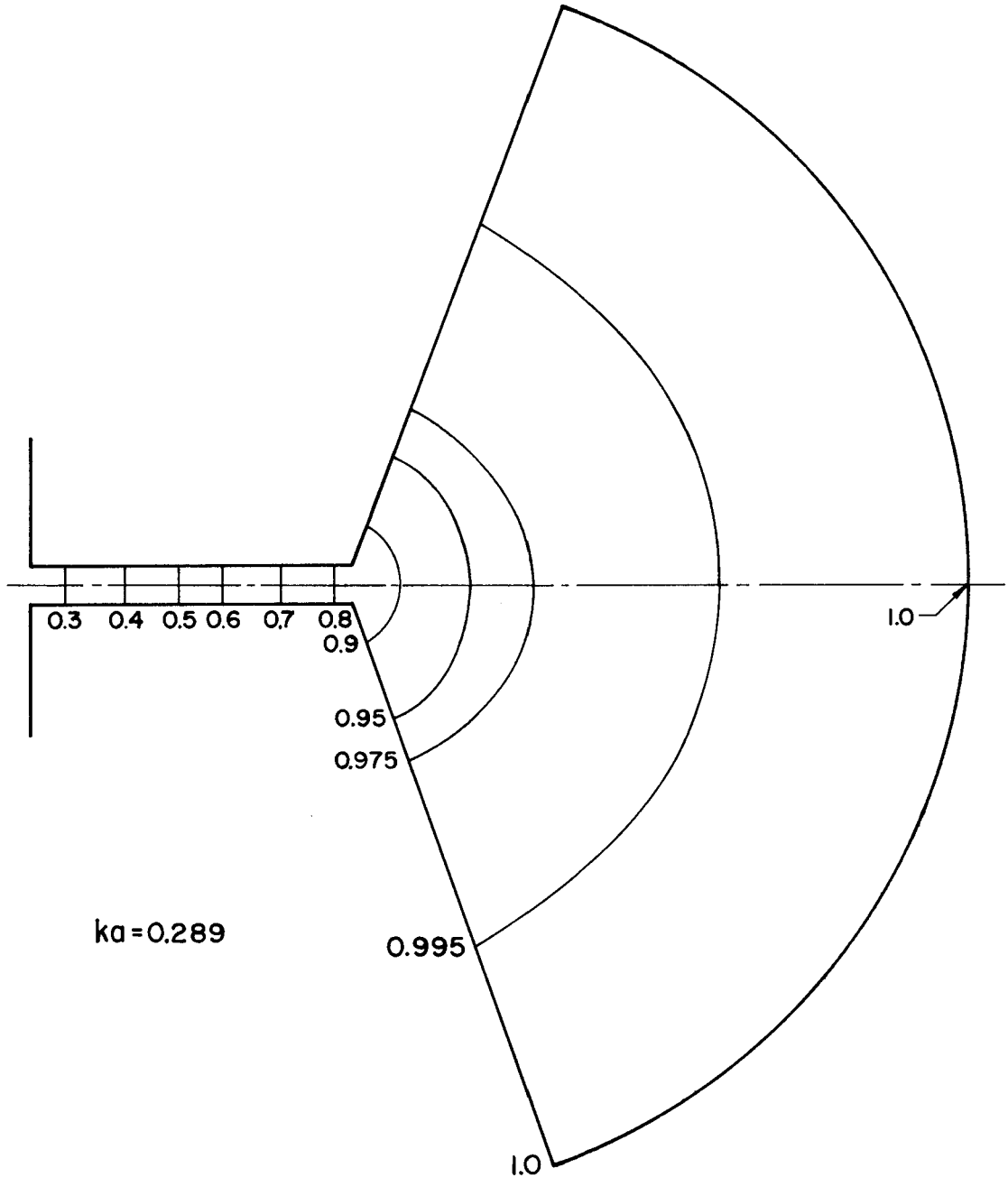

Fig. 37 Shape of Mode 1 for Circular-Segment Harbor; ka = 0.289

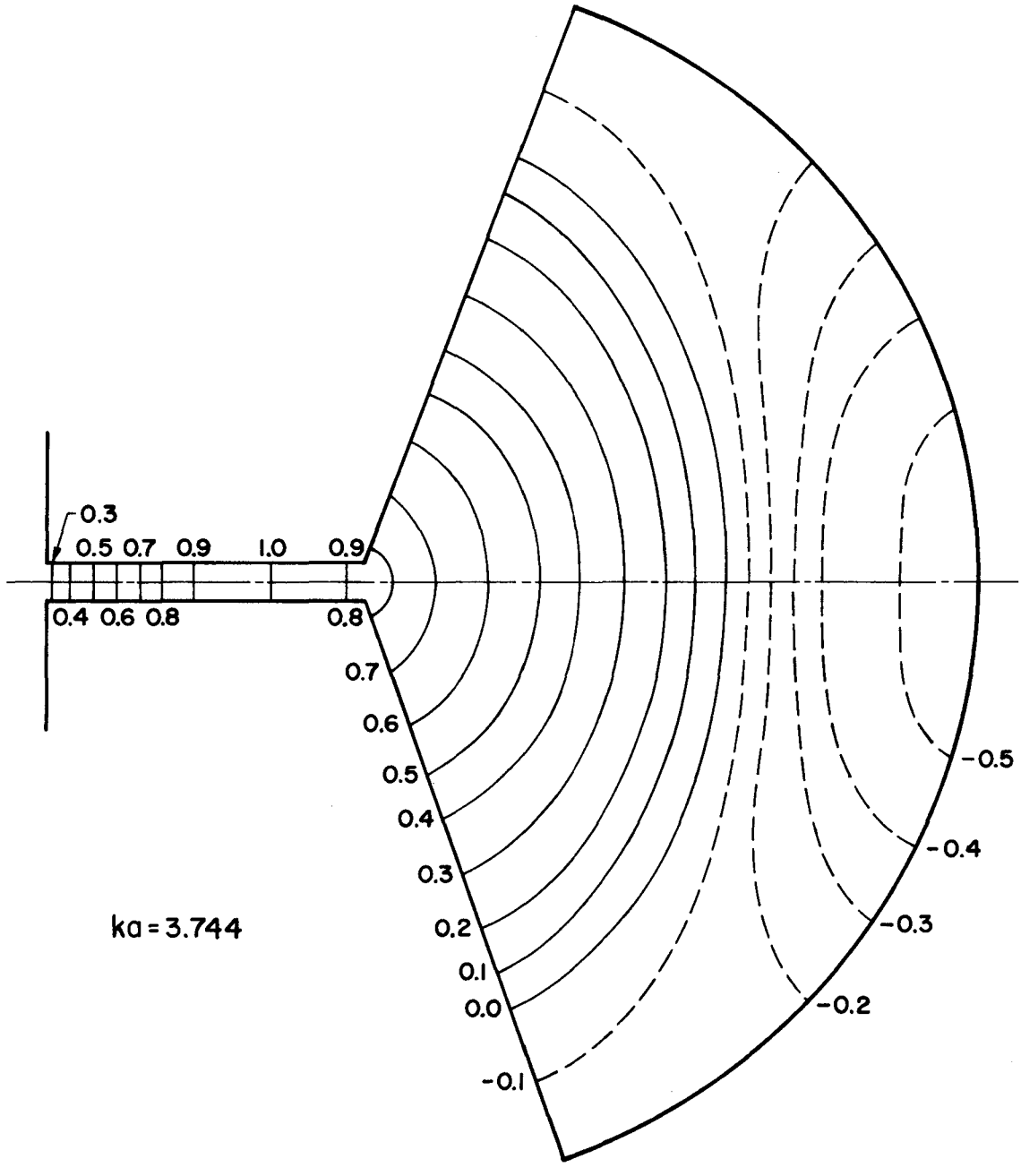

Fig. 38 Shape of Mode 2 for Circular-Segment Harbor; ka = 3.744

still be small compared to the wave length; the criterion suggested by Lee (1969) that the maximum boundary segment size be smaller than one-tenth of the smallest wave length studied also applies to the present theory.

4.4 THE EFFECT OF ENERGY DISSIPATION ON HARBOR RESONANCE

In this section the effect of energy dissipation on the response of a harbor will be discussed qualitatively with attention given to the differences between hydraulic models and the corresponding prototype harbors near resonance.

There are three major effects of viscous dissipation on the response of a dynamic system; to describe these it is useful to refer to the simple example of the forced oscillation of a single-degree-of-freedom oscillator (such as a spring-mass-dashpot system) described by the following equation of motion:

$$m\ddot{x} + c\dot{x} + k_* x = F_o \sin \omega t \tag{36}$$

where m is the mass of the oscillating body, c is a coefficient of damping for the system, k_* is the spring constant, x is the displacement, and F_o is the amplitude of an applied force with circular frequency ω. Eq. 36 may be rewritten as:

$$\ddot{x} + 2\zeta\omega_n\dot{x} + \omega_n^2 x = X_{ST}\omega_n^2 \sin \omega t \tag{37}$$

where $\zeta = c/c_c$, c_c is defined as a critical damping coefficient equal to $2m\omega_n$ where $\omega_n^2 = k_*/m$, and X_{ST} is the static displacement of the spring system under the applied force F_o and is equal to F_o/k_*. The dynamic

response of this system is then described by:

$$M = \frac{1}{\sqrt{\left[1-\left(\frac{\omega}{\omega_n}\right)^2\right]^2 + \left[2\zeta\frac{\omega}{\omega_n}\right]^2}} \tag{38}$$

In Eq. 38 M is the ratio of the maximum excursion of the oscillating mass at the given frequency to the static movement of the mass caused by F_o, i.e., X_{ST}. Eq. 38 is the well known expression for the system amplification which indicates that the amplification goes to infinity for zero damping when the forcing frequency equals the natural frequency, i.e., $\omega/\omega_n = 1$. The phase angle between the forcing function and the system output is given by:

$$\tan \phi = \frac{2\zeta\frac{\omega}{\omega_n}}{1 - \left(\frac{\omega}{\omega_n}\right)^2} \quad . \tag{39}$$

From Eq. 38 it is seen that the amplitude at resonance can be expressed as a first approximation for small damping as:

$$M_R = 1/2\zeta \, , \tag{40}$$

where the subscript R refers to resonance. The shift of the resonant frequency caused by damping can be shown to be:

$$(\omega/\omega_n)_R = \sqrt{1 - 2\zeta^2} \quad . \tag{41}$$

The peakedness of a response curve is usually described by the frequency bandwidth of the half-power point, i.e., the point at which the power has dropped to one-half its peak value or the amplitude to 0.707 of

its peak. For small values of the damping factor, ζ, the frequency limits of the half-power point are given approximately by:

$$\omega/\omega_n = \sqrt{1 \pm 2\zeta}\,. \tag{42}$$

which gives a bandwidth for the half-power point of $\Delta(\omega/\omega_n) \cong 2\zeta$.

Eqs. 40, 41, and 42 are shown in Fig. 39 with the damping factor as the abscissa and the ordinate as the amplification factor at resonance, the shift of the resonant frequency due to damping, and the frequency bandwidth of the half-power point. One obvious feature of these curves is that the amplification factor and the bandwidth of the half-power point are affected much more by damping than is the resonant frequency. For the range of damping factor shown ($0.05 < \zeta < 0.3$) the amplification factor at resonance and the half-power bandwidth change by a factor of six while the resonant frequency shifts by only about 4% to lower frequencies. Therefore, for the single-degree-of-freedom oscillator the major effect of increased damping on the resonant response are to decrease the amplification at resonance and increase the frequency bandwidth at the half-power point while maintaining approximately the same resonant frequency of the system.

Miles and Munk (1961) and Ippen and Goda (1963) have shown that the dynamics of a harbor near resonance, at least for the lowest mode of oscillation, are similar to the single-degree-of-freedom oscillator. Therefore, in qualitative sense one would expect similar effects of damping on the harbor response with respect to the amplification at resonance, the frequency bandwidth of the half-power point and the shift in the resonant frequency.

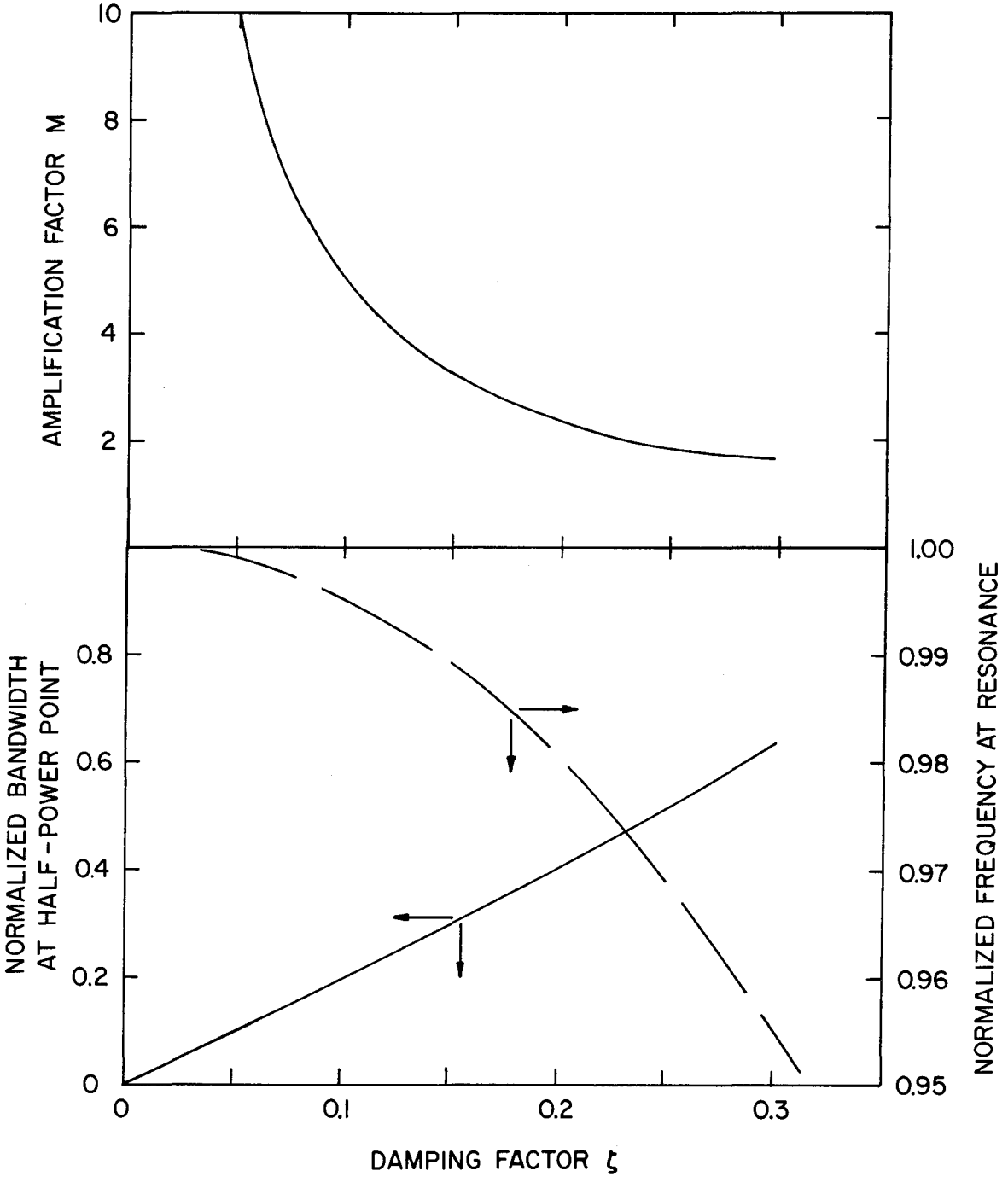

Fig. 39 The Effect of Damping in a Simple Spring-Mass-Dashpot System

These effects would apply in the same way to both a hydraulic model and the corresponding prototype harbor; however, the relative energy dissipation (or the damping factor) in the two cases may be quite different, i.e., scale effects may be important. In both model and prototype generally there are at least five regions where energy dissipation can be important: at the harbor entrance, at the internal boundaries of the harbor, along the bottom, at internal structures such as piers, moles etc., and internal viscous dissipation in the wave system. These forms of dissipation will be discussed with respect to the model and the prototype, and some attempt will be made to indicate the importance of scale effects, i.e., the reliability of scaling up response characteristics of the model to the prototype.

The dissipation of energy at the harbor entrance can be divided into two parts: the energy loss associated with separation and that due to boundary friction. For the lower modes of oscillation where wave periods and entrance velocities are relatively large the former would probably be more important. If the effect of separation is important in defining the entrance losses probably it is equally important in both model and prototype and scale effects for this type of dissipation would be relatively unimportant. Thus, if this loss could be determined in the model it could be directly scaled to the prototype. The effect of this loss has been demonstrated by Ippen and Raichlen (1962) in the study of the response of two highly reflective coupled rectangular basins. In that case the resonant response of a small rectangular harbor was investigated with and without a screen (16 mesh/inch) stretched across the entrance.

Depending upon the peakedness of the response curve, the response at resonance was reduced to 80% to 40% of the value without the screen by the increased entrance loss. Such dissipation could be quite important in reducing harbor resonance problems. The other aspect of entrance dissipation, that due to boundary friction at the entrance, will be discussed later.

Keulegan (1959) reported on an investigation of the boundary damping and internal dissipation associated with finite amplitude standing waves in a small rectangular basin of width b. In his study the waves were considered to be damped exponentially and an exponential modulus of decay, α, was defined such that:

$$\frac{A}{A_o} = e^{-\alpha \frac{t}{T}} \tag{43}$$

and α was found to be:

$$\alpha = \left(\frac{\nu T}{\pi b^2}\right)^{\frac{1}{2}} \frac{(\pi + kb) + kb(\pi - 2kh)}{\sinh 2kh} + 2(kb)^2\left(\frac{\nu T}{b^2}\right) \tag{44}$$

wherein ν is the kinematic viscosity and all other quantities have been defined previously. The first term on the right in Eq. 44 represents laminar damping due to the boundaries (the walls and the bottom) and the second term describes the internal dissipation. Since the first term is usually much greater than the second, the effect of the latter will not be considered in this discussion.

Considering only the possibility of laminar dissipation at the boundaries, it is interesting to use Eq. 44 (the first term) to see how this modulus varies with the size of a hydraulic model. If two

geometrically scaled models are considered the value of the ratio of α for the two models is considered to be an indication of the relative importance of dissipation in the two models. The subscript r is used to denote the ratio of a quantity in the smaller model to the corresponding quantity in the larger model. For the same relative wave number in both models, i.e., $(kb)_r = (kh)_r = 1$, Eq. 44 reduces to the following for the ratio of the boundary dissipation moduli:

$$\alpha_r = \frac{T_r^{\frac{1}{2}}}{b_r} \tag{45}$$

Since the models are operated as Froude models, $T_r = L_r^{\frac{1}{2}}$ and $b_r = L_r$ and Eq. 45 becomes:

$$\alpha_r = \frac{1}{L_r^{\frac{3}{4}}} \quad . \tag{46}$$

Eq. 46 shows, for geometrically similar models, the smaller model would have greater relative dissipation than the larger model. However, if the models are not geometrically similar then, as will be shown, the complete first term of Eq. 44 must be used in making a comparison.

Lee (1969) presented the results of both theory and experiment for a model of the East and West Basins of Long Beach Harbor. (These results are also presented in Figs. 8 through 11 of this report and compared to the results obtained from the coupled-basins theory.) Knapp and Vanoni (1945) used a hydraulic model to investigate the alignment of a mole to protect this part of Long Beach Harbor and some selected results of their experiments were also presented and

discussed by Lee (1969). Lee's experiments were conducted in a constant depth model with a horizontal length scale of 1/4700 and an average vertical length scale of 1/40. The model of Knapp and Vanoni more realistically modeled depth effects (although these effects are very small for this harbor) since a horizontal scale of 1/480 and a vertical scale of 1/240 was used. For the resonant mode of oscillation which corresponds to a period of about 6 min. ($ka \cong 3.3$, where "a" is a typical length dimension of 6768 ft in the prototype) it was found that Lee's model gave an amplification factor nearly 2.5 times that observed in the Knapp and Vanoni model. This is contrary to what Eq. 46 predicts if the horizontal scales alone are considered; for these scales Eq. 46 says that the damping modulus for the smaller harbor should be nearly six times that for the larger model. This contradiction is explained by the fact that the two models are not geometrically similar and the complete first term of Eq. 44 must be used in making a comparison.

The characteristics of these two models for the 6 min. mode in the prototype are shown in Table 1. In this table, the parameter "a" denotes the length of the North side of the West Basin and "b" is the maximum width of that basin. Using these data and applying Keulegan's analysis for the sloshing in a rectangular basin, considering only boundary dissipation, the ratio of the damping modulus α for Lee's model to the modulus for Knapp and Vanoni's model is 1/1240. This shows that the expected dissipation in the larger model would be much

Table 1. Characteristics of Two Hydraulic Models of Long Beach Harbor.

	Lee	Knapp & Vanoni
L_{r_h}	1/4700	1/480
L_{r_v}	1/40	1/240
a (ft)	1.44	14.1
b (ft)	0.95	9.27
h (ft)	1.0	0.167
k (1/ft)	2.26	0.23
T (sec)	0.745	11.8

greater than that in the smaller model primarily because the models are not geometrically similar and the vertical scale of the smaller model is more exaggerated. Obviously the magnitude of the damping modulus ratio given is only an indication of the relative importance of dissipation at the two scales and it is not an exact measure of the relative dissipation in the two models.

A different problem arises when model results are to be scaled up to prototype systems, since the boundary layers in a model are probably laminar whereas in the prototype turbulent boundary layers are most probable. Since Keulegan's treatment considers laminar damping only, this approach is not applicable. However, to determine trends in dissipation, steady flow considerations could be applied to this problem for the lower modes of oscillation, once the wave periods of these modes are usually very large. Assuming steady flow, the boundary drag

can be defined in terms of an average skin friction coefficient, C_f, which takes on different forms for laminar and turbulent flow. The power dissipated due to boundary shear can be expressed as:

$$P_d = C_f B \frac{\rho}{2} U^3 \qquad (47)$$

where B is a surface area and U is a characteristic velocity of the system.

If the model were truly a Froude model the power dissipated would scale up in the prototype by $L_r^{7/2}$ which assumes the same skin friction coefficient in the model as in the prototype, i.e., $C_{f_r} = C_{f_m} / C_{f_\rho} = 1$. Since the model is assumed to operate in the laminar flow region and the prototype in turbulent flow, this ratio will not be unity and the magnitude of C_{f_r} will indicate whether proportionately more energy is dissipated in the model than in the prototype, e.g., if $C_{f_r} > 1$ the model would dissipate relatively more energy than the prototype and for $C_{f_r} < 1$ the opposite is true. These skin friction coefficients can be expressed as:

for laminar flow: $$C_{f_m} = \frac{1.33}{\mathbb{R}_m^{\frac{1}{2}}} ,$$

and for turbulent flow: $$C_{f_p} = \frac{0.074}{\mathbb{R}_p^{1/5}}$$

where $\mathbb{R}$ is the Reynolds Number based on a horizontal length, and as before the subscripts m and p indicate model and prototype respectively. Hence, for a Froude model the skin friction coefficient ratio becomes:

$$C_{f_r} = \frac{18}{L_r^{\frac{3}{4}} R_p^{0.3}} \tag{48}$$

wherein L_r is the ratio of a horizontal model dimension to its corresponding prototype dimension. For the sake of this discussion where only trends are important the velocity which will be used in defining the Reynolds Number is the maximum water particle velocity in a wave and the wave length will be used as the characteristic length dimension of the system.

It is conceivable that for large values of L_r and the Reynolds Number, C_{f_r} would be less than unity indicating proportionately more dissipation in the prototype than in the model. However, consider the following example: the length scale (L_r) is 1/100, the prototype depth is 30 ft, and the wave period is 2.8 min. (the wave length would be 5000 ft). Taking a wave height of 2 ft, as a first approximation, the maximum water particle velocity for this long wave would be 1 ft/sec. The Reynolds Number based on this velocity and wave length would be about 5×10^8. Therefore, from Eq. 48, C_{f_r} would be 1.4, and for this case proportionately more energy would be dissipated on the bottom in the model than in the prototype.

Two aspects of energy dissipation in harbors have not been discussed yet. The first deals with the damping of waves inside the harbor due to the permeability of the bottom and the second deals with energy dissipation at the boundaries due to wave run-up and breaking on rough embankments and structures within the harbor.

Reid and Kajuira (1957) have treated the problem of viscous effects associated with percolation into a permeable sea bed of infinite thickness caused by temporal and spacial pressure distributions at the sea bed. Considering exponential damping with distance ($a = a_o e^{-Dx}$ the damping modulus given by them is at worse:

$$D = 0.123 \frac{\beta\sqrt{2\pi g}}{\nu h^{3/2}} \tag{49}$$

and less for values of h/L_o greater and less than 0.13. The quantity β in Eq. 49 is a permeability coefficient equal to about 10^{-9} ft^2 for ordinary sand. Thus, for a 30 ft depth Eq. 49 gives a value of D of a about 10^{-6} ft^{-1} which indicates that for most purposes this aspect of dissipation can be neglected compared to other forms of boundary dissipation.

Energy dissipation around the harbor periphery due to wave run up and breaking on beaches and revetted structures cannot be evaluated specifically due to the wide range of structures which may be located at the boundaries of each particular harbor. It is possible that with the proper design of internal structures the energy loss in a harbor due to this type of dissipation can completely overshadow any other form of energy loss.

Ippen and Goda (1963) analytically investigated the effect of energy dissipators on the response of a fully open narrow rectangular harbor connected to the open-sea; their development is quite instructive in describing the effect of the reflective characteristics of the structures

on the response and it is summarized here. They determined the response of the harbor as a function of a reflection coefficient defined in terms of the standing wave amplitude in the harbor as:

$$A = A_o(1 + K)$$

where A is the standing wave amplitude, A_o is the amplitude of a progressive wave within the harbor, and K is the reflection coefficient. Thus, for K = 1 (perfect reflection) $A = 2A_o$ and for K = 0 (zero reflection) $A = A_o$. When the response is determined assuming a two dimensional oscillation in the harbor matched at the entrance to the solution for the open-sea, the following simple expression can be obtained which is a first approximation to the response of the narrow, fully-open harbor at resonance:

$$R_R \cong \frac{1}{kb + \delta} \leq \frac{2}{1 - K} \qquad (50)$$

where b is the width of the harbor and is equal to the entrance width for the fully-open harbor and $\delta = (1 - K)/(1 + K)$. As an example, consider a fully open harbor where the ratio of the width of the harbor to its length is 0.02 and the normalized resonant wave number of the fundamental mode is $k\ell \cong \pi/2$. From Eq. 50 the undamped amplification at resonance would be 63.6. For boundary reflection coefficients of K = 0.9, 0.7, and 0.5 the corresponding amplification factors at resonance are R_R = 14.7, 5.2, and 2.9 respectively. Thus, with a general internal reflection coefficient of only 0.9 the harbor response would be decreased more than four times from its undamped value.

In the case of a harbor with a more complicated shape, at the present time it is not possible to evaluate the effect of this type of boundary dissipation on the response. However, the example just presented indicates that this effect can be important and makes it very difficult to scale up the results of a model study to a prototype scale with any reliability. The only obvious assurance one has is that the response would be less than an inviscid theory predicts. Nevertheless some of the methods describe here can provide a guide to an engineering decision; but more attention must be given to this aspect of the problem in future research to lead to a more generally applicable theory. On the other hand, as mentioned earlier, the inviscid theory developed and presented in this report effectively describes the important wave periods for resonance even if there is moderate dissipation in the prototype; this in itself is a useful guide for engineering design.

CHAPTER 5

CONCLUSIONS

The following major conclusions can be drawn from this study:

1. The theory developed herein and termed the coupled-basins theory predicts the response of an arbitrary shape harbor with constant depth which can be divided into several interconnected basins.
2. The theory agrees well with experimental results obtained from two connected circular harbors as well as with results obtained in a previous study dealing with the oscillations of the East and West Basins of Long Beach Harbor.
3. The coupled-basins theory reduces both the computer time and the required computer storage in predicting the response of a harbor. Therefore, this increase in economy and storage may allow this type of approach to be used in predicting the response of a harbor to shorter wavelengths than would be possible using the single basin theory.
4. When harbors of simple geometry are connected, the response of the resultant harbor system in some ways appears to be a superposition of the response of the individual harbors. This indicates that care must be taken in adding internal basins to real harbors so that additional response problems do not occur after the addition is completed.

5. The effect of the superposition can be seen also in the amplitude distributions within the harbors for the various resonant modes of oscillation.
6. The effect of an entrance channel on the response of the harbor can be significant. Again, superposition is important and as the length of the entrance channel increases the response of the main harbor changes considerably.
7. Side channel resonators added to an entrance channel may or may not improve the resonant conditions depending upon the importance of viscous effects in the problem as well as the length and location of the chambers and the wave periods involved.
8. Certain general conclusions can be drawn regarding viscous effects in harbor resonance studies. Two important regions for viscous dissipation are at the entrance and at the boundaries. Only general indications can be given as to the importance of these two effects in reducing the effect of resonance as predicted by an inviscid theory. Some conclusions can be drawn about the effect of boundary dissipation on model scaling and model - prototype relations. However, at the present time, these results are not conclusive and additional research in this area is needed.

LIST OF REFERENCES

1. Apté, A. S. (1957), "Recherches Theoriques et Experimentales sur Les Mouvements des Liquids Pesants Avec Surface Libre", Publications Scientifiques et Techniques du Ministere de L'Air, No. 333.

2. Baker, B. B., and Copson, E. T. (1950), The Mathematical Theory of Huygen's Principle, Oxford University Press, London.

3. Banaugh, R. P., and Goldsmith, W. (1963), "Diffraction of Steady Acoustic Waves by Surfaces of Arbitrary Shape", The Journal of the Acoustical Society of America, Vol. 35, No. 10, pp. 1590-1601.

4. Biesel, F., and LeMehaute, B. (1955), "Etude Theorique de La Reflexion de La Houle sur Certains Obstacles," LaHouille Blanche, March-April, pp. 130-140.

5. Biesel, F., and LeMehaute, B. (1956), Mouvements de Resonance a Deux Dimensions dans une Enceinte Sous L'Action d'Ondes Incidentes", LaHouille Blanche, July-August, pp. 348-374.

6. Carrier, G. F., Shaw, R. P., and Miyata, M., "The Response of Narrow-Mouthed Harbors in a Straight Coastline to Periodic Incident Waves", Journal of Applied Mechanics, Vol. 38, Series E, No. 2, pp. 335 - 344.

LIST OF REFERENCES (Continued)

7. Hwang, L. S., and Tuck, E. O. (1970), "On the Oscillations of Harbors of Arbitrary Shape", Journal of Fluid Mechanics, Vol. 42, pp. 447-464.

8. Ippen, A. T., Editor (1966), Estuary and Coastline Hydrodynamics, McGraw-Hill Book Company, New York.

9. Ippen, A. T., and Goda, Y. (1963), "Wave Induced Oscillations in Harbors: The Solution for a Rectangular Harbor Connected to the Open-Sea", Report No. 59, Hydrodynamics Laboratory, M. I. T.

10. Ippen, A. T., and Raichlen, F. (1962), "Wave Induced Oscillations in Harbors: The Problem of Coupling of Highly Reflective Basins", Report No. 49, Hydrodynamics Laboratory, M. I. T.

11. Ippen, A. T., Raichlen, F., and Sullivan, R. K. (1962), "Wave Induced Oscillations in Harbors: Effect of Energy Dissipators in Coupled Basin Systems", Report No. 52, Hydrodynamics Laboratory, M. I. T.

12. James, W. (1968), "Rectangular Resonators for Harbor Entrances", Proceeding of the 11th Conference on Coastal Engineering, pp. 1512-1530.

13. Keulegan, G. H. (1959), "Energy Dissipation in Standing Waves in Rectangular Basins", Journal of Fluid Mechanics, Vol. 6, pp. 33-50.

LIST OF REFERENCES (Continued)

14. Knapp, R. T., and Vanoni, V. A. (1945), "Wave and Surge Study for the Naval Operating Base, Terminal Island, California", Hydraulic Structure Laboratory of the California Institute of Technology.

15. Kravtchenko, J., and McNown, J. S. (1955), "Seiche in Rectangular Ports", Quarterly of Applied Mathematics, Vol. 13, pp. 19-26.

16. Lee, J. J. (1969), "Wave-Induced Oscillations in Harbors of Arbitrary Shape", Report KH-R-20, W. M. Keck Laboratory of Hydraulics and Water Resources, California Institute of Technology.

17. Lee, J. J., and Raichlen, F. (1970), "Resonance in Harbors of Arbitrary Shape", Proceedings of the 12th Conference on Coastal Engineering, Washington, D. C., Chapter 131, pp. 2163-2180.

18. Lee, J. J. (1971), "Wave-Induced Oscillations in Harbors of Arbitrary Geometry", Journal of Fluid Mechanics, Vol. 45, pp. 375-394.

19. Leendertse, J. J. (1967), "Aspects of a Computational Model for Long-Period Water Wave Propagation", Memorandum, RM-5294-PR, The Rand Corporation.

20. LeMehaute, B. (1955), "Two Dimensional Seiche in a Basin Subjected to Incident Waves", Proceeding Fifth Conference on Coastal Engineering, Berkeley, California, pp. 119-150.

LIST OF REFERENCES (Continued)

21. LeMehaute, B. (1960), "Periodical Gravity Wave on a Discontinuity", Journal of the Hydraulics Division, ASCE, Vol. 86, No. HY 9, pp. 11-41.

22. LeMehaute, B. (1961), "Theory of Wave Agitation in a Harbor", Journal of the Hydraulics Division, ASCE, Vol. 87, No. HY 2, pp. 31-50.

23. LeMehaute, B. (1962), Discussion of the paper "Harbor Paradox" by J. Miles and W. Munk, Journal of the Waterways and Harbors Division, ASCE, Vol. 88, No. WW 2, pp. 173-185.

24. McNown, J. S. (1952), "Waves and Seiche in Idealized Ports", Gravity Wave Symposium, National Bureau of Standards Circ. 521.

25. Mikhlin, S. G., and Smolitskiy, K. L. (1967), Approximate Methods for Solution of Differential and Integral Equations, American Elsevier Publishing Company, New York.

26. Miles, J., and Munk, W. (1961), "Harbor Paradox", Journal of the Waterways and Harbors Division, ASCE, Vol. 87, No. WW 3, pp. 111-130.

27. Miles, J. (1970), "Resonant Response of Harbors (Harbor Paradox Revisited)", 8th Symposium on Naval Hydrodynamics, Pasadena, California, (in press).

28. Morse, P. M., and Feshback, H. (1953), Method of Theoretical Physics, Vol. I and II, McGraw-Hill Book Company, New York.

29. Muskhelishvili, N. I. (1946), Singular Integral Equations, P. Noordhoff Ltd., Groningen, Holland.

30. Raichlen, F. (1965), "Wave-Induced Oscillations of Small Moored Vessels", Report KH-R-10, W. M. Keck Laboratory of Hydraulics and Water Resources, California Institute of Technology.

31. Raichlen, F. and Ippen, A. T. (1965), "Wave Induced Oscillations In Harbors", Journal of the Hydraulics Division, ASCE, Vol. 91, No. HY 2, pp. 1-26.

32. Reid, R. O. and Kajuira, K. (1957), "On the Damping of Gravity Waves Over a Permeable Sea Bed", Trans. AGU, Vol. 38, (5), pp. 662-666.

33. Valembois, J. (1953), "Investigation of the Effect of Resonant Structures on Wave Propagation", Proceedings Minnesota Intern. Hydraulics Convention, St. Anthony Falls Hydraulic Lab., Minneapolis, Minn., pp. 193-199.

34. Wilson, B. W. (1959), "Research and Model Studies on Wave Action in Table Bay Harbor, Cape Town", Transactions of the South African Institution of Civil Engineers, Vol. I, No. 6 and 7 (June, July 1959); Vol. II, No. 5 (May 1960).

35. Wilson, B. W., Hendrickson, J. A., and Kilmer, R. C. (1965), "Feasibility Study for a Surge-Action Model of Monterey Harbor, California", Report 2-136, Science Engineering Associates, San Marino, California.

LIST OF NOTATIONS

A	Wave amplitude
A_i	Incident wave amplitude
a	Characteristic dimension of a harbor, the radius of a circular harbor
$a_A (a_B)$	Radius of the circular harbor referred in Basin A (or Basin B)
B	Surface area
b	Width of a rectangular entrance channel
$\underline{C}$	A Dx1 vector representing the values of $\partial f_{21}/\partial n$ at the harbor entrance, and at the common boundaries between Region II-1 and II-2 as well as between Region II-1 and II-3.
D	A number equal to $p + d_1 + d_2$
d_1 (d_2)	The total number of segments at the common boundary between Regions II-1 and II-2 (II-3)
F_o	Amplitude of an amplified force
$\underline{F}_1$ ($\underline{F}_2$, $\underline{F}_3$)	A N_1x1 (N_2x1, N_3x1) vector representing the value of wave function at the boundary of Region II-1 (Region II-2, or Region II-3)
f	Wave function which describes the variation of the velocity potential in the x and y directions
f_1	Wave function in Region I (in the open-sea)
f_{21} (f_{22} or f_{23})	Wave function in Region II-1 (Region II-2 or Region II-3)
f_3	Radiated wave function

LIST OF NOTATIONS (Continued)

f_i	Incident wave function
f_r	Reflected wave function
G	An $N_1 x N_1$ matrix defined in Eqs. 11, 12e and 12f (in Eq. 18 G is an $N_2 x N_2$ matrix while in Eq. 22 G is an $N_3 x N_3$ matrix)
G_n	An $N_1 x N_1$ matrix defined in Eqs. 11, 12c, and 12d (in Eq. 18 G_n is an $N_2 x N_2$ matrix while in Eq. 22 G_n is an $N_3 x N_3$ matrix)
g	Acceleration due to gravity
H_{ij}	Radiation matrix (a pxp matrix, see Eq. 30)
H_A	A DxD matrix defined in Eq. 32
$H_o^{(1)}$, $H_1^{(1)}$	Zero and first orders of the Hankel function of first kind
h	Water depth
I	Identity matrix
λ	$\sqrt{-1}$
K	Reflection coefficient
k	Wave number
L	Wave length, or representing a length scale
ℓ	Length of a rectangular entrance channel
log	Logarithm to the Naperian base (e = 2.7128)
M	The ratio of the maximum excursion of the oscillating mass to the static movement of the mass.

LIST OF NOTATIONS (Continued)

M_A	A DxD matrix defined in Eq. 32
M_1	An N_1 xD matrix defined in Eq. 15
M_2	An $N_2 x d_1$ matrix defined in Eq. 20
M_3	An $N_3 x d_2$ matrix defined in Eq. 24
N_1 (N_2 or N_3)	Total number of segments into which the boundary of Region II-1 (Region II-2 or Region II-3) is divided
n	Outward normal to the boundary of the region
P_1 (P_2 or P_3)	A vector representing the value of the normal derivative of the wave function at the boundary of Region II-1 (Region II-2 or Region II-3)
p	Total number of segments into which the harbor entrance is divided
R	Amplification factor
$\mathbb{R}$	Reynold's number
r	Distance between points or radial position in a polar coordinates
s	Tangent to the boundary of the domain in a counter-clockwise direction
Δs	Length of the boundary segments
T	Wave period, or representing a time scale
t	Time
U_1	Is a N_1 xD matrix defined in Eqs. 13 and 14
U_2	Is a $N_2 x d_1$ matrix defined in Eq. 19

LIST OF NOTATIONS (Continued)

U_3	Is a $N_3 x d_2$ matrix defined in Eq. 23
$\vec{u}$	Velocity vector with components u, v, w
x	Coordinate axis in horizontal direction parallel to the coastline
$\vec{x}$	Position vector for the point (x, y)
y	Coordinate axis in horizontal direction perpendicular to the coastline
Z	Function which describes the variation of the velocity potential in depthwise direction z
z	Coordinate axis in vertical direction
$( )_j$	Quantities at the j^{th} segment of the boundary
$( )_r$	The ratio of a quantity in the smaller model to the corresponding quantity in a larger model or in the prototype
γ	Euler's constant (γ = 0.577216 ...)
ζ	Damping factor (see Eq. 37)
η	Displacement of water surface elevation from the mean water level
θ	Angular position
$\theta_A(\theta_B)$	Inclined central angle of the opening of circular harbor referred in Basin A (Basin B)
α	Exponential modulus of decay defined in Eq. 43
σ	Circular wave frequency ($2\pi/T$)

LIST OF NOTATIONS (Continued)

Φ	Velocity potential
ω	Forcing frequency
ω_n	Natural frequency
∇	Gradient operator
∇^2	Laplacian operator
$\lvert\ \rvert$	Absolute value

APPENDIX

COMPUTER PROGRAM

The computer program for calculating the response of an arbitrary shape harbor to the periodic incident waves which propagate normal to the coastline is presented in this Appendix. In order to illustrate the computer program, its application to the East and West Basins of the Long Beach Harbor will be presented. Subroutines used in the main program are also listed for reference.

The main computer program as well as the subroutines used in the main probram will be listed first (pp. 126 to 132). In this program, the region of consideration is divided into three regions: an open-sea region, Region II-1 (referred to herein as Basin A), and Region II-2 (referred to herein as Basin B). If a particular harbor geometry requires that it be divided into more regions then the program must be modified slightly.

The input data needed for using this program are:

(i) the number of boundary segments of Basin A (NA) and that of Basin B (NB), the number of segments at the entrance (NP), the number of segments at the common boundary between Basin A and Basin B (ND), and the following quantities:

NC = NP + ND The total of the entrance segments plus the total of the segments at the common boundary between Basin A and Basin B.

NP1 = NP + 1

NM = The segment number in Basin A prior to the first segment of the common boundary between Basin A and Basin B.

NM1 = NM + 1

MA = The total number of the interior points in Basin A to be calculated.

NM2 = NM + ND

(ii) the coordinates of the beginning and the end of each boundary segment in Basin B and Basin A. (This program is written to process first the boundary segments of Basin B and then those of Basin A's; thus, it must be supplied in this order.)

(iii) the value of the characteristic dimension (A), the width of the harbor opening (HAOP), and the water depth (DEPTH). "HAOP" is for identification only because it does not enter the computation.

(iv) the total number of interior points in Basin A plus those of Basin B (M) and the coordinates of these interior points (PX(I), PY(I)), and

(v) the incident wave number (K)

These input data for the Long Beach Harbor model for one particular wave number ($k = 2.35\ ft^{-1}$) are listed on p. 133. There are 50 boundary segments in Basin A and 34 boundary segments in Basin B. The total number of interior points in Basin A is 63, and the total number of interior points in Basin B is 25. The coordinates of

these boundary points and interior points are arranged according to the coordinates used in Fig. 7. The number associated with each interior point listed herein is essentially the same as used by Lee (1969); this allows one to check the results more rapidly in comparing both methods. Thus, point A of Fig. 7 corresponds to MESH (26), point B corresponds to MESH (88), point C corresponds to MESH (81), and point D corresponds to MESH (68).

The output data for the Long Beach Harbor model are presented on pp. 134 to 135. They contain the complex value and the absolute value of the normal derivative of the wave function at the harbor entrance and at the common boundary. The complex value and the absolute value of the wave function at the boundary of both Basin A and Basin B are also shown. Finally, the complex value and the absolute value of the wave function (F2) for the 88 interior points are printed on p.135; they are arranged so that those points in Basin A are printed first followed by those of Basin B. These output results can be checked with those presented in pp. 262 and 263 of Lee (1969) in which the single basin computer program was used to calculate the response of the same harbor model and at the same wave number To calculate the response at other wave numbers, data cards for these wave numbers can be added to the last data card presented here. It is also noted that this program is written in FORTRAN IV compatible with the IBM 360/75 digital computer.

Some of the symbols used in the computer program and not previously defined in this appendix are as follows:

M = Total no. of interior points to be calculated (Basin A plus Basin B)

NSEG(I) = Number which defines the boundary segments of Basin A or Basin B (also used to define the interior points to be calculated)

PX(I) = The x-coordinate at the beginning of the i^{th} segment of the boundary of Basin A (or Basin B) (also used as the x-coordinate of the interior points)

PY(I) = The y-coordinate at the beginning of the i^{th} segment of the boundary of Basin A (or Basin B) (also used as the y-coordinate of the interior points)

MESH(I) = Number which defines a particular interior point

EKA = Wave number parameter (ka)

R(I, J) = Distance between field and source points

DX(I) (or DY(I)) = x (or y) projection of the length of the i^{th} boundary segment of Basin A or Basin B

DS(I) = Length of the i^{th} boundary segment of Basin A or Basin B

PERT = Wave period

DFDN(I, J) = An N_1 x D matrix (for Basin A) equivalent to the matrix U_1 defined in Eqs. 13 and 14; for Basin B it is an $N_2 x d_1$ matrix equivalent to matrix U_2 defined in Eq. 19.

AN(I, J) = A matrix defined as $\left(\frac{\lambda}{2} G_n - I\right)$, it represents an $N_1 x N_1$ matrix for Basin A, and is an $N_2 \times N_2$ matrix for Basin B.

DRDN = $\partial r / \partial n$

XSS (YSS) = $\partial^2 x / \partial s^2$ $(\partial^2 y / \partial s^2)$

TEMP = $\frac{\Delta s}{\pi} \left(\frac{\partial x}{\partial s} \frac{\partial^2 y}{\partial s^2} - \frac{\partial^2 x}{\partial s^2} \frac{\partial y}{\partial s} \right)$

G(I, J) = An $N_1 x N_1$ matrix for Basin A (Eqs. 12e and 12f) or an $N_2 x N_2$ matrix for Basin B (Eq. 18)

Q(I, J) = An $N_1 x D$ matrix for Basin A equal to the matrix $\frac{\lambda}{2} GU_1$ defined in Eq. 15; for Basin B it is an $N_2 x d_1$ matrix

CSLECD = A subroutine for solving complex systems of linear equations

Q(I, J) = (After the statement CALL CSLECD) It represents the matrix M_1 defined in Eq. 15 for Basin A; for Basin B it represents M_2 defined in Eq. 20.

H(I, J) = A DxD matrix defined in the process of matching (see Eq. 33)

DFDC (I, 1) = A Dx1 complex numbered vector represents the normal derivative of the wave function at the entrance and that at the common boundary

ADFDC (I, 1) = Absolute value of DFDC (I, 1)

Q(I, 1) = Complex number representing the value of the wave function at the boundary segments of Basin A

QB (I, 1) = Complex number representing the value of the wave function at the boundary segments of Basin B

ABBF (I, 1) = Absolute value of Q (I, 1) (or QB (I, 1))

F1 (I) = The complex value of f for the interior points (either in Basin A or in Basin B)

F2 (I) = Absolute value of F1 (I) with the sign equal to that of the real part of F1 (I)

FR (I) = The ratio of F2 (I)/F2 MAX

MAXMIN = Subroutine to find maximum and minimum elements of an array

MAIN PROGRAM

```
      INTEGER P
      REAL K
      COMPLEX AN(50,50),Q(50,10),QB(34,10),H(50,10),DFDC(50,3),G(50,50)
      COMPLEX F1(100),DET,C,D,DGDN,F
      DIMENSION ADFDC(50,1),DFDN(50,10),ABBF(50,1),F2(100),FR(100),
     1  PX(100),PY(100),NSEG(100),R(50,50),RA(50,50),RB(34,34),
     2  XO(1),X(51),YO(1),Y(51),DSO(1),DS(51),DX(50),DY(50),
     3  BXO(1),BX(35),BYO(1),BY(35),DSBO(1),DSB(35),DXB(34),DYB(34),
     4  AXO(1),AX(51),AYO(1),AY(51),DSAO(1),DSA(51),DXA(50),DYA(50)
      DATA PI/3.1415926/
      PI3=3.0*PI
      C=CMPLX(0.,-1.0/2.0)
      D=CMPLX(0.,-0.25)
      TWOOPI=2.0/PI
C     READ INPUT DATA
      READ (5,1) NA,NB,NP,ND,NC,NP1,NM,NM1,MA,MM2
    1 FORMAT (14I5)
      N=NB
      KTIME=1
   11 READ (5,2) (NSEG(I),PX(I),PY(I),I=1,N)
    2 FORMAT (I5,2F13.0)
      NMR = N - 1
      PX(N+1)=PX(1)
      PY(N+1)=PY(1)
      PX(N+2)=PX(2)
      PY(N+2)=PY(2)
C     CALCULATE MIDPOINT OF EACH SEGMENT
      DO 5 I=1,N
      X(I)=0.5*(PX(I)+PX(I+1))
      Y(I)=0.5*(PY(I)+PY(I+1))
      DX(I)=PX(I+1)-PX(I)
      DY(I)=PY(I+1)-PY(I)
      DS(I)=SQRT(DX(I)**2+DY(I)**2)
    5 CONTINUE
      XO(1)=X(N)
      X(N+1)=X(1)
      YO(1)=Y(N)
      Y(N+1)=Y(1)
      DSO(1)=DS(N)
      DS(N+1)=DS(1)
      R(N,N) = 0
      DO 15 I=1,NMR
      I1=I+1
      R(I,I)=0
      DO 25 J=I1,N
      R(I,J)=SQRT((X(I)-X(J))**2+(Y(I)-Y(J))**2)
      R(J,I)=R(I,J)
   25 CONTINUE
   15 CONTINUE
      IF (KTIME.EQ.2) GO TO 100
C     STORE HARBOR GEOMETRY OF THE SECONARY BASIN
      BX(NB+1)=X(NB+1)
      BY(NB+1)=Y(NB+1)
      DSB(NB+1)=DS(NB+1)
      DSBO(1)=DSO(1)
      BYO(1)=YO(1)
      BXO(1)=XO(1)
      DO 415 I=1,NB
      DXB(I)=DX(I)
      DYB(I)=DY(I)
      DSB(I)=DS(I)
      BX(I)=X(I)
      BY(I)=Y(I)
      DO 415 J=1,NB
      RB(I,J)=R(I,J)
  415 CONTINUE
      N=NA
      KTIME = 2
      GO TO 11
  100 CONTINUE
C     STORE GEOMETRICAL INFORMATIONS OF FIRST BASIN
      AX(NA+1)=X(NA+1)
      AY(NA+1)=Y(NA+1)
      DSA(NA+1)=DS(NA+1)
      AXO(1)=XO(1)
      AYO(1)=YO(1)
      DSAO(1)=DSO(1)
      DO 425 I=1,NA
      AX(I)=X(I)
      AY(I)=Y(I)
      DXA(I)=DX(I)
      DYA(I)=DY(I)
      DSA(I)=DS(I)
      DO 425 J=1,NA
      RA(I,J)=R(I,J)
  425 CONTINUE
```

```
      READ (5,4) A
    4 FORMAT (4F10.0)
      READ (5,4) HADP,DEPTH
C     READ COORDINATES OF INTERIOR POINT INTO PX AND PY
      READ (5,1) M
      READ (5,2) (NSEG(I),PX(I),PY(I),I=1,M)
   16 READ (5,17) K
   17 FORMAT (F10.0)
      EKA=A*K
      PERT=(2.0*PI)/(SQRT(32.2*K*TANH(K*DEPTH)))
C     CALCULATE UNIT MATRIX DFDN  FOR SECONARY BASIN
      N=NB
      NN=ND
      XO(1)=BXO(1)
      YO(1)=BYO(1)
      DSO(1)=DSBO(1)
      X(NB+1)=BX(NB+1)
      Y(NB+1)=BY(NB+1)
      DS(NB+1)=DSB(NB+1)
      DO 435 I=1,NB
      X(I)=BX(I)
      Y(I)=BY(I)
      DX(I)=DXB(I)
      DY(I)=DYB(I)
      DS(I)=DSB(I)
      DO 435 J=1,NB
      R(I,J)=RB(I,J)
  435 CONTINUE
  110 CONTINUE
      DO 175 I=1,NB
      DO 175 J=1,ND
      IF ((I+J)-(ND+1)) 185,190,185
  190 DFDN(I,J)=-1.0
      GO TO 175
  185 DFDN(I,J)=0.0
  175 CONTINUE
      GO TO 60
  160 CONTINUE
C     CALCULATE UNIT MATRIX DFDN FOR MAIN BASIN
      DO 115 I=1,NA
      DO 115 J=1,NC
      DFDN(I,J)=0.0
  115 CONTINUE
      DO 125 I=1,NP
      DFDN(I,I)=1.0
  125 CONTINUE
      DO 105 J=NP1,NC
      I=NM-NP+J
      DFDN(I,J)=1.0
  105 CONTINUE
   60 CONTINUE
C     CALCULATE ELEMENTS OF THE MATRIX AN=(C*GN-I)
      DO 35 I=1,N
      DO 45 J=1,N
      IF (J .EQ. I) GO TO 10
      ARG=K*R(I,J)
      DRDN=((Y(I)-Y(J))*DX(J)- (X(I)-X(J))*DY(J))/R(I,J)
      AN(I,J)=-C*K*CMPLX(BESJ1(ARG),BESY1(ARG))*DRDN
      GO TO 45
   10 CONTINUE
      YSS=
     =6.0*((Y(I+1)-Y(I))/(DS(I+1)+DS(I))-(Y(I)-Y(I-1))/(DS(I)+DS(I-1)))/
     /  (DS(I-1)+DS(I)+DS(I+1))
      XSS=
     =6.0*((X(I+1)-X(I))/(DS(I+1)+DS(I))-(X(I)-X(I-1))/(DS(I)+DS(I-1)))/
     /  (DS(I-1)+DS(I)+DS(I+1))
      TEMP=(DX(I)*YSS-XSS*DY(I))/PI
      AN(I,I)=CMPLX(0.0,TEMP)*C-1.0
   45 CONTINUE
   35 CONTINUE
C     CALCULATE THE RIGHT HAND SIDE VECTOR Q
      DO 135 P=1,NN
      DO 55 I=1,N
      Q(I,P)=CMPLX(0.,0.)
      DO 65 J=1,N
      IF (P.NE.1) GO TO 30
      IF (J .EQ. I) GO TO 20
      ARG=K*R(I,J)
      G(I,J)=CMPLX(BESJ0(ARG),BESY0(ARG))*DS(J)
      GO TO 30
   20 G(I,I)=CMPLX(1.,TWOOPI*(ALOG(K*DS(J)*.25)-0.42279))*DS(I)
   30 Q(I,P)=Q(I,P)+G(I,J)*DFDN(J,P)
   65 CONTINUE
      Q(I,P)=C*Q(I,P)
   55 CONTINUE
  135 CONTINUE
      CALL CSLECD(AN,N,Q,NN,DET,IER)
      IF (N.EQ.NA) GO TO 70
```

```
C     STORE INFORMATION FOR SECONDARY BASIN
      DO 255 I=1,NB
      DO 255 J=1,ND
      QB(I,J)=Q(I,J)
  255 CONTINUE
      N=NA
      NN=NC
      XO(1)=AXO(1)
      YO(1)=AYO(1)
      DSO(1)=DSAO(1)
      X(NA+1)=AX(NA+1)
      Y(NA+1)=AY(NA+1)
      DS(NA+1)=DSA(NA+1)
      DO 275 I=1,NA
      X(I)=AX(I)
      Y(I)=AY(I)
      DX(I)=DXA(I)
      DY(I)=DYA(I)
      DS(I)=DSA(I)
      DO 275 J=1,NA
      R(I,J)=RA(I,J)
  275 CONTINUE
      GO TO 160
   70 CONTINUE
      DO 145 I=1,NA
      DO 145 J=1,3
      DFDC(I,J)=CMPLX(0.0,0.0)
  145 CONTINUE
C     CALCULATE WAVE FUNCTION OF EXTERIOR PROBLEM AND MATCHING
      DO 205 I=1,NC
      DO 205 J=1,NC
      H(I,J)=CMPLX(0.0,0.0)
  205 CONTINUE
      DO 215  I=1,NP
      DO 215  J=1,NP
      IF (I.EQ.J) GO TO 210
      H(I,J)=CMPLX(BESJO(K*R(I,J)),BESYO(K*R(I,J)))*DS(J)*C
      GO TO 215
  210 H(I,I)=CMPLX(1.0,TWOOPI*(ALOG(K*DS(I)*.25)-0.42279))*DS(I)*C
  215 CONTINUE
      DO 315 I=NP1,NC
      DO 315 J=NP1,NC
      II=NC-I+1
      JJ=J-NP
      H(I,J)=QB(II,JJ)
  315 CONTINUE
      DO 325 I=1,NP
      DO 325 J=1,NC
      H(I,J)=Q(I,J)-H(I,J)
  325 CONTINUE
      DO 335 I=NP1,NC
      DO 335 J=1,NC
      II=NM+I-NP
      H(I,J)=Q(II,J)-H(I,J)
  335 CONTINUE
      DO 225 I=1,NP
      DFDC(I,1)=CMPLX(1.0,0.0)
  225 CONTINUE
      CALL CSLECD(H,NC,DFDC,1,DET,IER)
      WRITE (6,6)
    6 FORMAT (1H1)
      WRITE (6,19) K
   19 FORMAT (2X3HK =F10.5,2X,'(1/FT)')
      WRITE (6,38)
   38 FORMAT (///,2X,'COMPLEX VALUE OF DFDC AT THE ENTRANCE AND AT THE C
     *OMMON BOUNDARY (1/FT)',/)
      WRITE (6,8) (DFDC(I,1),I=1,NC)
    8 FORMAT (1X,6F13.5)
      DO 305 I=1,NC
  305 ADFDC(I,1)=CABS(DFDC(I,1))
      WRITE (6,68)
   68 FORMAT(///,2X,'ABSOLUTE VALUE OF DFDC AT THE ENTRANCE (1/FT)',/)
      WRITE (6,8) (ADFDC(I,1),I=1,NP)
      WRITE (6,69)
   69 FORMAT (///,2X,'ABSOLUTE VALUE OF DFDC AT THE COMMON BOUNDARY (1/F
     *T)')
      WRITE (6,8)  (ADFDC(I,1),I=NP1,NC)
C     CALCULATE BOUNDARY WAVE FUNCTION F OF PRIMARY BASIN
      DO 235 I=1,NA
      DO 235 J=1,NC
  235 DFDC(I,2)=DFDC(I,2)+Q(I,J)*DFDC(J,1)
      DO 245 I=1,NA
      Q(I,1)=DFDC(I,2)
      ABBF(I,1)=CABS(Q(I,1))
  245 CONTINUE
```

```
      WRITE (6,48)
   48 FORMAT (///,2X,'COMPLEX VALUE OF THE BOUNDARY F FUNCTION Q(I,1)')
      WRITE (6,47)
   47 FORMAT (2X,'(BASIN A)',/)
      WRITE (6,8) (Q(I,1),I=1,N)
      WRITE (6,148)
  148 FORMAT (///,2X,'ABSOLUTE VALUE OF THE BOUNDARY F FUNCTION')
      WRITE (6,47)
      WRITE (6,8)(ABBF(I,1),I=1,N)
C     CALCULATE BOUNDARY WAVE FUNCTION F OF SECONDARY BASIN
      DO 385 I=1,NB
      DFDC(I,2)=CMPLX(0.0,0.0)
      DFDC(I,3)=CMPLX(0.0,0.0)
      DO 375 J=1,ND
      JJ=NP+J
  375 DFDC(I,2)=DFDC(I,2)+QB(I,J)*DFDC(JJ,1)
      QB(I,1)=DFDC(I,2)
      ABBF(I,1)=CABS(QB(I,1))
  385 CONTINUE
      WRITE (6,48)
      WRITE (6,49)
   49 FORMAT (2X,'(BASIN B)',/)
      WRITE(6,8) (QB(I,1),I=1,NB)
      WRITE(6,148)
      WRITE (6,49)
      WRITE(6,8) (ABBF(I,1),I=1,NB)
C     NUMBERING BOUNDARY F DERIVATIVES FOR SECONDARY BASIN
      DO 355 I=1,ND
      L=NC-I+1
      DFDC(I,3)=DFDC(L,1)
  355 CONTINUE
C     RENUMBERING BOUNDARY DERIVATIVES OF PRIMARY BASIN
      DO 365 I=NM1,NM2
      J=I-NM1+NP1
      DFDC(I,1)=DFDC(J,1)
      DFDC(J,1)=CMPLX(0.0,0.0)
  365 CONTINUE
C     CALCULATE WAVE FUNCTION F FOR INTERIOR POINTS
      DO 75 J=1,M
      F=CMPLX(0.0,0.0)
      IF (J.GT.MA) GO TO 395
      DO 85 I=1,NA
      R1=SQRT((AX(I)-PX(J))**2+(AY(I)-PY(J))**2)
      RK=K*R1
      DGDN=K*CMPLX(BESJ1(RK),BESY1(RK))*((PX(J)-AX(I))*DYA(I)
     *     -(PY(J)-AY(I))*DXA(I))/R1
      F=F+Q(I,1)*DGDN-DFDC(I,1)*CMPLX(BESJ0(RK),BESY0(RK))*DSA(I)
   85 CONTINUE
      GO TO 200
  395 DO 495 I=1,NB
      R1=SQRT((BX(I)-PX(J))**2+(BY(I)-PY(J))**2)
      RK=K*R1
      DGDN=K*CMPLX(BESJ1(RK),BESY1(RK))*((PX(J)-BX(I))*DYB(I)
     *     -(PY(J)-BY(I))*DXB(I))/R1
      F=F+QB(I,1)*DGDN+DFDC(I,3)*CMPLX(BESJ0(RK),BESY0(RK))*DSB(I)
  495 CONTINUE
  200 F=D*F
      F1(J)=F
      F2(J)=SIGN(CABS(F),REAL(F))
   75 CONTINUE
      CALL MAXMIN(F2,M,F2MX,F2MN)
      F2MAX=AMAX1(ABS(F2MX),ABS(F2MN))
      DO 605 J=1,M
  605 FR(J)=F2(J)/F2MAX
      WRITE (6,6)
      WRITE (6,119) HAOP,DEPTH
  119 FORMAT (2X,'HARBOR OPENING (FT.)=',F 7.3,5X,'DEPTH (FT.)=',F7.3)
      WRITE (6,19) K
      WRITE (6,26) EKA
   26 FORMAT (2X3HKA=F10.5)
      WRITE (6,129) PERT
  129 FORMAT (2X,'PERIOD T =',F10.5,2X,'(SEC.)')
      WRITE (6,199) F2MAX
  199 FORMAT (//,2X,'F2MAX=',F10.5)
      WRITE (6,99)
   99 FORMAT (//,2X,'MESH', 8X,'PX', 9X,'PY',14X,'FCMPLX',15X,'F2',
     *   10X,'FRA.',/)
      WRITE (6,9) (NSEG(J),PX(J),PY(J),F1(J),F2(J),FR(J),J=1,M)
    9 FORMAT (1X,I5,F11.3,F11.3,2F13.5,F13.5,F11.3)
      GO TO 16
      END
```

SUBROUTINES

(1)

```
      SUBROUTINE  CSLECD( A, M, B, N, DET, ILL)
C     SOLUTION OF COMPLEX SYSTEM  OF LIN.EQUAT.WITH N RIGHT HAND VECTORS
C      AND/OR COMPUTATION OF COMPLEX DETERMINANT
      COMPLEX A, B, AT, FAC, DET
      DIMENSION A(50,M),B(50,N)
      ILL= 0
      CALL OVERFL(IO)
      SIGN= +1
      IMA= M-1
      DO 35 I=1,IMA
      AMAX= REAL(A(I,I)) * REAL(A(I,I)) + AIMAG(A(I,I)) * AIMAG(A(I,I))
      JMAX= I
      I1= I+1
      DO 20  J=I1,M
      ARE= REAL(A(J,I))
      AIM= AIMAG(A(J,I))
      AJI= ARE*ARE + AIM*AIM
      IF(AMAX-AJI)  18,20,20
   18 AMAX= AJI
      JMAX= J
   20 CONTINUE
      IF(AMAX) 21,90,21
   21 IF(I-JMAX)  23,25,23
   23 SIGN= -SIGN
      DO 24  K=I,M
      AT= A(I,K)
      A(I,K)= A(JMAX,K)
   24 A(JMAX,K)= AT
      IF(N.LE.0) GO TO 25
      DO 241  K=1,N
      AT= B(I,K)
      B(I,K)= B(JMAX,K)
  241 B(JMAX,K) = AT
   25 DO 35  J=I1,M
      FAC= A(J,I)/A(I1-1,I1-1)
      DO 30  K=I1,M
   30 A(J,K)= A(J,K) - FAC*A(I,K)
      IF(N.LE.0) GO TO 35
      DO 32  K=1,N
   32 B(J,K) = B(J,K) -FAC*B(I,K)
   35 CONTINUE
C     TRIANGULAR MATRIX READY
      IF(N.LE.0)  GO TO 70
      IF      (CABS(A(M,M)) .EQ. 0.)  GO TO 90
      DO 40  K=1,N
   40 B(M,K) = B(M,K)/ A(M,M)
      DO 60  I=1,IMA
      J= M-I
      K1= J+1
      DO 50  K=K1,M
      DO 50  L=1,N
   50 B(J,L)= B(J,L) -A(J,K)*B(K,L)
      DO 60  L=1,N
   60 B(J,L) = B(J,L) / A(J,J)
   70 DET= A(1,1)
      DO 74 I=2,M
   74 DET= DET*A(I,I)
      DET= DET* SIGN
      CALL OVERFL(IO)
      IF(IO.EQ.1)  GO TO 91
      RETURN
   90 DET= (0.,0.)
   91 WRITE(6,92)
   92 FORMAT(46HODET A = 0  OR OVERFLOW   IN SUBROUTINE CSLECD )
      ILL= -1
      RETURN
      END
```

```
      FUNCTION BESJ0(X)
C     BESSEL FUNCTION J0(X)
      IF (X .GT. 3.) GO TO 10
      IF (X .LT.-3.) GO TO 20
      X03=X/3.
      T=X03*X03
      BESJ0=1.+T*(-2.2499997+T*(1.2656208+T*(-.3163866 +T*(.0444479
     1     +T*(-.0039444 +T*.0002100)))))
      RETURN
   10 T=3./X
      F0=.79788456+T*(-.00000077+T*(-.00552740+T*(-.00009512
     1  +T*(.00137237+T*(-.00072805+T*.00014476)))))
      THETA0=X-.78539816+T*(-.04166397+T*(-.00003954
     1      +T*(.00262573+T*(-.00054125+T*(-.00029333+T*.00013558)))))
      BESJ0=F0*COS(THETA0)/SQRT(X)
      RETURN
   20 WRITE (6,6)
    6 FORMAT (44H ARGUMENT LESS THAN -3 , NO J0(X) CALCULATED)
      RETURN
      END
```

(3)

```
      FUNCTION BESJ1(X)
C     BESSEL FUNCTION J1(X)
      IF (X .GT. 3.) GO TO 10
      IF (X .LT.-3.) GO TO 20
      X03=X/3.
      T=X03*X03
      BESJ1=.5+T*(-.56249985+T*(.21093573+T*(-.03954289+T*(.00443319
     1     +T*(-.00031761+.00001109)))))
      BESJ1=BESJ1*X
      RETURN
   10 T=3./X
      F1=.79788456+T*(.00000156+T*(.01659667+T*(.00017105
     1     +T*(-.00249511+T*(.00113653-T*.00020033)))))
      THETA1=X-2.35619449+T*(.12499612+T*(.00005650+T*(-.00637879
     1     +T*(.00074348+T*(.00079824-T*.00029166)))))
      BESJ1=F1*COS(THETA1)/SQRT(X)
      RETURN
   20 WRITE (6,6)
    6 FORMAT (44H ARGUMENT LESS THAN -3 , NO J1(X) CALCULATED)
      RETURN
      END
```

(4)

```
      FUNCTION BESY0(X)
C     NEUMANN FUNCTION Y0(X)
      IF (X .LE. 0.) GO TO 20
      IF (X .GT. 3.) GO TO 10
      X03=X/3.
      T=X03*X03
      BESY0=2./3.1415926*ALOG(.5*X)*BESJ0(X)+.36746691+T*(.60559366
     1     +T*(-.74350384+T*(.25300117+T*(-.04261214+T*(.00427916
     2     -T*.00024846)))))
      RETURN
   10 T=3./X
      F0=.79788456+T*(-.00000077+T*(-.00552740+T*(-.00009512
     1  +T*(.00137237+T*(-.00072805+T*.00014476)))))
      THETA0=X-.78539816+T*(-.04166397+T*(-.00003954
     1      +T*(.00262573+T*(-.00054125+T*(-.00029333+T*.00013558)))))
      BESY0=F0*SIN(THETA0)/SQRT(X)
      RETURN
   20 WRITE (6,6)
    6 FORMAT (48H ARGUMENT LESS THAN OR = 0 , NO Y0(X) CALCULATED)
      RETURN
      END
```

(5)

```
      FUNCTION BESY1(X)
C     NEUMANN FUNCTION Y1(X)
      IF (X .LE. 0.) GO TO 20
      IF (X .GT. 3.) GO TO 10
      X03=X/3.
      T=X03*X03
      BESY1=2./3.1415926*X*ALOG(0.5*X)*BESJ1(X)
     1     -.6366198+T*(.2212091+T*(2.1682709+T*(-1.3164827
     2     +T*(.3123951+T*(-.0400976+T*.0027873)))))
      BESY1=BESY1/X
      RETURN
   10 T=3./X
      F1=.79788456+T*(.00000156+T*(.01659667+T*(.00017105
     1     +T*(-.00249511+T*(.00113653-T*.00020033)))))
      THETA1=X-2.35619449+T*(.12499612+T*(.00005650+T*(-.00637879
     1     +T*(.00074348+T*(.00079824-T*.00029166)))))
      BESY1=F1*SIN(THETA1)/SQRT(X)
      RETURN
   20 WRITE (6,6)
    6 FORMAT (48H ARGUMENT LESS THAN OR = 0 , NO Y1(X) CALCULATED)
      RETURN
      END
```

```
MXMN     TITLE 'MAXMIN--SUBROUTINE FINDING MAX AND MIN'
*
*        THE SUBROUTINE 'MAXMIN' FINDS THE UPPER AND LOWER BOUNDARIES
*        OF AN ARRAY, EITHER REAL OR INTEGER. THE CALLING SEGUENCE IS
*        AS FOLLOWS,
*
*              CALL MAXMIN(A,N,AMX,AMN)
*
*        WHERE A = ONE DIMENSIONAL ARRAY, REAL OR INTEGER.
*              N = LENGTH OF THE ARRAY. N MUST BE GREATER OR EQUAL TO 1
*                = POSITIVE, IF A IS A FLOATING-POINT ARRAY.
*                = NEGATIVE, IF A IS AN INTEGER ARRAY.
*            AMX = MAXIMUM VALUE OF THE ARRAY, REAL OR INTEGER.
*            AMN = MINIMUM VALUE OF THE ARRAY, REAL OR INTEGER.
*
R0       EQU   0
R1       EQU   1
R2       EQU   2
R3       EQU   3
I        EQU   4
A        EQU   5
AMX      EQU   6
AMN      EQU   7
BASE     EQU   8
N        EQU   9
AAMX     EQU   10
AAMN     EQU   11
FMX      EQU   0
FMN      EQU   2
FR       EQU   4
         ENTRY MAXMIN
MAXMIN   SAVE  (14,12),,*
         BALR  BASE,0
         USING *,BASE
         L     AAMX,8(R1)          GET ADDR. OF AMX.
         L     AAMN,12(R1)         GET ADDR. OF AMN.
         L     R2,4(R1)
         L     N,0(R2)             GET N.
         C     N,=F'1'             IS N = 1 ?
         BNE   NNE1                NO. BRANCH.
         L     R2,0(R1)            YES. SET
         L     R2,0(R2)            AMX = A(1).
         ST    R2,0(AAMX)          AMN = A(1).
         ST    R2,0(AAMN)          AND RETURN.
RETN     RETURN (14,12),T
NNE1     LTR   N,N
         BNZ   NNZ                 BRANCH IF N .NE. 0.
         L     15,=V(IBCOM#)       IF N = 0, PRINT
         CNOP  0,4                 AN ERROR MESSAGE
         BAL   14,4(15)            AND TERMINATE THE JOB.
         DC    A(6),AL1(1),AL3(FM)
         BAL   14,16(15)
         CALL  EXIT
NNZ      L     A,0(R1)             INITIALIZE ARRAY POINTER.
         LPR   R3,N                REG.3 = IABS(N).
         BCTR  R3,0                SET UP UPPER LIMIT OF ARRAY
         SLL   R3,2                BY SETTING REG.3 = (N-1)*4.
         LA    I,4                 SET I = 4 TO START THE LOOP.
         LA    R2,4                REG.2 = 4, INCREMENT OF I.
         LTR   N,N                 IS N PLUS ?
         BP    FLOATPT             YES. A IS FLOATING-PT. BRANCH.
         L     AMX,0(A)            SET AMX = A(1) .
         LR    AMN,AMX             AMN = A(1) INITIALLY.
LOOP1    L     R0,0(A,I)           GET A(I).
         CR    AMX,R0              IS AMX >= A(I) ?
         BL    SETAMX              NO. BRANCH.
         CR    AMN,R0              IS AMN <= A(I) ?
         BNH   BXLE                YES. BRANCH.
         LR    AMN,R0              NO. SET AMN = A(I)
         B     BXLE                AND BRANCH.
SETAMX   LR    AMX,R0              IF AMX < A(I), SET AMX = A(I).
BXLE     BXLE  I,R2,LOOP1          STEP I AND LOOP BACK.
         ST    AMX,0(AAMX)         STORE THE INTEGER RESULTS
         ST    AMN,0(AAMN)         AND RETURN.
         B     RETN
FLOATPT  LE    FMX,0(A)            SET FMX = A(1),
         LE    FMN,0(A)            FMN = A(1) INITIALLY.
LOOP2    LE    FR,0(A,I)           GET A(I).
         CER   FMX,FR              IS FMX >= A(I) ?
         BL    SETFMX              NO. BRANCH.
         CER   FMN,FR              IS FMN <= A(I) ?
         BNH   FBXLE               YES. BRANCH.
         LER   FMN,FR              NO. SET FMN = A(I)
         B     FBXLE               AND BRANCH.
SETFMX   LER   FMX,FR              IF FMX < A(I), SET FMX = A(I).
FBXLE    BXLE  I,R2,LOOP2          STEP I AND LOOP BACK.
         STE   FMX,0(AAMX)         STORE THE FLOATING-POINT
         STE   FMN,0(AAMN)         RESULTS AND RETURN
         B     RETN
FM       DC    C'(/'' ERROR RETURN FROM MAXMIN--N = 0.'')'
         END
```

```
50   34    2    4    6    3    7    8   63   11
 1     -0.285    -0.698
 2     -0.330    -0.645
 3     -0.390    -0.570
 4     -0.450    -0.495
 5     -0.491    -0.450
 6     -0.555    -0.465
 7     -0.675    -0.486
 8     -0.809    -0.509
 9     -0.930    -0.530
10     -0.990    -0.545
11     -1.023    -0.585
12     -1.073    -0.720
13     -1.115    -0.842
14     -1.161    -0.975
15     -1.199    -1.079
16     -1.202    -1.115
17     -1.179    -1.146
18     -1.079    -1.184
19     -0.954    -1.229
20     -0.825    -1.280
21     -0.774    -1.302
22     -0.719    -1.310
23     -0.585    -1.335
24     -0.524    -1.349
25     -0.450    -1.350
26     -0.339    -1.350
27     -0.285    -1.320
28     -0.300    -1.254
29     -0.360    -1.140
30     -0.383    -1.071
31     -0.375    -1.007
32     -0.345    -0.884
33     -0.315    -0.750
34     -0.299    -0.705
 1     -0.105     0.000
 2     -0.203     0.000
 3     -0.300     0.000
 4     -0.323    -0.060
 5     -0.369    -0.180
 6     -0.411    -0.287
 7     -0.461    -0.405
 8     -0.491    -0.450
 9     -0.450    -0.495
10     -0.390    -0.570
11     -0.330    -0.645
12     -0.285    -0.698
13     -0.255    -0.690
14     -0.158    -0.690
15     -0.060    -0.690
16     -0.023    -0.705
17     -0.015    -0.750
18     -0.015    -0.885
19     -0.015    -1.005
20     -0.009    -1.040
21      0.030    -1.050
22      0.165    -1.050
23      0.315    -1.053
24      0.450    -1.056
25      0.585    -1.058
26      0.720    -1.061
27      0.855    -1.062
28      0.990    -1.064
29      1.125    -1.067
30      1.260    -1.068
31      1.365    -1.070
32      1.418    -1.050
33      1.425    -1.005
34      1.425    -0.870
35      1.425    -0.735
36      1.425    -0.600
37      1.421    -0.525
38      1.380    -0.480
39      1.260    -0.416
40      1.140    -0.344
41      1.022    -0.273
42      0.902    -0.207
43      0.797    -0.144
44      0.735    -0.120
45      0.660    -0.117
46      0.510    -0.117
47      0.360    -0.119
48      0.210    -0.119
49      0.075    -0.111
50     -0.036    -0.066
1.440
0.20       1.00
```

```
88
 1     -0.210    -0.105
 2      0.750    -0.225
 3      0.600    -0.225
 4      0.450    -0.225
 5      0.300    -0.225
 6      0.150    -0.225
 7      0.000    -0.225
 8     -0.150    -0.225
 9     -0.270    -0.225
10      1.035    -0.405
11      0.900    -0.375
12      0.750    -0.375
13      0.600    -0.375
14      0.450    -0.375
15      0.300    -0.375
16      0.150    -0.375
17      0.000    -0.375
18     -0.150    -0.375
19     -0.300    -0.375
20      1.200    -0.525
21      1.050    -0.525
22      0.900    -0.525
23      0.750    -0.525
24      0.600    -0.525
25      0.450    -0.525
26      0.300    -0.525
27      0.150    -0.495
28      0.000    -0.495
29     -0.180    -0.495
30     -0.345    -0.480
35      1.305    -0.585
36      1.305    -0.705
37      1.200    -0.675
38      1.050    -0.675
39      0.900    -0.675
40      0.750    -0.675
41      0.600    -0.675
42      0.450    -0.675
43      0.300    -0.675
44      0.150    -0.675
45      0.075    -0.600
46     -0.075    -0.600
47     -0.225    -0.600
71      1.320    -0.825
72      1.200    -0.825
73      1.050    -0.825
74      0.900    -0.825
75      0.750    -0.825
76      0.600    -0.825
77      0.450    -0.825
78      0.300    -0.825
79      0.150    -0.825
80      0.090    -0.750
81      1.320    -0.960
82      1.200    -0.960
83      1.050    -0.960
84      0.900    -0.960
85      0.750    -0.960
86      0.600    -0.960
87      0.450    -0.960
88      0.300    -0.960
89      0.150    -0.960
90      0.090    -0.885
32     -0.600    -0.570
33     -0.750    -0.585
34     -0.900    -0.600
49     -0.450    -0.675
50     -0.600    -0.675
51     -0.750    -0.675
52     -0.930    -0.690
53     -0.450    -0.825
54     -0.600    -0.825
55     -0.750    -0.825
56     -0.900    -0.825
57     -1.005    -0.825
58     -0.480    -0.975
59     -0.600    -0.975
60     -0.750    -0.975
61     -0.900    -0.975
62     -1.050    -0.975
63     -0.480    -1.125
64     -0.600    -1.125
65     -0.750    -1.125
66     -0.900    -1.125
67     -1.050    -1.095
68     -0.450    -1.245
69     -0.600    -1.245
70     -0.750    -1.215
2.35
```

K = 2.35000 (1/FT)

COMPLEX VALUE OF DFDC AT THE ENTRANCE AND AT THE COMMON BOUNDARY (1/FT)

-1.29793	-9.20573	-1.17960	-8.18918	-1.57852	-8.27092
-1.09136	-5.84153	-1.16054	-6.40026	-1.71354	-9.60764

ABSOLUTE VALUE OF DFDC AT THE ENTRANCE (1/FT)

9.29678	8.27370

ABSOLUTE VALUE OF DFDC AT THE COMMON BOUNDARY (1/FT)

8.42021	5.94260	6.50463	9.75925

COMPLEX VALUE OF THE BOUNDARY F FUNCTION Q(I,1)
(BASIN A)

0.34629	1.45456	0.34037	1.39798	0.36667	1.64139
0.43034	2.11007	0.43959	2.29322	0.37951	2.06259
0.29358	1.64680	0.24941	1.42348	0.24769	1.42556
0.24661	1.44330	0.24957	1.48275	0.27716	1.63593
0.36870	2.16062	0.44250	2.61231	0.49460	2.97566
0.48700	2.99361	0.46333	2.93952	0.44983	2.93968
0.40990	2.71710	0.41472	2.75151	0.43526	2.87409
0.37550	2.50065	0.26589	1.83511	0.12728	0.99263
-0.03264	0.01485	-0.19773	-1.00370	-0.35529	-1.98789
-0.48970	-2.84220	-0.58436	-3.46495	-0.63129	-3.80009
-0.62415	-3.78956	-0.60483	-3.67437	-0.64303	-3.87777
-0.63171	-3.78176	-0.60752	-3.62347	-0.58419	-3.48298
-0.55838	-3.32547	-0.54655	-3.23006	-0.44466	-2.58781
-0.31513	-1.79269	-0.17160	-0.92932	-0.03718	-0.13393
0.04134	0.32324	0.09129	0.61347	0.18700	1.16321
0.31682	1.88821	0.42339	2.44775	0.47922	2.67833
0.47367	2.51123	0.43217	2.09534		

ABSOLUTE VALUE OF THE BOUNDARY F FUNCTION
(BASIN A)

1.49521	1.43882	1.68185	2.15351	2.33497	2.09721
1.67277	1.44516	1.44692	1.46422	1.50361	1.65924
2.19185	2.64952	3.01648	3.03297	2.97581	2.97389
2.74785	2.78259	2.90686	2.52869	1.85427	1.00076
0.03585	1.02299	2.01939	2.88408	3.51388	3.85217
3.84061	3.72382	3.93072	3.83415	3.67404	3.53164
3.37202	3.27597	2.62573	1.82018	0.94503	0.13899
0.32587	0.62022	1.17814	1.91460	2.48410	2.72087
2.55551	2.13945				

COMPLEX VALUE OF THE BOUNDARY F FUNCTION Q(I,1)
(BASIN B)

0.24957	1.48275	0.24661	1.44330	0.24769	1.42556
0.24941	1.42348	0.18508	1.07651	0.08154	0.49197
-0.02073	-0.09970	-0.09078	-0.51546	-0.11865	-0.68622
-0.12439	-0.72387	-0.15202	-0.89069	-0.18830	-1.11269
-0.22136	-1.31929	-0.23941	-1.44184	-0.22454	-1.36291
-0.22380	-1.35925	-0.24600	-1.48099	-0.24450	-1.44753
-0.24120	-1.40105	-0.24022	-1.37715	-0.23895	-1.36033
-0.23483	-1.31758	-0.23688	-1.30970	-0.23901	-1.31001
-0.24552	-1.32932	-0.23484	-1.25921	-0.23855	-1.27718
-0.23120	-1.24359	-0.19272	-1.03660	-0.14719	-0.78037
-0.07073	-0.34280	0.05222	0.36133	0.16735	1.01662
0.16802	1.01165				

ABSOLUTE VALUE OF THE BOUNDARY F FUNCTION
(BASIN B)

1.50361	1.46422	1.44692	1.44516	1.09230	0.49868
0.10183	0.52339	0.69640	0.73448	0.90357	1.12851
1.33773	1.46158	1.38129	1.37755	1.50128	1.46803
1.42166	1.39794	1.38115	1.33834	1.33094	1.33163
1.35180	1.28092	1.29926	1.26489	1.05436	0.79413
0.35002	0.36508	1.03030	1.02551		

HARBOR OPENING (FT.)= 0.200 DEPTH (FT.)= 1.000
K = 2.35000 (1/FT)
KA= 3.39400
PERIOD T = 0.72890 (SEC.)

F2MAX= 3.90599

MESH	PX	PY	FCMPLX		F2	FRA.
1	-0.210	-0.105	0.42423	2.04361	2.08717	0.534
2	0.750	-0.225	0.02710	0.24676	0.24825	0.064
3	0.600	-0.225	0.16902	1.07050	1.08376	0.277
4	0.450	-0.225	0.30452	1.83239	1.85752	0.476
5	0.300	-0.225	0.41714	2.43353	2.46902	0.632
6	0.150	-0.225	0.48211	2.72735	2.76963	0.709
7	0.0	-0.225	0.49389	2.69062	2.73557	0.700
8	-0.150	-0.225	0.47472	2.49220	2.53701	0.650
9	-0.270	-0.225	0.45247	2.33993	2.38328	0.610
10	1.035	-0.405	-0.32289	-1.83039	-1.85865	-0.476
11	0.900	-0.375	-0.17552	-0.94066	-0.95690	-0.245
12	0.750	-0.375	-0.01827	-0.00353	-0.01861	-0.005
13	0.600	-0.375	0.13945	0.91960	0.93011	0.238
14	0.450	-0.375	0.28466	1.74857	1.77159	0.454
15	0.300	-0.375	0.40116	2.38653	2.42000	0.620
16	0.150	-0.375	0.47398	2.74838	2.78895	0.714
17	0.0	-0.375	0.49676	2.80875	2.85234	0.730
18	-0.150	-0.375	0.47457	2.62322	2.66580	0.682
19	-0.300	-0.375	0.42244	2.30591	2.34429	0.600
20	1.200	-0.525	-0.50131	-2.92889	-2.97148	-0.761
21	1.050	-0.525	-0.38394	-2.19427	-2.22760	-0.570
22	0.900	-0.525	-0.23230	-1.26624	-1.28737	-0.330
23	0.750	-0.525	-0.06350	-0.24966	-0.25761	-0.066
24	0.600	-0.525	0.10664	0.75868	0.76614	0.196
25	0.450	-0.525	0.26156	1.65897	1.67946	0.430
26	0.300	-0.525	0.38474	2.35326	2.38450	0.610
27	0.150	-0.495	0.46471	2.75896	2.79782	0.716
28	0.0	-0.495	0.48740	2.83180	2.87344	0.736
29	-0.180	-0.495	0.43965	2.49926	2.53763	0.650
30	-0.345	-0.480	0.34517	1.94195	1.97239	0.505
35	1.305	-0.585	-0.57306	-3.38578	-3.43393	-0.879
36	1.305	-0.705	-0.60161	-3.56173	-3.61218	-0.925
37	1.200	-0.675	-0.54690	-3.20432	-3.25066	-0.832
38	1.050	-0.675	-0.43143	-2.47493	-2.51225	-0.643
39	0.900	-0.675	-0.27750	-1.52355	-1.54862	-0.396
40	0.750	-0.675	-0.10237	-0.45771	-0.46902	-0.120
41	0.600	-0.675	0.07556	0.61037	0.61503	0.157
42	0.450	-0.675	0.23778	1.56969	1.58759	0.406
43	0.300	-0.675	0.36694	2.31830	2.34716	0.601
44	0.150	-0.675	0.44810	2.76858	2.80461	0.718
45	0.075	-0.600	0.47306	2.84340	2.88248	0.738
46	-0.075	-0.600	0.46640	2.74025	2.77966	0.712
47	-0.225	-0.600	0.37945	2.19967	2.23215	0.571
71	1.320	-0.825	-0.62805	-3.73627	-3.78869	-0.970
72	1.200	-0.825	-0.57639	-3.39036	-3.43901	-0.880
73	1.050	-0.825	-0.46387	-2.67032	-2.71031	-0.694
74	0.900	-0.825	-0.30952	-1.70642	-1.73426	-0.444
75	0.750	-0.825	-0.13144	-0.61157	-0.62554	-0.160
76	0.600	-0.825	0.05078	0.49499	0.49758	0.127
77	0.450	-0.825	0.21757	1.49660	1.51233	0.387
78	0.300	-0.825	0.35135	2.29143	2.31821	0.594
79	0.150	-0.825	0.43873	2.80463	2.83874	0.727
80	0.090	-0.750	0.46054	2.88010	2.91669	0.747
81	1.320	-0.960	-0.64349	-3.85262	-3.90599	-1.000
82	1.200	-0.960	-0.59489	-3.51605	-3.56602	-0.913
83	1.050	-0.960	-0.48333	-2.79269	-2.83420	-0.726
84	0.900	-0.960	-0.32810	-1.81508	-1.84449	-0.472
85	0.750	-0.960	-0.14808	-0.70063	-0.71611	-0.183
86	0.600	-0.960	0.03528	0.42068	0.42216	0.108
87	0.450	-0.960	0.20252	1.43492	1.44914	0.371
88	0.300	-0.960	0.33697	2.24635	2.27149	0.582
89	0.150	-0.960	0.42130	2.75772	2.78971	0.714
90	0.090	-0.885	0.45028	2.90394	2.93864	0.752
32	-0.600	-0.570	0.07017	0.42361	0.42938	0.110
33	-0.750	-0.585	-0.04051	-0.21789	-0.22162	-0.057
34	-0.900	-0.600	-0.11072	-0.63643	-0.64598	-0.165
49	-0.450	-0.675	0.12541	0.75249	0.76287	0.195
50	-0.600	-0.675	0.02105	0.14474	0.14626	0.037
51	-0.750	-0.675	-0.06691	-0.37197	-0.37794	-0.097
52	-0.930	-0.690	-0.14112	-0.81831	-0.83039	-0.213
53	-0.450	-0.825	0.00355	0.06822	0.06831	0.017
54	-0.600	-0.825	-0.06240	-0.32821	-0.33409	-0.086
55	-0.750	-0.825	-0.12331	-0.69709	-0.70791	-0.181
56	-0.900	-0.825	-0.16927	-0.98180	-0.99628	-0.255
57	-1.005	-0.825	-0.19048	-1.11804	-1.13415	-0.290
58	-0.480	-0.975	-0.11508	-0.60975	-0.62052	-0.159
59	-0.600	-0.975	-0.14334	-0.78854	-0.80147	-0.205
60	-0.750	-0.975	-0.17999	-1.02290	-1.03861	-0.266
61	-0.900	-0.975	-0.21017	-1.22209	-1.24003	-0.317
62	-1.050	-0.975	-0.22932	-1.35796	-1.37719	-0.353
63	-0.480	-1.125	-0.19528	-1.06415	-1.08191	-0.277
64	-0.600	-1.125	-0.20480	-1.13769	-1.15597	-0.296
65	-0.750	-1.125	-0.22114	-1.25896	-1.27823	-0.327
66	-0.900	-1.125	-0.23631	-1.37532	-1.39548	-0.357
67	-1.050	-1.095	-0.24143	-1.43407	-1.45425	-0.372
68	-0.450	-1.245	-0.23324	-1.27102	-1.29224	-0.331
69	-0.600	-1.245	-0.23346	-1.29992	-1.32072	-0.338
70	-0.750	-1.215	-0.23077	-1.31389	-1.33400	-0.342